# OPTIMAL POWER FLOW FOR HYBRID AC-DC MICROGRID

**2022**
**PhD THESIS**
**ELECTRICAL-ELECTRONICS ENGINEERING**

**Salem Faraj ALARABI ALJRIBI**

**Thesis Advisor**
**Prof. Dr. Ziyodulla YUSUPOV**

# OPTIMAL POWER FLOW FOR HYBRID AC-DC MICROGRID

**Salem Faraj Alarabi ALJRIBI**

**T.C.**
**Karabuk University**
**Institute of Graduate Programs**
**Department of**
**Electrical-Electronics Engineering**
**Prepared as PhD Thesis**

**Thesis Advisor**
**Prof. Dr. Ziyodulla YUSUPOV**

**KARABUK**
**June 2022**

I certify that in my opinion the thesis submitted by Salem Faraj Alarabi ALJRIBI titled "OPTIMAL POWER FLOW FOR HYBRID AC-DC MICROGRID" is fully adequate in scope and in quality as a thesis for the degree of PhD.

Prof. Dr. Ziyodulla YUSUPOV .....
Thesis Advisor, Department of Electrical-Electronics Engineering

This thesis is accepted by the examining committee with a unanimous vote in the Department of Electrical-Electronics Engineering as a PhD thesis. June 27, 2022

| Examining Committee Members (Institutions) | Signature |
|---|---|
| Chairman : Assist. Prof. Dr. Huseyin ALTINKAYA (KBU) | ..... |
| Member : Assist. Prof. Dr. Zafer ALBAYRAK (SUBU) | ..... |
| Member : Prof. Dr. Ziyodulla YUSUPOV (KBU) | ..... |
| Member : Assist. Prof. Dr. Mümtaz MUTLUER (NEU) | …… |
| Member: Assist. Prof. Dr. Cevat RAHEBI (Istanbul Topkapı Univ.) | …… |

The degree of PhD by the thesis submitted is approved by the Administrative Board of the Institute of Graduate Programs, Karabuk University.

Prof. Dr. Hasan SOLMAZ .....
Director of the Institute of Graduate Programs

*“I declare that all the information within this thesis has been gathered and presented in accordance with academic regulations and ethical principles and I have according to the requirements of these regulations and principles cited all those which do not originate in this work as well.”*

Salem Faraj Alarabi ALJRIBI

## ABSTRACT

**Ph.D. Thesis**

**OPTIMAL POWER FOLW FOR HYBRID AC-DC MICROGRID**

**Salem Faraj Alarabi ALJRIBI**

**Karabük University**
**Institute of Graduate Programs**
**The Department of Electrical-Electronics Engineering**

**Thesis Advisor:**
**Prof. Dr. Ziyodulla YUSUPOV**
**June 2022, 114 pages**

Over the past two decades, the use of new energy sources has also received significant attention due to the trend of public acceptance of clean energy as well as privatization in the electricity industry and the issue of power systems restructuring. The use of new energy sources, depending on the type of energy source, cannot be done like conventional power plants. Therefore, it causes production to be scattered across the network. These issues have led to dispersed production as a suitable choice for production and responding to increasing consumer demand. In this thesis, grey wolf optimization is used to optimize the microgrid system for effective dispatching of power to load with economic manner. In this thesis, hybrid microgrid system consisting of diesel engines (DE), photovoltaic (PV) panels and battery unit is developed and investigated on MATLAB/Simulink platform. In this model, the variation of renewable energy power price of spinning reserve and electricity price from grid purchase have been considered. The grey wolf optimization method is used

to optimize the microgrid system for effective dispatching of power to load with economic manner. The vital objective of the proposed grey wolf algorithm is to minimize the overall cost of the microgrid operation. Six scenarios are analyzed in the microgrid with considering island and grid-connected modes. Each scheduling scheme power flow and cost factor are analyzed in depth by MATLAB/Simulink program. Priority is provided to either for main grid or distributed generation in the grid-connected mode for power sharing between microgrid and main grid. The PV panel, diesel generator and battery are mostly operated to supply the power to load instead of the grid during island mode.

**Key Words :** Microgrid, Renewable energy sources, Grey Wolf Optimization, Economic load dispatch, Storage, Reserve.

**Science Code :** 90502

# ÖZET

**Doktora Tezi**

**HİBRİT AC-DC MİKRO ŞEBEKE İÇİN OPTİMAL GÜÇ AKIŞI**

**Salem Faraj Alarabi ALJRIBI**

**Karabük Üniversitesi**
**Lisansüstü Eğitim Enstitüsü**
**Elektrik-Elektronik Mühendisliği Anabilim Dalı**

**Tez Danışmanı:**
**Prof. Dr. Ziyodulla YUSUPOV**
**Haziran 2022, 114 sayfa**

Son yirmi yılda, temiz enerjinin kamu tarafından kabul edilmesi eğiliminin yanı sıra elektrik endüstrisindeki özelleştirme ve güç sistemlerinin yeniden yapılandırılması sorunu nedeniyle yeni enerji kaynaklarının kullanımı da önemli ölçüde ilgi görmüştür. Enerji kaynağının türüne bağlı olarak yeni enerji kaynaklarının kullanımı konvansiyonel santraller gibi yapılamamaktadır. Bu nedenle, üretimin ağ boyunca dağılmasına neden olur. Bu sorunlar, üretim için uygun bir seçim olarak dağınık üretimi ve artan tüketici talebine cevap vermesini sağlamıştır. Bu tezde, gücün ekonomik bir şekilde yüke etkin bir şekilde dağıtılması için mikro şebeke sistemini optimize etmek için gri kurt optimizasyonu kullanılmıştır. Bu tezde, MATLAB/Simulink platformu üzerinde dizel motorlar (DE), fotovoltaik (FV) paneller ve pil ünitesinden oluşan hibrit mikro şebeke sistemi geliştirilmiş ve incelenmiştir. Bu modelde, eğirme rezervinin yenilenebilir enerji güç fiyatı ile şebeke alımından elektrik fiyatının değişimi dikkate alınmıştır. Gri kurt optimizasyon yöntemi, gücün ekonomik bir şekilde yüke etkin bir şekilde dağıtılması için mikro şebeke sistemini optimize etmek için kullanılır. Önerilen gri kurt algoritmasının hayati amacı, mikro şebeke

operasyonunun toplam maliyetini en aza indirmektir. Ada ve şebeke bağlantılı modlar dikkate alınarak mikro şebekede altı senaryo analiz edilmiştir. Her bir çizelgeleme şeması güç akışı ve maliyet faktörü, MATLAB/Simulink programı ile derinlemesine analiz edilir. Mikro şebeke ve ana şebeke arasındaki güç paylaşımı için şebekeye bağlı modda ana şebekeye veya dağıtılmış üretime öncelik verilir. PV paneli, dizel jeneratör ve akü, ada modunda şebeke yerine yüke güç sağlamak için çoğunlukla çalıştırılır..

**Anahtar Kelimeler :** Mikro şebeke, Yenilenebilir enerji kaynakları, Gri kurt optimizasyonu, Ekonomik yük dağıtımı, Depolama, Rezerv.

**Bilim Kodu :** 90502

**ACKNOWLEDGMENT**

First of all, I would like to thank Allah for helping me with this work.

I thank to my supervisor Prof. Dr. Ziyodulla YUSUPOV, and my monitoring committee members Assistance Prof. Dr. Zafer ALBAYRAK and Assistance Prof. Huseyin ALTINKAYA, for their professional supervision, notes and many beneficial propositions during my research work.

I would like to give thanks to my parents, wife, children and brothers for their prayer, encouragement and support at all times.

## CONTENTS

**Page**

**Page**

**Page**

**Page**

## LIST OF FIGURES

**Page**

**Page**

## LIST OF TABLES

**Page**

## SYMBOLS AND ABBREVITIONS INDEX

### SYMBOLS

$\alpha$ : Alpha

$\beta$ : Beta

$\delta$ : Delta

ω : Omega

### ABBREVITIONS

MILP : Mixed Integer Linear Programming

GAMS : General Algebraic Modeling System

MG : Microgrid

PV : Photovoltaic

AC : Alternating Current

DC : Direct Current

ABC : Artificial Bee Colony Algorithm

DE : Diesel Generator

WT : Wind Turbine

FC : Fuel Cell

DERs : Distributed Energy Resources

RES : Renewable Energy Sources

DOE : Department of Energy

CRS : Congressional Research Service

LV : Low-voltage

DG : Distributed Generation

IGBTs : Insulated-gate Bipolar Transistors

QV : Reactive power – voltage

PQ : Active – reactive Power

PCC : Point of Common Coupling

| | |
|---|---|
| STS | : Static Transfer Switch |
| QoP | : Quality of Power |
| CERTS | : Consortium for Electric Reliability Technology Solutions |
| EMS | : Energy Management System |
| PI | : Proportional and Integral |
| PID | : Proportional Integral Derivative |
| KBU | : Karabuk University |
| OPF | : Optimal Power Flow |
| GA | : Genetic Algorithm |
| PSO | : Particle Swarm Optimization |
| DQLF | : Decoupled Quadratic Load Flow |
| SPEA | : Strength Pareto Evolutionary Algorithm |
| FACTS | : Flexible Alternating Current Transmission System |
| MAS | : Multi-agent System |
| GWO | : Grey Wolf Optimizer |
| EES | : Energy Storage System |

# PART 1

## INTRODUCTION

Due to the high costs of fuel and environmental damage, as well as the increasing demand for energy, the world has tended to change the ways of generating energy in other ways that are suitable for the environment and with sustainable resources. These methods have led to a reduction in the harmful environmental emissions resulting from burning fossil fuels.

These problems have led to a new concept of Smart Grid. a smart grid (SG) is an electricity network that meets future requirements for energy-efficient and economical operation of the power system through the coordinated management and using modern two-way communications between the elements of electrical networks, power plants, accumulating devices and consumers. Microgrid (MG) is a basic element of SG and as a key component of the smart grid are intended to improve energy efficiency, the reliability of power system and decrease carbon dioxide emissions. The term microgrid refers to the concept of single electrical power subsystems associated with a small number of distributed energy resources (DERs), both renewable and/or conventional sources, including photovoltaic, wind power, hydro, internal combustion engine, gas turbine, and microturbine together with a cluster of loads [1]. Last decades with rapidly penetration of DER to the power system, the interest on MG is growing.

Existing power systems are expected to transition from passive power systems to more active power systems resulting in difficulties in stability and energy flow management issues within the grid [2-5].

Moreover, for the successful operation of small networks, the integration of DERs has become an important aspect of other technical and operational difficulties encountered [6-9].

Centralized control of several distributed energy resources at distribution voltage levels can be problematic, as they are not feasible to implement economically, which requires other alternative strategies to the management of emerging DERs. A variety of distributed/decentralized approaches have been suggested to improve manage operations of the power system with the merging of a number of DERs at distribution networks for medium/low voltage levels [10,11].

In this work, the microgrid is planned, designed and modeled for Engineering faculty building at Karabuk university (KBU) campus. Mathematical simulation of the MG with complex economic power dispatch problem is developed in MATALB/Simulink.

### 1.1. PROBLEM STATEMENT AND MOTIVATION OF THE RESEARCH

The high demand for energy and high fuel prices, in addition to the environmental pollution caused by fuel combustion, have led to the emergence of a new concept of the smart grid that relies on renewable energy sources in power generation because of its positive impact.

Conventional power systems generally allow energy to flow in one direction and only accommodate customer loads, but over the past few years, many reasons have prompted experts to highlight small grid schemes. These include reducing carbon dioxide and other gaseous emissions, energy efficiency and diversity in sources energy.

Distributed generation (DG) is focused on renewable energy resources and its economic load dispatch problems are getting more attention in the microgrid (MG) system. There are a lot of research papers on the cost-effective operation of MGs have been established because MGs are environmentally sustainable, versatile and provide better quality of power. Solar PV technology helps to generate power with lowest cost and also enhance the environment factor to the environment. PV energy volatility, however, creates numerous issues, for example, economic losses from the hybrid power grid.

Dynamic and static load dispatches are group of economic dispatch for power systems. The dynamic load dispatch is favored to the steady approach these days since this approach not only minimizes costs although it assists to communicate among all DGs. However, owing to volatility, instability and unpredictability in renewable resources, the objective role of economic dispatch with a competitive approach is difficult to solve in MG.

Most of papers have considered the economic dispatch of MGs in an island operation mode, and there are no works related to dynamic economic dispatch in two operation modes of MG – grid-connected mode and island mode including energy reserve. Also, abovementioned issue has not studied as case study for university campuses which differ from industrial, residential, and commercial objects.

## 1.2. AIM AND OBJECTIVE OF THESIS

The purpose of this study is to design and develop grey wolf optimization technic-based control of Karabuk university microgrid. The following objectives are implemented to achieve the purpose:

- Design and modeling of microgrid for the university campus in Karabuk conditions
- The dynamic economic power dispatch (EPD) optimization for both operating modes of microgrid, i.e. island and grid-connected modes using grey wolf optimization (GWO) technique
- Developing the microgrid based on multi-agent system control and optimization
- The comparison GWO and MAS-based results of KBU MG for EPD.

## 1.3.METHODOLOGY OF THE RESEARCH

In this dissertation, grey wolf optimization is used to optimize the microgrid system for effective dispatching of power to load with economic manner. The microgrid

system consisting of following components diesel engines (DE), photovoltaic (PV) and battery models and it is developed and investigated in the MATLAB/Simulink platform. The control and optimization of Microgrid based on multi-agent system (MAS) is implemented on the JADE-platform. Finally, microgrid optimization results on GWO and MAS GWO have compared. The methodology flow-chart of the research work is illustrated in Figure 1.1.

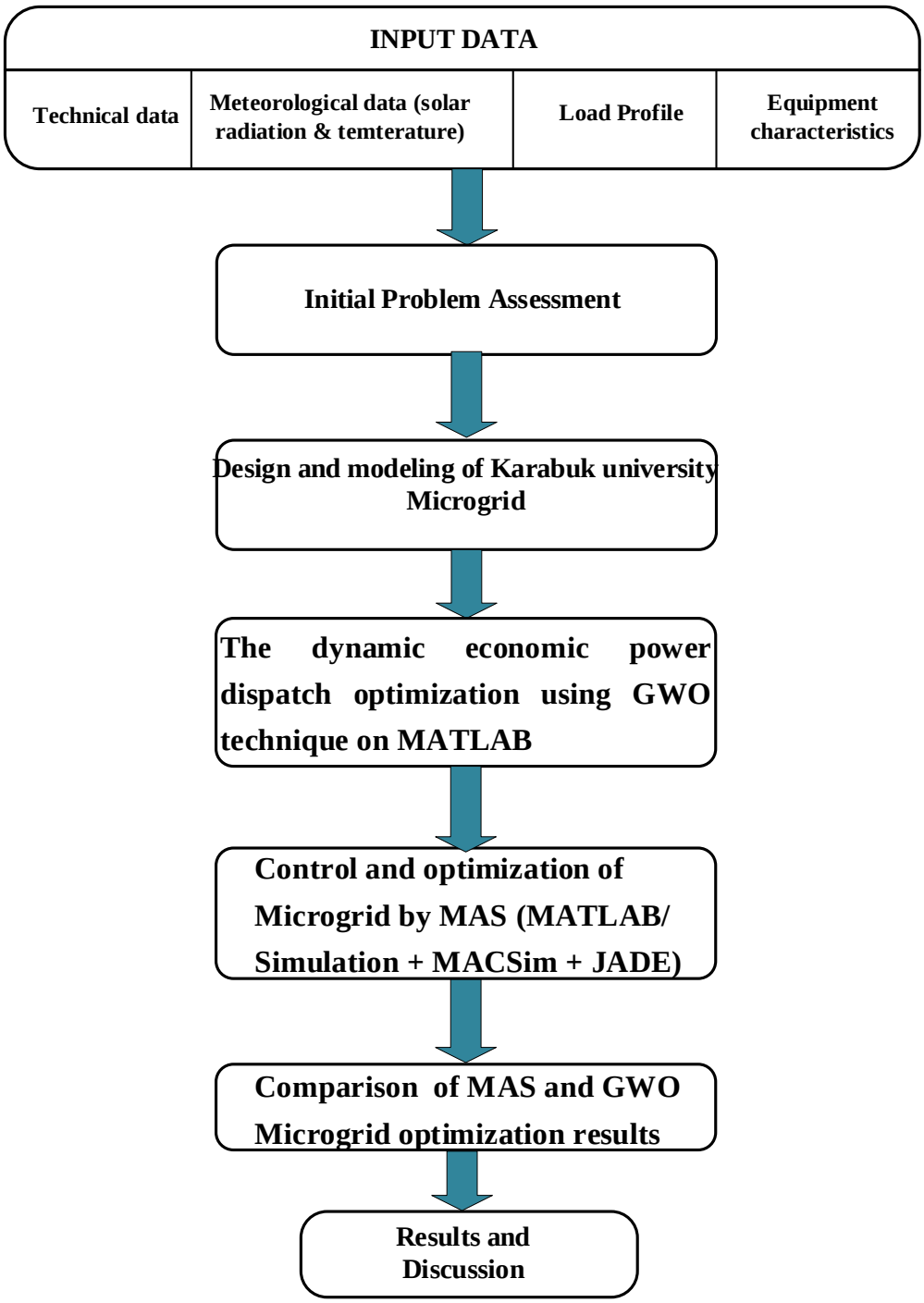


Figure 1.1. Methodology flow-chart of the research work.

## 1.4. LITERATURE REVIEW

The optimal design of grid-connected photovoltaic power systems is based on choosing the best components and sizes and adapting an appropriate operational strategy to provide efficient, cheap, clean, and reliable alternative energy. Several researchers have investigated the design and component sizes of grid-connected PV systems and their power quality. Their contributions are given below:

Through their technical and economical method, Ahmad et al. [12] optimized an MG-based system using a mixed-integer linear programming (MILP) model. They mentioned how programming benefits in terms of power generation through managing the volatility and intermittency of this form of power generation and distributed sources. They also attempted to reduce the load peaks through their approach. They solved the cost function using a general algebraic modeling system (GAMS) as a part of linear programming. They used software called HOMER for simulations to optimize the MG size.

A study by Das et al. [13] attempted to understand the effects of adding gas turbines and internal combustion engines to a hybrid MG equipped with PVs. They optimized the system using a multi-objective genetic algorithm to make it efficient in terms of the overall efficiency and the energy costs. For this purpose, they used a thermo-electric strategy to track the load. Their proposed system fulfilled all electricity demands and provided cooling and heating simultaneously.

In a linear programming algorithm by Delgado and Domínguez-Navarro [14], an MG energy management process was used for optimal generator operations, uncontrollable and controllable loads. They made efforts to meet the economic and operational constraints which emerged because of the energy sale/purchase for the components (storage systems, loads, and generators). They optimized the problem through the diesel generators' optimal dispatch.

Through their control strategy for hybrid systems to manage energy, Dufo-López et al. [15] presented a GA-based hybrid system. The proposed method used multiple

renewable resources (wind, hydro, and PV), electrolyzer, fuel cells, and AC generators. To minimize the operating costs, energy management is optimized that allows excessive renewable power generation to produce hydrogen or charge the batteries. The load, which the renewable sources cannot supply, can be obtained by either using fuel cells or discharging the battery.

Luna et al. [16] discussed a practically operational energy management system. They studied three cases considering imperfect, perfect, and exact predictions. Despite significant generation-load imbalances, they tested their optimization model on isolated and grid-connected systems.

Through their intelligent multi-objective management system for an MG, Chaouachi et al. [17] attempted to minimize power generation's environmental impact and operational costs. They developed an artificial neural network (ANN) for predicting PV-based and wind-based power generation in advance (24hr and 1hr). The multi-objective linear programming lies at the core of the mentioned system. Using a fuzzy logic-based expert system, battery scheduling can be obtained.
In a study on MG optimization based on the particle swarm algorithm, Li et al. [18] proposed an approach to operate a connected or isolated MG and consider the power fluctuations in an MG, with 24 hours advanced forecasts to handle fluctuations.

In their isolated MG energy management system, Marzband et al. [19] used an algorithm called the artificial bee colony (ABC) algorithm and a stochastic approach for economic analysis of the MG's generating units, given that all the renewable generation sources have an intermittent nature. According to the results, the costs decreased by 30%. Using Markov chains and neural networks, they managed load uncertainty and non-dispatchable generation quite effectively.

To optimize an interconnected MG, Kuitaba et al. [20] combined a meta-heuristic algorithm (Grey Wolf Optimization) in combination with a fuzzy logic-based expert system. This method minimized the generating costs and emission levels (fossil fuel sources). It reduced the MG costs and consumption of fossil fuels by optimizing the battery capacity.

A new technique presented by Ogunjuyigbe et al. [21] is based on a genetic algorithm, and it is effective for optimal renewable generation and battery usage in a stand-alone MG. The author demonstrated that the proposed multi-purpose technique reduces operational and life cycle costs. This extracts data from a load profile for MG optimization and allows wind and solar variations.

Another algorithm was presented by Wu et al. [22]. They based their algorithm on dynamic programming to control and manage a stand-alone MG. It is a deep-learning algorithm with practical applications, allowing scheduling for a control strategy to optimize an MG. It transmits information throughout the centralized management framework through local controllers.

In his energy management system, Zhuo [23] used dynamic programming for MG management using renewable generation batteries and sources. He aimed to maximize renewable energy sales and cost minimization to fulfill the power demands. For this purpose, the researcher selected an unregulated energy market with fluctuating power prices and used dynamic programming to determine the battery control actions.

In a study on managing energy on two grid-connected MGs, Raju et al. [24] used two MGs with local loads, and their system had two PVs and wind generators. For generation cost minimization from the solar resource and keeping in view the load randomness, they selected a multi-agent management system. That system was based on a differential evolution algorithm (JADE). The mentioned system has addressed the grid's price variation, considered the critical loads, and selected the best option.

Another research [25] was conducted on decentralized energy management using MG multi-agents with fuzzy logic and cognitive maps. The author termed batteries, distributed generators, electrolyzers, and fuel cells as intelligent agents. The author has compared decentralized and centralized approaches and discovered additional advantages of partial operation of the decentralized approach in specific situations like a system failure/malfunction.

Research by Lu et al. [26] shows a novel dynamic pricing mechanism to optimize the operational performance of grid-connected MGs. The author evaluated the uncertainty of integrating renewable energy into the grid. There are two levels of the mentioned optimization scheme: In the upper level, the pricing strategy guarantees a smooth energy operation, and the MG transactions were developed in the lower level.

In a study, Hu et al. [27] used another optimization process to operate an interconnected grid in a two-stage operational procedure: First, they used a common generator and then initiated the economic dispatch of the distributed and conventional generation. The mentioned combination helps manage the uncertainty, which has been observed in renewable power generation, for which the researcher used the Lyapunov method.

In their research work, Zachar and Daoutidis [28] presented a hierarchic control system for load regulation, supervision, and dispatch-able MG energy. They used Stochastic optimization on a small scale to avoid errors in the renewable energy generation forecasts. They also applied time-saving Deterministic optimization for updating optimal dispatch conditions.

A study conducted by Wu et al. [29] shows an optimization approach to operating a hybrid system with the help of battery storage and solar energy. They used battery storage because it stores significant power to supply to the customers during peak and off-peak periods. Thus, the researcher proved that scheduling a hybrid system minimizes the power consumption from the grid and, at the same time, reduces a customer's power cost.

Another optimization scheme was proposed by Astaneh et al. [30] in research to explore a stand-alone MG's most economical configuration when equipped with a lithium battery. They considered different power management strategies and estimated the lithium batteries' lifetimes and performances by applying an electrochemical model.

Yadav et al. [31] considered MG economic dispatch for an MG system, including a wind turbine (WT), some diesel engines (DE), a battery, and a fuel cell (FC). In this paper, a model for MG was developed and analyzed, keeping in view the effects of emissions, reserve power, renewable power fluctuations, and price variation for the grid. They used GAMS software to minimize operational and pollution-treatment costs.

A research paper by Han et al. [32] evaluates economic dispatches of the complex MG systems. The considered system had the following operating possibilities: Grid-connected and islanded modes. They also considered abrupt changes in the renewable source due to changes in the environmental conditions.

Grey wolf optimizer – a meta-heuristic algorithm firstly has been mentioned by Mirjalili et al. in 2014 [33]. The authors developed swarm intelligence-based algorithm which inspired by wolves to search the optimal way for hunting their preys in nature. This algorithm is not only novel, also it is easy-to-understand and feasible-to-implement algorithm because it is nature and animal-inspired.

Comprehensive simulation studies have conducted, and it was determined that GWO proved more effective compared to other optimization algorithms (DE, backtracking search algorithm, and BAT algorithm) for set-point, trajectory, and step tracking. Moreover, GWO has shown another capability, and that is, it supports other optimization and AI methods because of fewer random and user-preferred parameters [33-36]. It should be noted, the comparison of GWO with another computational intelligence methods, for example, with Gravitational Search Algorithm (GSA), differential evolution (DE), PSO, evolution strategy, and evolutionary programming through 29 test functions, show the following rewards of GWO [33,34]:

- Adaptable, easy, and plain to apply for most processes in the environment.
- Easy-to-understand and feasible-to-implement algorithm because it is nature and animal-inspired.

- The mathematical model of GWO is novel that gives to relocate a solution around another in an n-dimensional search space to simulate chasing and encircling preys by wolves.
- GWO divides a dataset into four groups, assuming that different amounts of data (wolf population) exist in each part and applies the wolf-pack problem-solving method to address real-world issues. Specifically, when the performance analysis of different optimization methods is required
- GWO technique can solve several problems with single objective.

Summarizing literature survey and to justify the novelty of this work it could be concluded:

- GWO is novel algorithm which adaptable, easy, and plain to apply for most processes in the environment including power systems.
- It is adaptive and applicable to model of n-dimensional objects using GWO and can solve several problems with single objective.
- There are still insufficient and insignificant number of research works that compared different artificial intelligence methods and attempted to determine the optimum of the components' configuration and sizes of hybrid MG system.
- There are few works for solution economic loads dispatch optimization problems in MGs using GWO algorithm.

## PART 2

## MICROGRID STRUCTURE AND CONTROL

In the recent times, several organizations have presented different definitions of microgrid; some of them are as follows:

A microgrid joins Energy Storage Systems (ESS), Renewable Energy Sources (RES), and Distributed Energy Resources (DERs) with elastic loads operating locally with a capacity to work in parallel as a single entity either in an intentional island mode or with the grid for providing customized levels of reliability while maintaining resilience to grid disturbances [34].

According to the U. S. Department of Energy (DOE) A microgrid integrates local elastic loads with distributed energy resources (DERs) that operate in parallel in an intentional island mode or with the grid to provide customized levels of reliability while managing grid disturbances. It is an integrated and advanced system that meets the customers' needs in remote locations assuring economically sensitive development and protection of critical loads [35].

With a slight difference, Congressional Research Service (CRS) defines a microgrid as [36]: “An MG is a local power system that operates independently of the bulk power networks”. It may combine a dual power generation and heating system when a gas combustion engine is attached to it (to cogenerate hot water or renewable energy) with the help of fuel cells or diesel generators. A microgrid serves the power requirements of colleges, factories, data centers, military installations, and hospitals.

Another definition has been mentioned in the EU research projects [37,38]: “A microgrid comprises LV distribution systems with storage devices (batteries, flywheels, and capacitors), flexible loads, and DERs (micro-turbines, PVs, and fuel

cells)". It is possible to operate such systems in a non-autonomous way when it is grid-connected and operates autonomously when it is disconnected. The micro sources' operations have several performance-related benefits if efficiently coordinated and managed. The mentioned definitions clearly indicate that the following are the features of a microgrid:

- A microgrid operates in disconnected or grid-connected modes.
- A microgrid integrates micro-sources, controllable loads, and storage units in a local grid.
- A microgrid demonstrates energy coordination and management between the available micro-sources.

The presented definitions show a common microgrid characteristic controlled as a single entity that operates through energy storage elements, co-located power generation sources, and end-user loads. On the other hand, a main discrepancy in the mentioned definitions is the generation units' total rating within a microgrid and whether it's grid-connected at a single point or multiple points. Microgrids can be operated by solving the technical challenges linked with their practical implementation. Moreover, solving the problems facilitates the transition from conventional grids to smart and more efficient grids.

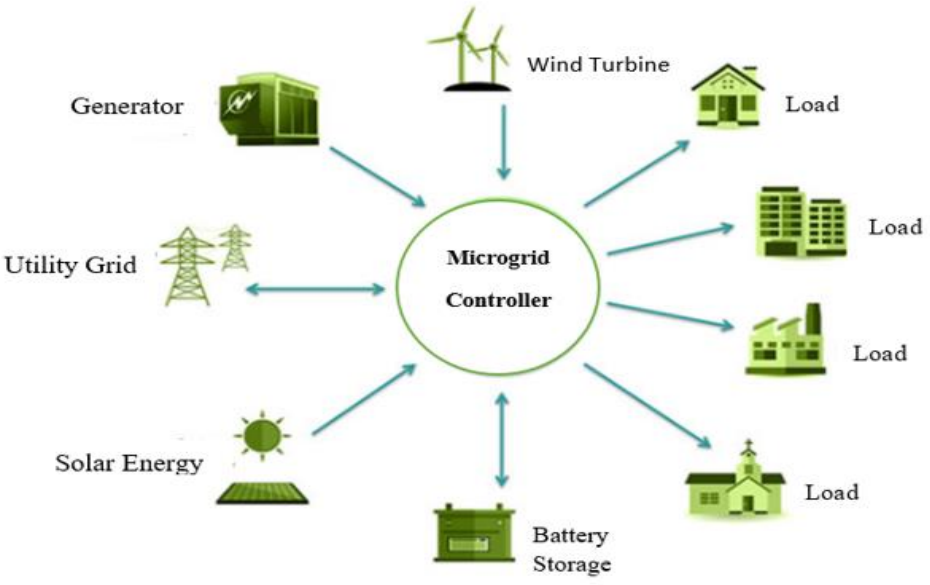


Figure 2.1. Typical Microgrid structure.

## 2.1. MICROGRID COMPONENTS

Microgrids, in general, consist of the following components:

- DG sources include small wind turbines, PV panels, diesel/gas microturbines, and fuel cells.
- Energy storage devices include supercapacitors, flywheels, and batteries.
- Power electronics devices (inverters, converters).
- Critical and non-critical loads.
- Common coupling point
- Static switch

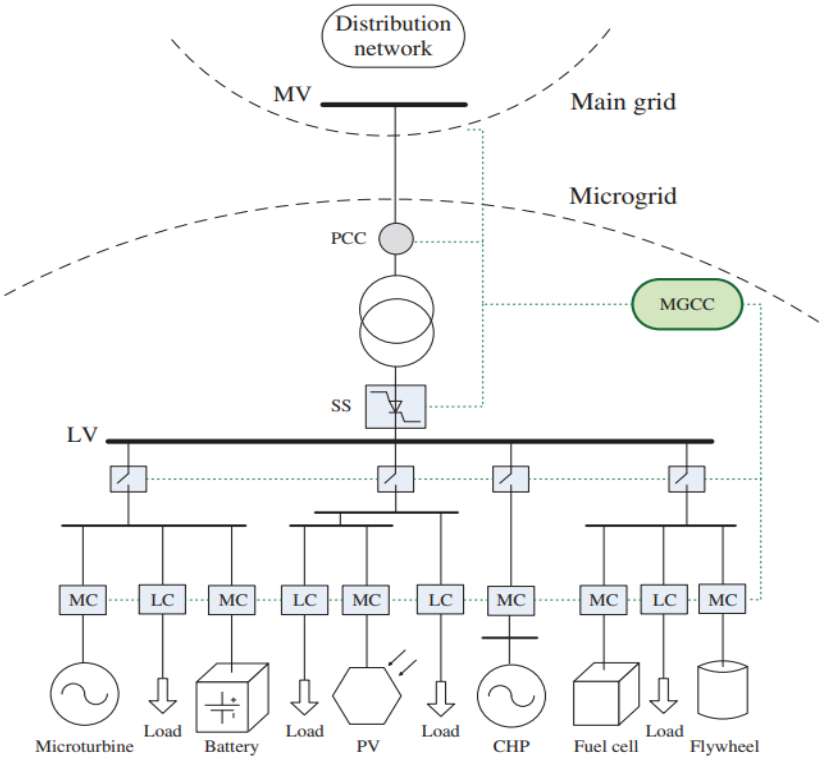


Figure 2.2. Microgrid components.

### 2.1.1. Distributed Generation (DG) Sources

Distributed generation sources are variety of technology that often generated close to the consumer, which reduces power loss. There is range of power generation sources

such as wind turbines which depend on the speed of the wind flow as they must be installed in place where the wind is adequately available to generate power.

Solar panels, which also depend in their work on sunlight, as these panels convert sunlight into electrical energy. There are also other sources of power generation sources such as fuel cell, diesel and gas microturbines etc.

Recently, power generation systems have become more and more popular for conventional central power generation near the load (consumer), and generation helps support clean energy delivery and reduce electricity losses along transmission and distribution lines [39].

### 2.1.2. Distributed Energy Storage Devices

Energy storage systems store excess energy and use it when needed. Batteries can provide power when electrical loads require more power than the distributed generation sources generate at a particular time. To compensate for the power loss in the generation process resulting from climatic effects, solar panels' efficiency decreases in cloudy conditions and at night because there is no sunlight to convert into electricity. Likewise, for wind energy, when there is not enough wind to rotate the wings of wind fans associated with generators to convert the wind's mechanical energy into electrical energy. And the simplest way to store electricity is to use rechargeable electric batteries when distributed generators produce the current required to charge the battery. Many storage devices are added to a microgrid, such as flywheels, batteries, and supercapacitors [40].

### 2.1.3. Inverter

The primary purpose of using an inverter is DC-AC power conversion that adjusts the output AC power frequency and controls the effective output voltage value. The significant characteristics of a PV inverter are its reliability and efficiency.

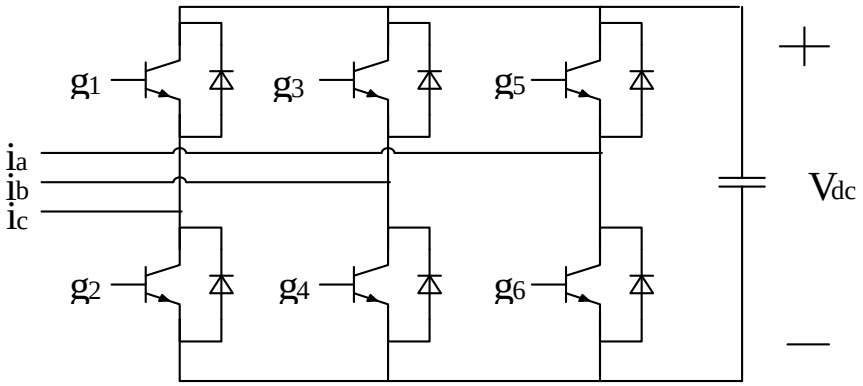


Figure 2.3. Inverter circuit.

The inverter circuit, shown in Figure 2.3, includes six insulated-gate bipolar transistors (IGBTs). It is evident that transistors $g_1$ and $g_2$ are unable to work simultaneously, and transistors $g_3$, $g_4$, $g_5$, and $g_6$ are the same. If we control the six gates, it controls two system variables: DC bus voltage and active/reactive power. It also uses a reactive power-voltage (QV) control for the following benefits:

- The system can get a stable DC bus voltage, so it will be easier to add DC load to a DC microsystem without any DC-DC converter to reduce the cost and be more convenient to expand the system.
- Increase the reliability of the DC microgrid: When there is a critical load in the DC microgrid, it uses a QV control strategy to control the inverter. While the load varies in a short span of time, the grid uses the QV control, which is likely to get more power from the large grid much faster compared to the grid using the PQ control strategy. Since the grid uses active–reactive power, the (PQ) control strategy should measure the power changes in the microgrid.

The inverters are manufactured to work at approximately the maximum power point of the PV system. Generally, inverter efficiencies vary from 90% to 96% at full load. When finalizing a size for the inverters used in grid-connected PV systems, the efficiency and ability to withstand an overload situation must be considered.

### 2.1.4. Converter

In most MGs, a bidirectional converter connects the battery and the grid. The battery output voltage usually is less than the DC bus voltage; therefore, a DC bus is linked to the battery using a boost converter. A buck converter is also used for a battery-DC bus connection. The diagram of the bidirectional converter is illustrated in Figure 2.4.

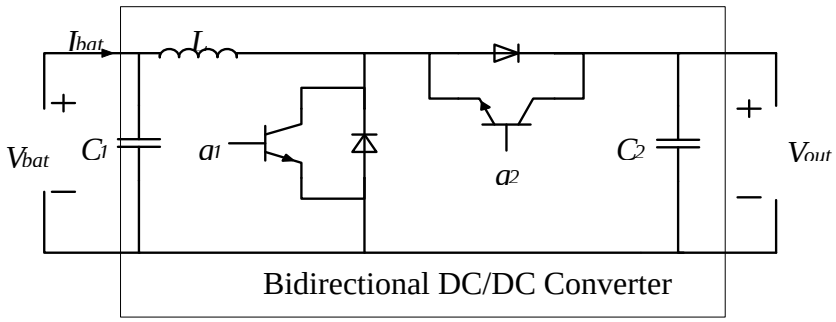


Figure 2.4. Schematic diagram of a bidirectional converter.

In case of gate $S_2$ has 0 signal while the signal at gate $S_1$ is 1; so, the bi-directional converter will be in a boost mode, in which power transmits to a DC bus while battery operation will take place in the discharge mode. If the signal at gate $S_2$ is 1, but gate $S_1$ has 0 signal, the bi-directional converter operation will be in buck mode, through which power transmission takes place to the battery. The battery is likely to operate in a charged mode.

### 2.1.5. Critical and Non-critical Loads

Microgrids serve thermal and/or electrical loads, despite that the discussion will be only about electrical loads in this section. Either electrical loads are critical or non-critical. In critical loads, the power should be reliable and high-quality, so it must remain uninterrupted. Non-critical loads, on the other hand, are sometimes disconnected for specific time periods for microgrid maintenance. A microgrid's load management behavior mainly depends on its operational mode, system requirements, market incentives, and strategies, such as operating an MG in an islanded or grid-connected mode.

When an MG is grid-connected, the system compensates for the power discrepancies between the generated and demanded power, maintaining a net power balance. It is also possible to mitigate any difference through load/generation shedding, specifically when operational or contractual obligations impose strict limits on the power export or import. Load shedding maintains the power balance and stabilizes the MG voltage. It also means that critical loads receive service priority when a convenient operational strategy is implemented. It is also possible to execute the load controls because they decrease peak loads and optimize dispatchable DG and ESS units' performances through smoothening out load profiles [41].

### 2.1.6. Point of Common Coupling (PCC)

It is a connecting point that connects MG to the main grid. MG is usually used in remote places where a public network is unavailable. The PCC location is illustrated in Figure 2.5 [42].

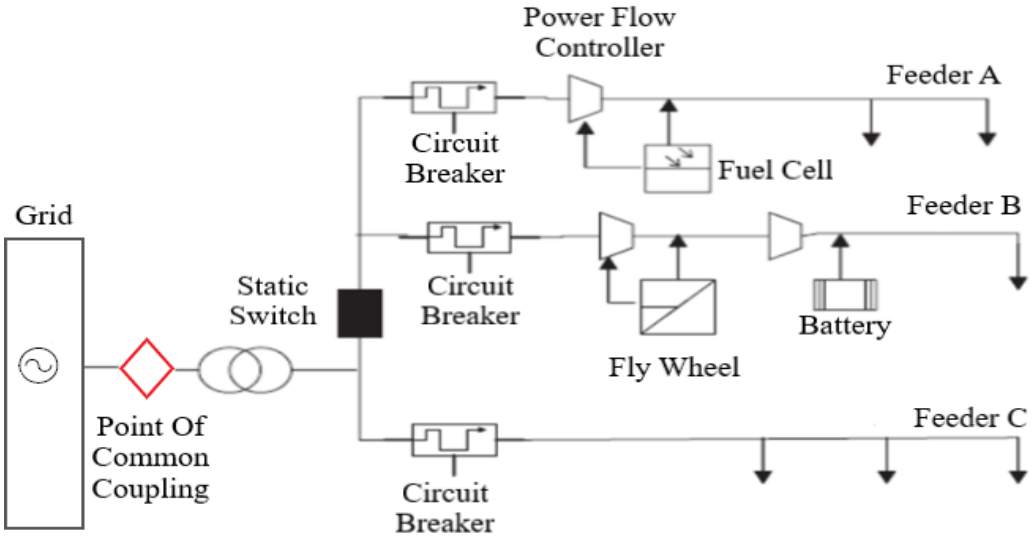


Figure 2.5. Location of Point common coupling (PCC) [42].

### 2.1.7. Static Switch

The static transfer switch (STS) is used to transfer, automatically or manually, one or more three-phase loads from one power source to another and back without interruption. If the source supplying the loads fails, transfer to the other source will be automatic. Figure 2.6 shows the STS structure.

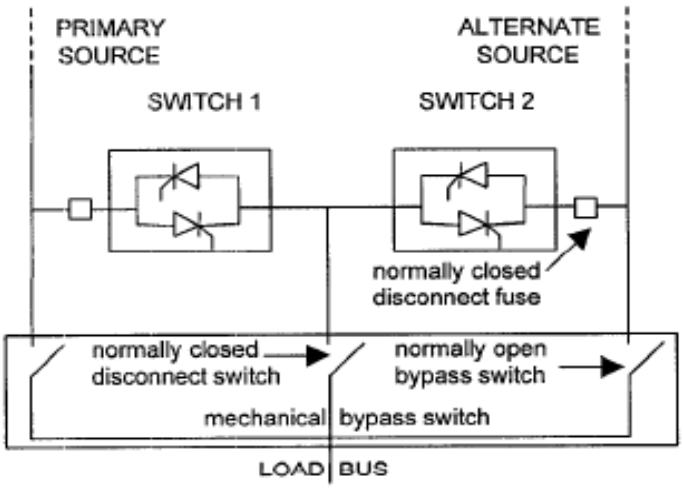


Figure 2.6. Static switch structure [43].

STS provides an effective solution to the following issues:

- STS completely separates two sources of the associated distribution systems
- Source redundancy issue with no-break load transfer in existing installations;
- Load separation to avoid mutual disturbances.

STS thus improves the availability of energy while facilitating operation and maintenance in installations supplying sensitive loads.

For microgrid reconnection to the main grid, STS should provide synchronization, as Figure 2.7 shows.

To synchronize a grid section with the power system, a static switch should be used to conduct phase estimation. A static switch has the following three tasks:

1- Microgrid-main grid synchronization
2- Reverse power detection
3- Short circuit detection

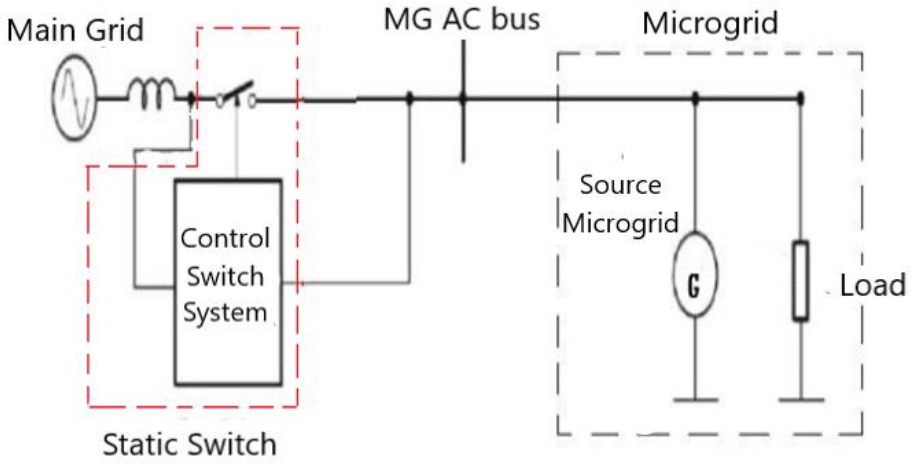


Figure 2.7. Microgrid-main grid connection using a static switch.

## 2.2. MICROGRID OPERATION MODE

A microgrid can autonomously operate, and it can also be grid-connected, where, in case of any fault, an MG can disconnect itself and operate independently. Hence, it only supplies the local load [43]. Thus, a microgrid's operational modes are islanded, grid-connected, and transitory [44].

When a microgrid functions parallel to the grid, the grid controls the frequency and voltage, but that depends on the grid's load. When a fault/disturbance occurs in the main grid, the microgrid disconnects and autonomously operates. This capability of a microgrid improves the power quality when it is supplied to its local customers because it provides voltage control on the local level.

While operating autonomously, a microgrid controls the frequency and voltage because it continuously adjusts the active/reactive powers and the output. It is a normal operational mode for a microgrid, through which it provides the load required in a geographically close location. For example, the local load may be the power requirement of a university, a small village, a commercial building, or an industry. A microgrid should address some main issues in the autonomous mode, such as Quality of Power (QoP), frequency and voltage management, communication among its components, and load-supply balance.

## 2.3. MICROGRID TYPES

Microgrids are classified as AC systems, DC systems, or hybrid systems based on the power drawn from them. These typical microgrids are identical to a small power system consisting of interconnected components like DG units, loads, and storage devices. Although controlling a large number of DGs is challenging considering the safety and efficiency of the system, modern technology plays a crucial role in overcoming these problems by using power electronic devices which interfere with DGs to create the architecture of a microgrid. Microgrids are connected to a power distribution network using the common coupling point, and it appears as a single unit.

### 2.3.1. DC Microgrid

A DC microgrid connects to the grid through an AC/DC converter if it has excessive generated power and the power interface is bi-directional. A DC microgrid is equipped with a DC bus, and voltage is regulated, so most DGs require an AC/DC or DC/DC bus-connected power electronic interface. Generally, DC/AC converters are needed for bus voltage adjustment in cases of AC loads. Sometimes, DC loads are directly DC bus-connected, and depending on the bus voltage; they possibly require a DC/DC converter. For fast and stable load steps, the bus is linked to a few capacitors without any electronic interface. An AC/DC converter regulates the DC bus voltage, and the DC bus voltage quality is excellent even when distribution grids have low quality. In case of distribution grid failures, a microgrid has to regulate its DC bus voltage with no support from the main AD/DC converter [45].

In terms of cost, system efficiency, and system size, DC microgrids have advantages over AC microgrids. It means that fewer power electronic converters are needed, improving the overall efficiency. Moreover, AC/DC converters generally do not need any transformer that significantly reduces the DC microgrid size. Like an AC microgrid, a DC microgrid needs an energy management system, but only voltage stabilization is needed in this case. A DC microgrid does not require support for

frequency stabilization, which is quite unlike an AC microgrid [46]. Figure 2.8 shows a DC MG architecture.

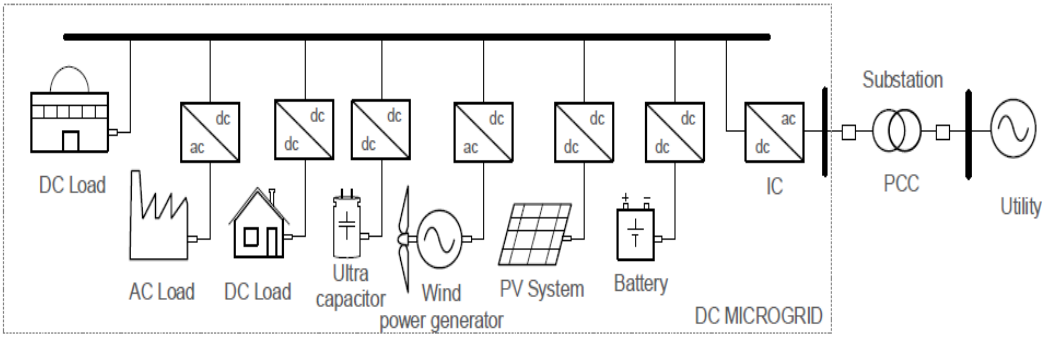


Figure 2.8. The basic structure of the DC microgrid.

### 2.3.2. AC Microgrid

Although the AC distribution is inspired by the traditional power systems, it is a very popular and common structure in microgrid studies and applications. AC infrastructure includes transformers, protections, and distribution. Generally, AC microgrids are feasible-to-use and easier to design because they are built based on reliable and proven technologies. An organization, Consortium for Electric Reliability Technology Solutions (CERTS), developed its first MG in 1998. It was only a cluster of storage devices and micro-generators back then, but it could seamlessly isolate itself from the grid without any load interruption [47]. Figure 2.9 shows an AC MG concept based on the CERTS microgrid.

This microgrid can adjust its generation to any possible operating condition by simply circuit breakers or changing its topology. A static switch manages the MG's grid connection. It disconnects a microgrid from the main grid in case of low-quality electrical distribution in the grid, so it performs in the islanded operational mode. It helps maintain excellent power reliability and quality against the DG-fed critical loads and the ESS devices' power storage. Whenever any grid issue emerges, the mentioned static switch opens up. The third bus has a circuit breaker that disconnects the non-critical loads to protect against a malfunction or damage [39].

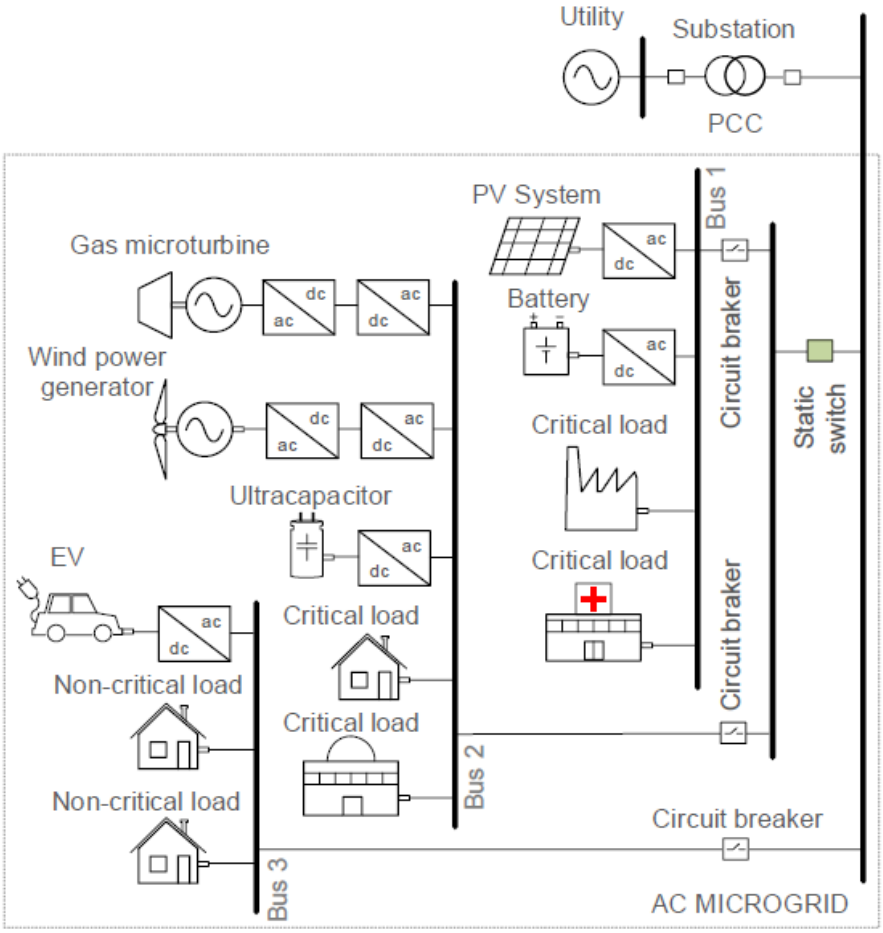


Figure 2.9. AC microgrid architecture [39].

### 2.3.3. Hybrid AC/DC Microgrid

This type of MG combines the AC and DC architectural advantages. Compared to other architectures, hybrid AC-DC microgrids are gaining interest because they integrate the two networks in the same grid and integrate AC- and DC-based loads and DERs.

Figure 2.10 shows a typical hybrid microgrid structure, and it is easy to distinguish between the AC and DC grids linked with an AC-DC bidirectional converter [48]. The DC bus is linked to the DC loads, and the AC bus is linked to the AC with a power converter to adapt to the needed voltage level. The ESS and DG units are linked to DC/AC buses, which minimizes the steps required for conversion. An AC bus functions with the existing equipment; however, a DC bus allows the usage of a few

simple converters. In addition, the mentioned architecture also permits the sensible loads' installation to a DC feeder, while to install more robust loads, an AC feeder is required [37].

In the case of integration problems, a hybrid AC-DC MG reduces the conversion stages and simplifies the electronic interfaces, ultimately reducing power losses, adding a DC device to a DC bus that assists in controlling the AC-side harmonic injections, which take place with the help of the main converter that guarantees the supply of high-quality AC power to the grid.

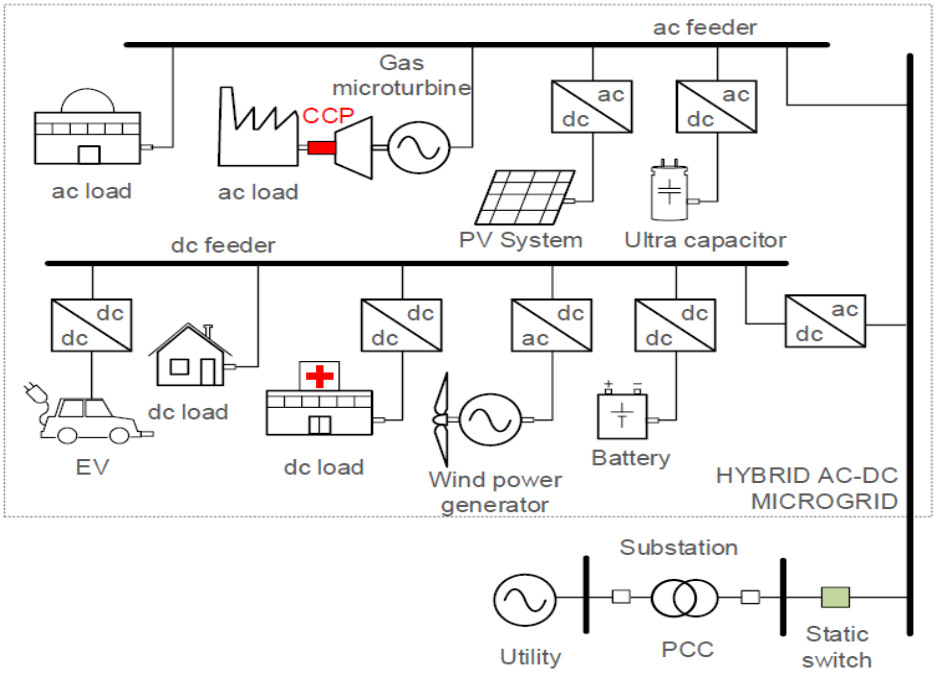


Figure 2.10. Hybrid AC/DC Microgrid [48].

## 2.4. MICROGRID CONTROL STRATEGIES

Most of the latest energy systems, such as MGs, are complex, so they need intelligent control systems, and the centralized or decentralized controls cannot control the entire system. Thus, MG control systems are mostly hierarchical control schemes, widely accepted as a standard MG management solution [48-50]. Most literature sources recommend hierarchical controls, which mainly have three levels [51-55]. At each level, there are different controls corresponding to various control tasks' timescales,

depending on certain control functions performed at each level. Most primary control levels have timescales of milliseconds up to seconds for each control task.

In most cases, this is locally performed, so it needs no communication in several MG controls. Local controls have a very quick response time [56]. The secondary or medium-level regulates an MG's economical operation within seconds or minutes. Still, it is generally less than an hour, and it takes place through centralized control. The tertiary control level performs within a few minutes/hours but usually less than 24 hours [57], and this level mostly deals with MG-main grid coordination. Despite the fact that in stand-alone MGs, three hierarchical levels are standardized, so they always operate in islanded mode. Since there is no grid connection, the second hierarchical level is the highest. Table 2.1 summarizes the control functions along with issues and references. It must be kept in mind that different authors have differently mapped the hierarchical levels of control functions [58]. The EM and its relevant functions are juggled between secondary [59] and tertiary levels [60-62].

Table 2.1. Microgrid control functions by hierarchical levels [63].

| **Microgrid control function by hierarchical level** | | |
|---|---|---|
| **Hierarchical level** | **Timescales** | **Control function** |
| 1 | 2 | 3 |
| **Primary level** | Milliseconds to seconds | • Primary voltage and frequency control<br>• Active and reactive power sharing control<br>• Islanding detection |
| **Secondary level** | Seconds – Minutes – One hour | • Voltage and frequency steady-state deviation<br>• Power quality control<br>• EM system (real-time optimization)<br>• Grid connected – Island mode and transition control<br>• Demand side management (includes load shedding) |

Continue of Table 2.1

| 1 | 2 | 3 |
|---|---|---|
| **Tertiary level** | Minutes-hours-days | • Grid – MG bidirectional power flow control and coordination<br>• Multiple MGs (MG cluster) coordination<br>• Ancillary service |

### 2.4.1. Primary Control Level

An MG operates the fastest at the primary control level compared to the other three levels because it handles control power converters' output current and voltage, local DER output controls, independent active/reactive power-sharing controls, and islanding detection.

The inverter output control typically has an inner loop to regulate current and an outer loop to control voltage [50]. For these control loops, standard control methods are PI and PID controls [64]. A study [65] focused on islanded MGs and proposed a novel algorithm for frequency and voltage stabilization that is independent of line parameters, and that enables certain plug-and-play operations. In MGs, power-sharing is a popular method [66] but improving power-sharing accuracy is the main concern. Droop control is used in most power-sharing methods because it involves power balance when a classical synchronous generator provides the power and needs no communication link. For MGs, droop control is an artificially-crafted process to enable proportional controls of frequency, reactive power pairs, and active power and voltage. A benefit of the droop method is that it applies to just local measurements and requires no communication between local controllers. The major advantages of droop include instability issues, poor transient performance, no black start option, poor load behavior, and low power-sharing accuracy when line impedance inequalities occur. Another issue is load-dependent system frequency, which cannot be used for nonlinear loads, which led the researchers to investigate further for improving the standard droop control [67].

In droop control, droop coefficients are tuned and compensated for increasing power-sharing accuracy [59,68]. Generally, in the form of ESS, islanded MGs need more flexibility, which is important for control systems when voltage-based droop control is developed [69]. It is possible to apply droop control to hybrid AC-DC MGs that generalize the interlinking converter's autonomous control in a hybrid MG [70]. In addition, droop controls are also adapted to control islanded DC MGs [71]. The concept behind the droop approach is the master-slave concept, and in this case, the master unit injects frequency, and the slave units determine the output power based on droop characteristics and the frequency [72].

On a primary level, the control can be used for a frequency-based power management strategy to handle the MG loads and sources and active DC bus signals with multiple ESS [73,74]. During steady-state voltage fluctuations, decentralized power apportionment is another method that does not have bus frequency [58].

### 2.4.2. Secondary Control Level

In large power systems, load frequency control addresses the steady-state frequency drift, which occurs because of the droop characteristic [51] and is another part of the secondary control level. Other secondary controls include power quality control, voltage control, EMS-related tasks like optimization, load shedding, and working-mode transition control. Secondary controls help make the MG operations economical and reliable [49]. The mentioned secondary level moderates between the third and the primary levels and corrects the value mismatch between the tertiary level and the available MG power on the primary level [56]. According to multiple literature sources, secondary level functions are differentiable because most authors agree that the secondary frequency and voltage regulation should occur at this level. The difference exists in the EMS functions, and several authors believe that they should be performed at secondary or tertiary control levels. It is possible to perform all the EMS functions on the same level, but functions get divided between the two levels in some cases. In an already mentioned article, the authors presented no review on EMS may be because it is an enormous research area often reviewed by writing a separate article. Poor power-sharing/voltage regulation ratio is the main setback of the droop control

method. A substantial gain in droop means precise power-sharing, but it also implies poor voltage regulation; therefore, a secondary frequency/voltage control loop is essential. Fewer references are available on secondary control improvement by certain adaptations and not on adding a secondary controller to boost the performance. A few studies dealing with secondary level controls are available, which show their importance [75,76].

### 2.4.3. Tertiary Control Level

In the context of MG controls, tertiary control is the highest and the most controversial level of hierarchical control, which is evident from the literature. A main reason behind the controversy is researchers' lack of common stand on whether the tertiary controls are part of the MG control. Maybe that is why it is the least researched level. It is termed an MG component because most authors considered it part of MG control.

A major issue of this control is bidirectional power, which flows between the microgrid and the main grid [51]. Tertiary controls include a few MG clusters, their power exchange, cooperation, and communication [50]. In the energy markets, MG clusters and bidirectional power flows are considered important issues. They increased the interest of the researchers, and MG owners can gain significant incomes by operating their MGs. Active and reactive power exchanges are dealt with in the ancillary services markets whenever a need arises [50,52]. Excessive power production, which is significantly higher than the power demand at the MG level, is also a matter of tertiary control. It also affects the price at which MG owners are willing to trade the generated power in the energy market, for which they need to know the optimal long-term set-points for an MG that depend on the main grid requirements [56,61]. When grid-connected, MGs require both voltage and frequency regulation by the main grid [56]. In the MG cluster, reactive power management is needed [49] besides spinning and non-spinning reserves [52]. The mentioned issues should be considered when the MG's economic status is calculated before making it part of a power generation project. The listed tertiary control issues still have substantial room for research and further exploration, which is evident from an insufficient number of studies available on this topic.

## PART 3

## MODELING OF MICROGRID SYSTEM

In the present age, photovoltaic systems' modeling and simulation have made a great transition. Now, it has become an important part of power generation; however, PV system modeling is quite complex. The literature shows that so far, many researchers have proposed several computational methods [77] to model a stand-alone PV system's different component. Obviously, some methods are complicated, impractical, and need advanced computation, and, on the other hand, some of them are limited to simulating photovoltaic module characteristics. Some methods have been successfully simulated using MATLAB/Simulink, Labview, and PSpice [78,79].

Automatic data acquisition systems are currently used for system performance monitoring and operational control. To evaluate the plant efficiency, the obtained information can be used for long periods and optimize future system performance and reliability. The mentioned systems use microcontrollers and microprocessors for PV applications [80]. AI is now becoming a useful alternate to conventional processes and the integrated system's component. The mentioned methods can model PV arrays, predict the system's energy produced, and estimate the maximum power point tracker [81]. The research community has recently shown interest in using a bond graph to model and simulate the whole PV system [82]. To capture and model the physical systems' structures, a bond graph is an explicit graphical tool. Some studies further extended the bond graph as a concept to show the occurrences and phenomena. A bond graph is, in fact, a graphical modeling language that transforms a system into subsystems to demonstrate the physical connections and provides model formalism [83,84].

## 3.1. STUDIED SYSTEM CHARACTERISTICS

Karabuk University is a massive place that accommodates 53,000 students, academic staff, and professionals, which obviously consumes significant electricity. It faces issues such as the high maintenance cost of a complex power distribution system, increasing utility bills, and carbon emissions. The management of Karabuk University intends to decrease the overall power management costs by integrating a few solar PV panels into the campus grid. In five KBU buildings, PV panels are installed. The MG modeling, design, and planning have been conducted in the current work [85].

The central KBU campus is called Demir Celik, with a 3,500,000$m^2$ building area. The latitude of KBU is 41º 12' 22" N, while the longitude is 32° 39' 35" E. Figure 3.1 shows the Demir Celik campus of KBU. For studying a microgrid, we have selected the Engineering Faculty building of KBU.


Figure 3.1. Demir Celik campus and Engineering Faculty at KBU.

The KBU campus receives the electric power from the BAŞKENT EDAS A.Ş power supply substation. Figure 3.2 is a single-line diagram of the KBU Engineering faculty and the installed microgrid (MG). The mentioned KBU Engineering Faculty building is now our case study for examining the structure and functioning of a microgrid. The mentioned MG is a 0.4 kV LV 50 Hz network consisting of PV panels, two types of

loads: non-critical loads (non-controllable), a diesel generator, and critical (controllable) (Figure 3.2), and a battery storage system. Table 3.1 shows the KBU MG system components.

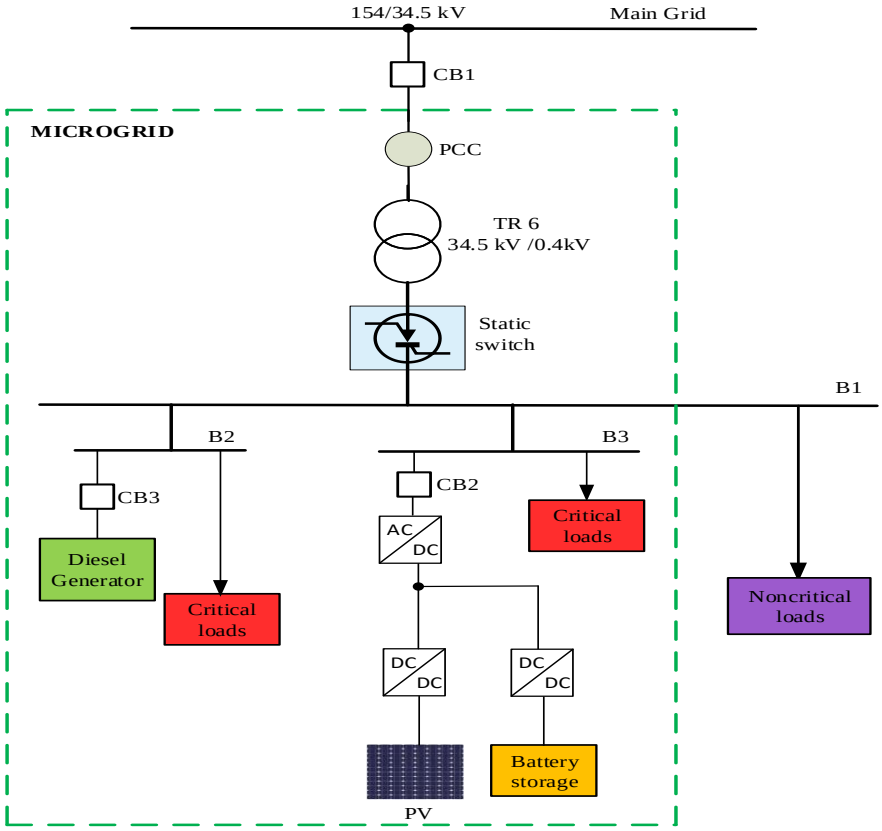


Figure 3.2. Single-line of microgrid diagram in KBU Engineering Faculty [85].

Figure 3.3 shows the overall grid-connected KBU MG structure and components. DG units are also located in the vicinity of electrical consumption to prevent electricity losses. The power supply against critical loads has been provided through a solar PV system's chemistry, hydraulics, and diesel generator. Usually, there is a distinct time granularity for these domains.

Table 3.1. Components of KBU MG system

| Component | Name | Size | Unit |
|---|---|---|---|
| **Generator** | Kohler 410kW Standby | 410 | kW |
| **PV** | Generic flat plate PV | 36.6 | kW |
| **Battery Storage** | Hitachi LL1500-W | 40 | kW |
| **System Inverter** | ABB Pro33 | 33.0 | kW |
| **Utility** | Safranbolu TEDAŞ | | |
| **Critical Load** | | 400 | kW |
| **Non-critical Load** | | 700 | kW |

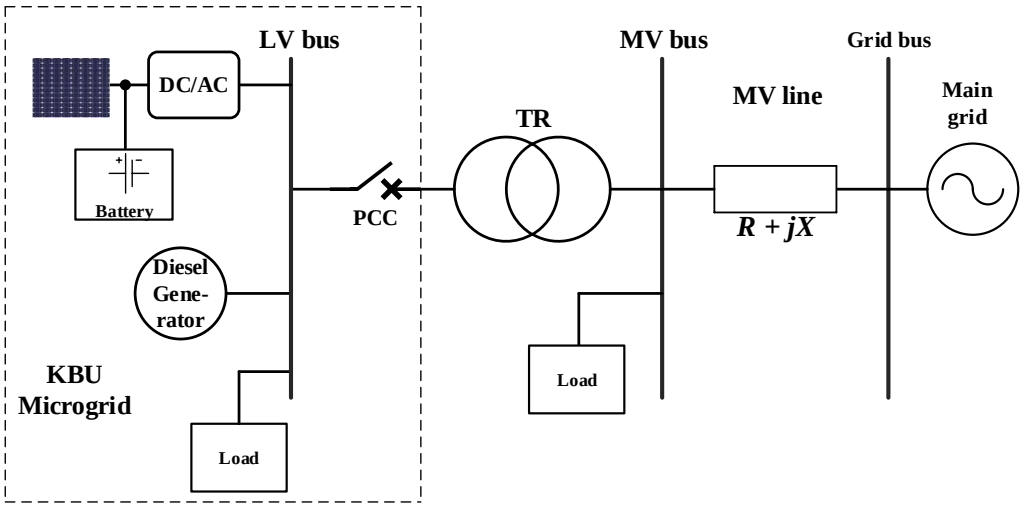


Figure 3.3. The overall structure of grid-connected KBU MG [85].

## 3.3. MODELING OF KBU MICROGRID SYSTEM

### 3.3.1. Modeling Passive Loads

Two types of receptors are used for the passive loads modeling: current receptor and voltage receptor.

And the output current can be mathematically stated as:

$$i_{-cp} = \frac{1}{R_{exl}} C_{ucs} \cdot u_{-mvb} \tag{3.1}$$

Here: $u_{-mvb} = [u_{tr13}, u_{tr23}]^T$ – the phase-to-phase voltage vector;

$i_{-cp} = [i_{cp1}, i_{cp2}]^T$ – the load currents' vector;

$R_{exl}$ – a resistor corresponding to the real load power ($P_{exl}$).

Figure 3.4 shows the voltage receptor load model.

$$R_{exl} = \frac{U_{nmvb}^2}{P_{exl}} \tag{3.2}$$

Here: $U_{mnvb}$ – the load voltages' nominal value.

Since it has a voltage output, the current receptor load is termed a "voltage-type" or "phase-to-phase" source load:

$$u_{-mvb} = C_{ucs} \cdot \left(R_{exl} i_{-cp}\right) \tag{3.3}$$

$R_{exl}$ – a resistor that corresponds to real load power ($P_{exl}$)

$C_{ucs}$ – the matrix calculated from a single-phase and phase-to-phase voltages.

$$R_{exl} = \frac{P_{exl}}{I_{nmvb}^2} \tag{3.4}$$

$I_{nmvb}$ is the load currents' nominal value.

Figure 3.5 shows the current receptor load model.

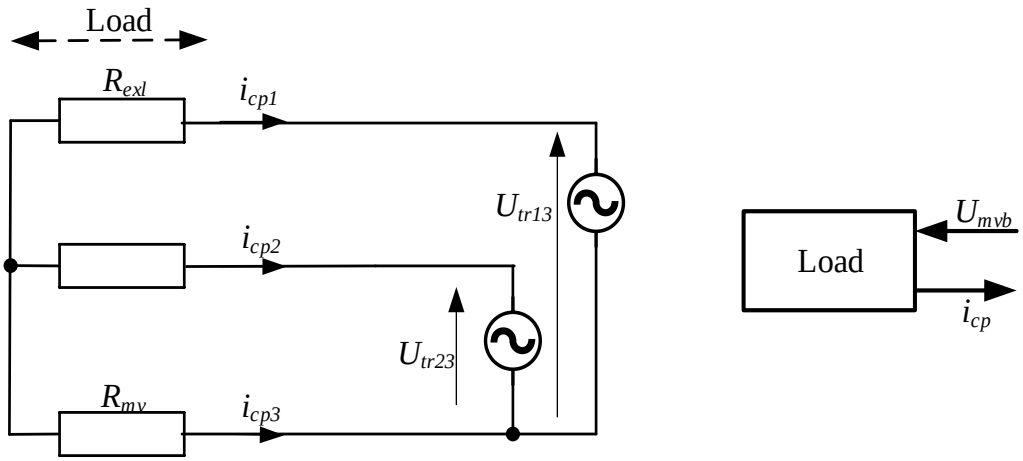


Figure 3.4. Model of voltage receptor load.

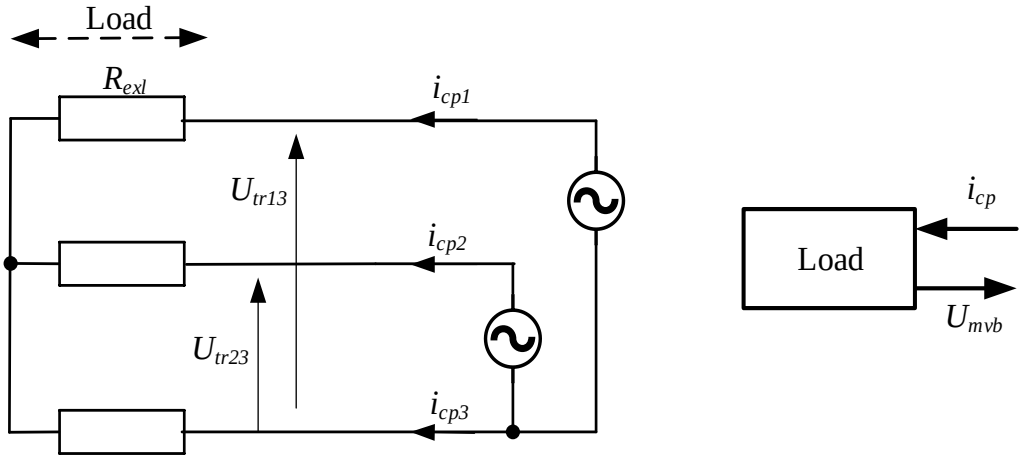


Figure 3.5. Model of current receptor load.

### 3.3.2. Modeling Relevant Buses

A grid architecture model is based on characterizing a coupling bus. If we assume that "*a unique voltage-type source unit must set the voltage at a bus*," it simplifies the bus modeling between the grid and the MG, so just a single unit should be a voltage-type source among the units (connected to a single bus) while others should be considered "current-type" sources. Thus, two buses exist between the main grid, and now, they will be modeled.

### 3.3.3. Grid Bus

Generally, a grid bus is linked with only the grid and the MV lines. A voltage-type source is a diesel group because it controls terminal voltages. Thus, modeling of the MV lines is done considering it a current-type source:

$$i_{-lmv} = i_{-gdb} \tag{3.5}$$

$$u_{-gdb} = u_{-gd} \tag{3.6}$$

Figures 3.6 (a) and (b), respectively, show single-line and block diagrams of a grid bus.

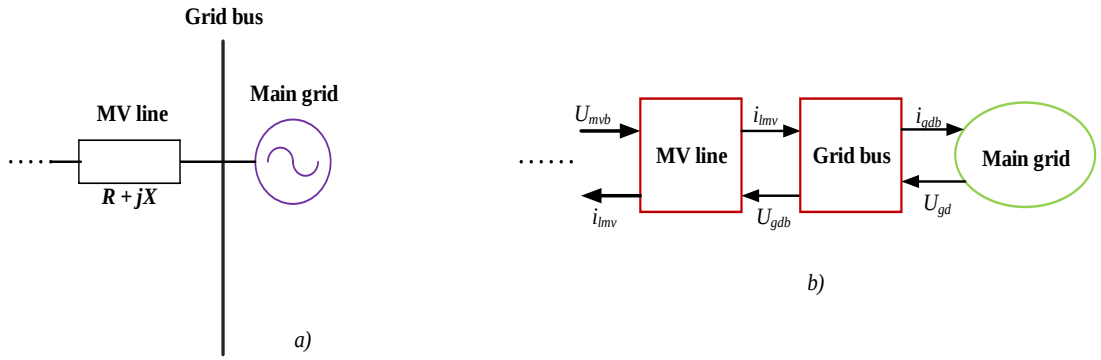


Figure 3.6. Grid bus representation: a) single-line diagram; b) block diagram.

### 3.3.4. Solar PV Generation of Power and Calculation of Solar PV Costs

The photovoltaic (PV) panel output power is calculated using Equation 3.7 in the adopted from:

$$P_{PV} = 3.24 \times N_{PV}[1 - 0.0041 \times (T_{PV} - 8)] \times G_h \tag{3.7}$$

where $N_{PV}$ – generating capacity of PV panels, $T_{PV}$ – temperature, $G_h$ – solar irradiance at h time (kW/m$^2$). The clean energy subsidy includes state tax and federal solar panel incentives; therefore, considering renewable energy conversion helps by lowering solar investment costs. The reduced investment costs due to the renewable energy conversion are estimated as follows

$$C'_P = C_P - (C_P \times S_h) - [C_P \times (1 - S_h) \times F_h] \tag{3.8}$$

Where: $C_P$ is the true investment expense ($/kW), $S_h$ is a national tax subsidy (percent) and $F_h$ is a state tax subsidy.

### 3.3.5. Battery Charging and Discharging Modeling

The formula for charging a battery ($E_B(h) < 0$):

$$Q_C(h) = (1 - \alpha) \times Q_C(h-1) - (E_B(h) \times \Delta h \times \eta_h) \quad (3.9)$$

$$-\eta_h \times E_B(h) \leq L_C \times Q_{Cmax} \quad (3.10)$$

The formula for discharging a battery ($E_B(h) > 0$):

$$Q_C(h) = (1 - \alpha) \times Q_C(h-1) - (E_B(h) \times \Delta h \times \eta_{h1}) \quad (3.11)$$

$$\frac{E_B(h)}{\eta_{h1}} \leq L_d \times Q_{Cmax} \quad (3.12)$$

Where: $E_B(h)$ – charging power, $\eta_h$ – charging efficiency, $\eta_{h1}$ – discharging efficiency and $\alpha$–self-discharge. These variables are expressed in percentages per hour. $L_C$ and $L_d$ are charging and discharging rated capacity of the battery, respectively [Ampere-hours]. $Q_{Cmax}$, $Q_C(h)$, $Q_C(h-1)$ reflects the maximum capacity of the battery and the battery's charge status in $h$ and $h-1$ cycles, respectively.

### 3.3.6. Modeling a Diesel Generator

A diesel generator combines electrical generators and internal combustion engines for power production. Usually, a diesel generator engine is designed to work and consume diesel as a fuel; however, some engines are redesigned to consume natural gas or other liquid fuels. Contrary to the microturbines' function, these generators can be linked to the grid without interfaces. When the operation takes place, the spinning speed is maintained low, and it is possible to fix the output frequency at 50 Hz. Figure 3.7 is the schematic diagram of a synchronous diesel engine generator.

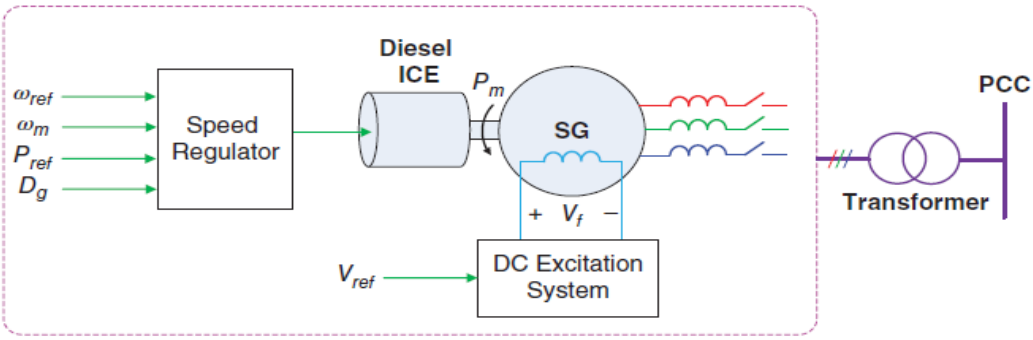


Figure 3.7. Conventional synchronous diesel engine generator model [88].

A transformer is used for connecting the synchronous machine to the grid. In accordance with a speed reference $\omega_{ref}$ and power reference *Pref*, the mechanical power *Pm* is dispatched. A DC excitation system is part of the synchronous generator system that controls the generator's field voltage $V_f$.

A study [89] shows the three-phase *abc* coordinate transformation into the *0dq* rotating reference frame, which is given below:

$$Qx_{abcn} = x_{0dq} \tag{3.13}$$

where: $Q$ – 3x3 (Park's transformation matrix)

$x$ – 3x1 electrical states vector.

We have rewritten Equation 3.13 in the matrix form and obtained the following:

$$Q = \frac{2}{3}\begin{bmatrix} 1/2 & 1/2 & 1/2 \\ cos\,(\omega t) & cos\,(\omega t - 2\pi/3) & cos(\omega t + 2\pi/3) \\ -sin(\omega t) & -sin(\omega t - 2\pi/3) & -sin(\omega t + 2\pi/3) \end{bmatrix} \tag{3.14}$$

Figure 3.8 illustrates the association between the *0dq* rotating frame and the synchronous machine *abc* stationary reference frame. In this case, Figures *a*, *b* and *c* apply to the stator phase windings, F applies to the field winding, D to the *d* axis damper winding, and Q to the *q* axis damper winding. Along the q axis, field flux has voltage induction, which directs along the *d* axis. Here, for generating conditions, power angle δ should have a greater-than-zero steady-state value. The following are

projections of *abc* quantities onto the *d* and *q* axes, considering *a* phase magnetic field axis as the reference:

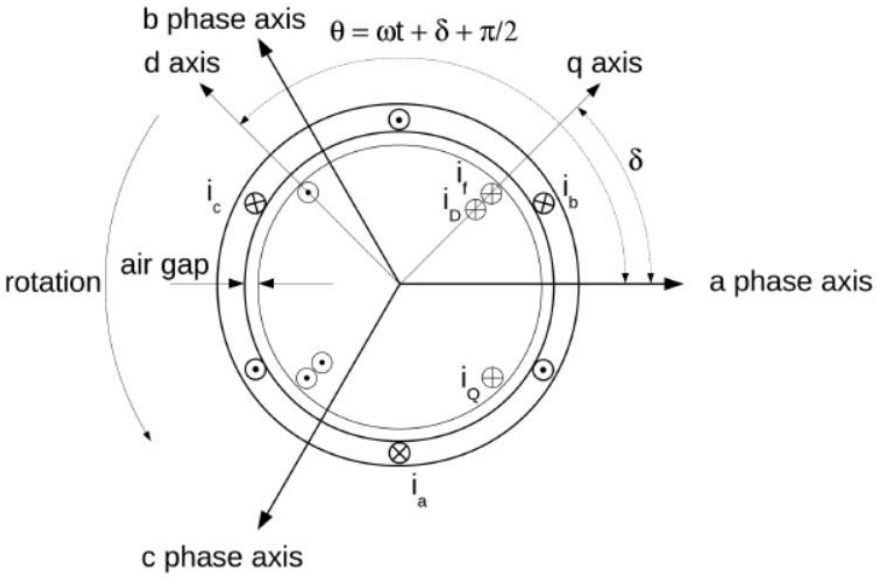


Figure 3.8. Association between *0dq* rotating frame and *abc* stationary frame.

$$x_d = \frac{2}{3\left[x_a\, cos(\theta) + x_b\, cos\left(\theta - \frac{2\pi}{3}\right) + x_c\, cos\left(\theta + \frac{2\pi}{3}\right)\right]} \tag{3.15}$$

$$x_q = \frac{2}{3\left[x_a\, sin(\theta) + x_b\, sin\left(\theta - \frac{2\pi}{3}\right) + x_c\, sin\left(\theta + \frac{2\pi}{3}\right)\right]} \tag{3.16}$$

The Park transform, i.e., the transformation from stationary reference frame *abc* to *0dq* rotation coordinates, can be written [90]

$$P = \sqrt{2/3}\begin{bmatrix} 1/\sqrt{2} & 1/\sqrt{2} & 1/\sqrt{2} \\ cos\,(\omega t) & cos\,(\omega t - 2\pi/3) & cos\,(\omega t + 2\pi/3) \\ sin\,(\omega t) & sin\,(\omega t - 2\pi/3) & sin\,(\omega t + 2\pi/3) \end{bmatrix} \tag{3.17}$$

Figure 3.9 shows the generator system's electrical system model in the *abc* frame. The figure also shows that all mutual inductances are not included, such as the mutual inductance $L_{Fc}$ is given that exists between the field winding and *c* phase winding. Still, $L_{Fa}$ and $L_{Fb}$ do not exist between the *a* and *b* phase windings and field winding. In the same way, the mutual inductance $L_{Da}$ $(L_{Qa})$ between *a* phase winding and the *d*

axis (*q* axis) damper winding is given, but $L_{Db}$ $(L_{Qb})$ and $L_{Dc}$ $(L_{Qc})$ are not. The exclusion of mutual inductance between the two windings (on the *d* and *q* axis) damper winding occurs because of the quadrature relationship. No mutual coupling exists between the mentioned windings.

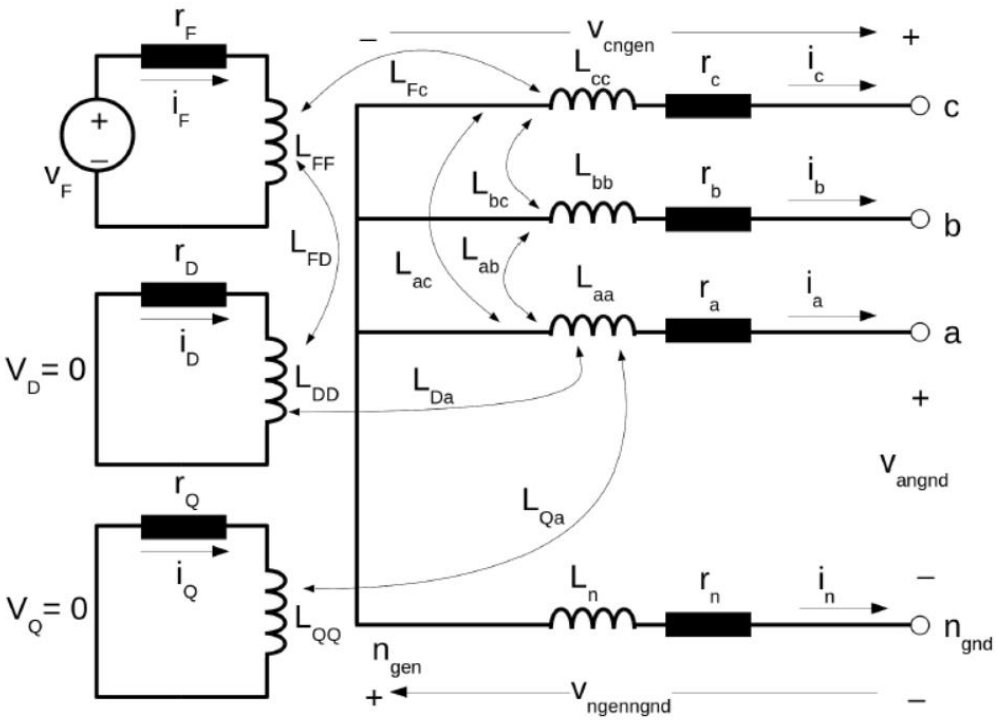


Figure 3.9. The electrical generator model in the *abc* frame.

Here, suppose: $L_{Da} = L_{aD}$, $L_{FD} = L_{DF}$, $L_{Fa} = L_{aF}$,…. For a simpler generator model, these symmetry properties will be used. A previous study [90] shows that inductances with two subscripts are time-varying while the ones with a single subscript are constant. Using a single upper case letter subscript, the rotor parameters are denoted:

- D – *d* axis damper winding
- Q – *q* axis damper winding
- F – field winding

In the *0dq* frame, the generator voltage equations are given below:

$$\begin{bmatrix} v_0 \\ v_d \\ v_q \\ -v_F \\ v_D \\ v_Q \end{bmatrix} = -\begin{bmatrix} r+3r_n & 0 & 0 & 0 & 0 & 0 \\ 0 & r & \omega L_q & 0 & 0 & \omega k M_Q \\ 0 & -\omega L_d & r & -\omega k M_F & -\omega k M_D & 0 \\ 0 & 0 & 0 & r_F & 0 & 0 \\ 0 & 0 & 0 & 0 & r_D & 0 \\ 0 & 0 & 0 & 0 & 0 & r_Q \end{bmatrix} \begin{bmatrix} i_0 \\ i_d \\ i_q \\ i_F \\ i_D \\ i_Q \end{bmatrix} \quad (3.18)$$

$$-\begin{bmatrix} L_0+3L_n & 0 & 0 & 0 & 0 & 0 \\ 0 & L_d & 0 & kM_F & kM_D & 0 \\ 0 & 0 & L_q & 0 & 0 & kM_Q \\ 0 & kM_F & 0 & L_F & M_R & 0 \\ 0 & kM_D & 0 & M_R & L_D & 0 \\ 0 & 0 & kM_Q & 0 & 0 & L_Q \end{bmatrix} \begin{bmatrix} \dot{i_0} \\ \dot{i_d} \\ \dot{i_q} \\ \dot{i_F} \\ \dot{i_D} \\ \dot{i_Q} \end{bmatrix} \quad (3.19)$$

Referring to all values to the stator:

$v_{0dq}$ – the voltages of generator stator in *0*, *d*, and *q* axis;

$v_{FDQ}$ – the voltages of rotor field, and in *d* and *q* axis damper winding

$i_{0dq}$ – the currents of generator stator in *0*, *d*, and *q* axis;

$i_{FDQ}$ – the currents of generator rotor field, and in d and q axis damper winding;

$r$ – the resistance of stator armature; $r_F$ – the resistance of rotor field;

$r_n$ – the resistance inserted in the neutral connection between the generator and system neutral;

$r_D$ and $r_Q$ – damper resistances in the *d* and *q* axis;

$\omega$ – electrical frequency;

$L_{FDQ}$ – the synchronous inductances of rotor field, in *d* and *q* axis damper;$L_{0dq}$ – the synchronous inductances of a stator in the *0*, *d*, and *q* axis;

$L_n$ – the inductance between the generator and system neutral;

$kM_D$ – the mutual inductance of stator *d* axis to rotor d axis damper;

$kM_Q$ – the mutual inductance of stator *d* axis to rotor *d* axis damper.

$L_{AD} = kM_F = kM_D = M_R$ and $L_{AQ} = kM_Q$ – the mutual inductance of the stator in $q$ axis to *q* rotor axis damper.

$kM_F$ – the mutual inductance of stator *d* axis to rotor field;

We state the following:

$$r = \begin{bmatrix} r + 3r_n & 0 & 0 & 0 & 0 & 0 \\ 0 & r & \omega L_q & 0 & 0 & \omega k M_Q \\ 0 & -\omega L_d & r & -\omega k M_F & -\omega k M_D & 0 \\ 0 & 0 & 0 & r_F & 0 & 0 \\ 0 & 0 & 0 & 0 & r_D & 0 \\ 0 & 0 & 0 & 0 & 0 & r_Q \end{bmatrix} \tag{3.20}$$

$$L = \begin{bmatrix} L_0 + 3L_n & 0 & 0 & 0 & 0 & 0 \\ 0 & L_d & 0 & kM_F & kM_D & 0 \\ 0 & 0 & L_q & 0 & 0 & kM_Q \\ 0 & kM_F & 0 & L_F & M_R & 0 \\ 0 & kM_D & 0 & M_R & L_D & 0 \\ 0 & 0 & kM_Q & 0 & 0 & L_Q \end{bmatrix} \tag{3.21}$$

By recognizing $v_d = v_q = 0$, handling $v_F$ as an input, and rearranging into first-order differential equations:

$$\begin{bmatrix} \dot{i_0} \\ \dot{i_d} \\ \dot{i_q} \\ \dot{i_F} \\ \dot{i_D} \\ \dot{i_Q} \end{bmatrix} = -L^{-1} r \begin{bmatrix} i_0 \\ i_d \\ i_q \\ i_F \\ i_D \\ i_Q \end{bmatrix} - L^{-1} \begin{bmatrix} v_0 \\ v_d \\ v_q \\ 0 \\ 0 \\ 0 \end{bmatrix} + L^{-1} \begin{bmatrix} 0 \\ 0 \\ 0 \\ v_F \\ 0 \\ 0 \end{bmatrix} \tag{3.22}$$

Thus, Equations 3.22 can be written as follows:

$$\begin{bmatrix} \dot{i_0} \\ \dot{i_d} \\ \dot{i_q} \\ \dot{i_F} \\ \dot{i_D} \\ \dot{i_Q} \end{bmatrix} = -L^{-1} r \begin{bmatrix} i_0 \\ i_d \\ i_q \\ i_F \\ i_D \\ i_Q \end{bmatrix} - L^{-1} \begin{bmatrix} P \begin{bmatrix} v_a \\ v_b \\ v_c \end{bmatrix} \\ 0 \\ 0 \\ 0 \end{bmatrix} + L^{-1} \begin{bmatrix} 0 \\ 0 \\ 0 \\ v_F \\ 0 \\ 0 \end{bmatrix} \tag{3.23}$$

Figure 3.10 shows the electrical generator model in the *0dq* reference frame.

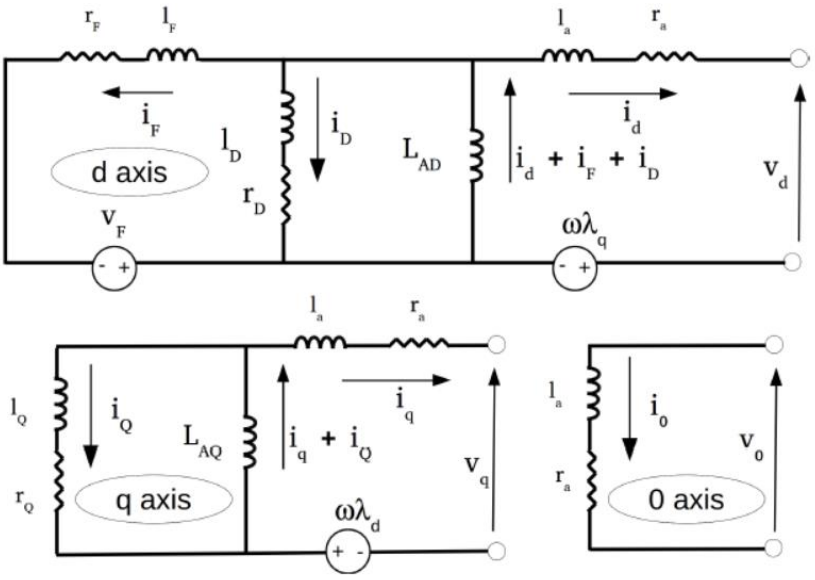


Figure 3.10. The electrical generator model in the *0dq* reference frame.

### 3.3.7. Inverter modeling

Inverters operate mainly as voltage source (also current source is known) and control the voltage magnitude of each phase. The sinusoidal voltage form can be obtained by using reference waveform and modulator, also controlled through use of low-frequency signals. The drawback of voltage-source inverters (VSIs) is there are high frequency distortions that become by switching action of the inverters. Three-phase VSIs are used in MGs for connecting the DC bus with the AC grid [91,92]. The purpose of the inverter is inverting DC into AC. The three-phase inverter model is shown in Figure 3.11. The circuit consists of voltage source $V_r$ in series and output impedance $Z0\angle\theta$, where $\delta$ is power angle – difference between $V_r$ and $V_0$, while $E$ is the amplitude of the voltage source and $\delta$.

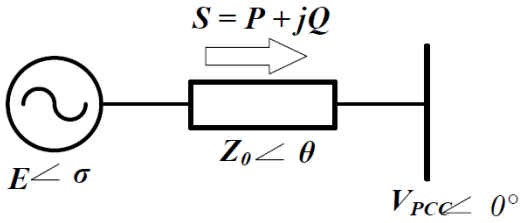


Figure 3.11. The equivalent model of three-phase inverter [93].

### 3.3.8. Economic Load Display of Microgrid

For an MG the device operating cost is listed below:

$$MG = MGC_{fuel} + MGC_{OM} + MGC_{DC} + GI\left(\sum Y_h^r R_h^r + C_{grid} + C_{diesel}\right) \quad (3.24)$$

$$MGC_{fuel} = L_{fc} \times E_i(h) \quad (3.25)$$

$$MGC_{OM} = L_{OM} \times E_i(h) \quad (3.26)$$

$$MGC_{DC} = \frac{DC}{E_{imax} \times 8760 \times FC} \times E_i(h) \quad (3.27)$$

$$DC = \frac{(I\_cost \times b \times (1+b)^m)}{((1+b)^m - 1)} \quad (3.28)$$

$$C_{grid} = a_2 + a_1 \times P_{G1} + a_0 \times {P_{G1}}^2 \quad (3.29)$$

$$C_{diesel} = a_2 + a_1 \times P_{G2} + a_0 \times {P_{G2}}^2 \quad (3.30)$$

Where: $MGC_{fuel}, MGC_{OM}$, $MGC_{DC}$, $C_{grid}$ and $C_{diesel}$illustrate the expenses of fuel consumption, costs of service maintenance, cost of depreciation, cost of the grid, and cost of diesel gen-set, respectively. $P_{G1}$ and $P_{G2}$ are power-sharing of the grid and diesel gen-set of the system. The $a_0$, $a_1$ and $a_2$ are constant values. The purchasing power and spinning reserve price, respectively, reflect $R_h^r$ $and$ $Y_h^r$. $GI$ equals 0 and 1, respectively, in islanded and grid-connected mode. $E_i(h)$ reflects the output power of the DGs, $L_{fc}$ and $L_{OM}$ reflects the fuel usage and operational control coefficients. $FC$, $DC$, and $I\_cost$ reflect the power factor, the cost of depreciation in kilowatt-hours, and the cost of installation, respectively. In this case, $b$ represents the rate of interest, which is 8%, and $m$ represents the lifetime of DGs [94].

### 3.3.9. Transmission Line Modeling

When the simulation is conducted, the model of a three-phase PI section line shows most transmission lines. This model is accessible in the SimPower Systems Library. In order to practically implement a balanced model (parameters lumped in a single PI section), we selected a three-phase PI section line model., contrary to the distributed

parameter line model, which has uniformly distributed inductance, capacitance, and resistance along the line. Figure 3.12 shows the mentioned model.

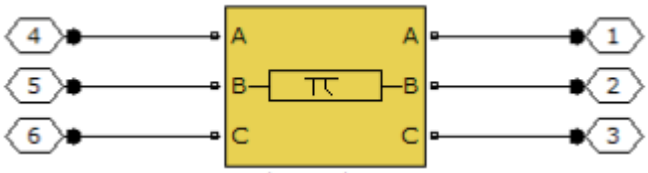


Figure 3. 12. Three-phase transmission line.

# PART 4

## OPTIMIZATION TECHNIQUES APPLIED TO MICROGRID

Microgrid studies mainly discuss control issues and energy management. The concept of energy management is based on optimal energy distribution, keeping in view different objective functions subject to different constraints. The control issues include frequency, active/reactive powers, and voltage issues, and in this context, they are the main variables [95].

For managing a microgrid, objective functions generally have different parts, which happens because of considering many objective functions. Table 4.1 shows the summary of objective functions mentioned in recent studies.

Table 4.1. Objective functions for microgrid control and energy management [96].

| Papers Type of Objective Function | | | | | | | | | | |
|---|---|---|---|---|---|---|---|---|---|---|
| Energy management Control | | Cost | Pollution | Losses | Voltage | Security | Peak Shaving | Loss of load | Adequacy | efficiency |
| | [23-75] | √ | X | X | X | X | X | X | X | X |
| | [76-95] | √ | √ | X | X | X | X | X | √ | X |
| | [173] | √ | X | √ | √ | √ | √ | X | √ | X |
| | [96] | √ | X | X | X | X | X | √ | X | X |
| | [97] | √ | X | X | √ | X | X | X | √ | √ |
| | [98] | X | X | √ | X | X | X | X | X | X |
| | [99] | √ | X | X | X | X | X | X | X | X |
| | [100] | √ | X | X | X | X | X | X | X | X |
| | [101,102] | X | X | √ | X | X | X | X | X | X |
| | [107-135] | X | X | X | √ | X | X | X | X | X |
| | [103-105] | X | X | X | X | X | X | X | X | X |
| | [106] | X | X | X | X | X | X | X | X | X |
| | [136-145] | X | X | X | X | X | X | X | X | X |
| | [146-160] | X | X | X | √ | X | X | X | X | X |
| | [161] | X | X | X | X | X | X | X | X | X |
| | [162,163] | X | X | X | X | X | X | X | X | X |
| | [164,165] | X | X | X | √ | X | X | X | X | X |
| | [166,167] | X | X | X | X | X | X | X | X | X |
| | [168-172] | X | X | X | X | X | X | X | X | X |

Figure 4.1 illustrates different aspects of MG management and the classification of its subsections. It has already been mentioned that energy management and microgrid control are divided based on objective function and parameters. Thus, the arrangement of different researches is based on energy and control subsections. Cost, losses, revenue, and emission optimization are considered the main microgrid energy management goals. The mentioned functions can be either considered as sole or combined functions. Moreover, control methods help solve various issues, including voltage, frequency, and active/reactive powers of a microgrid.

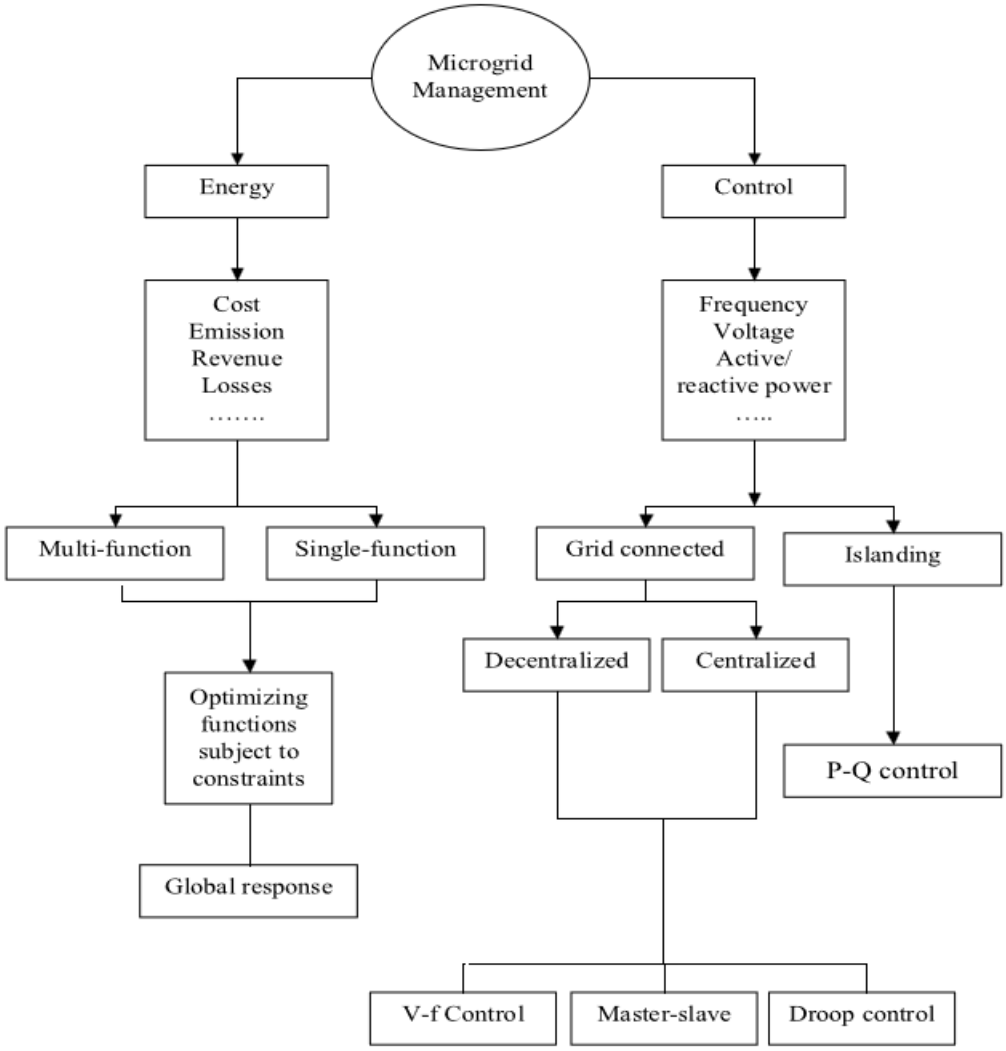


Figure 4.1. Microgrid management aspects based on energy and control [96].

Figure 4.2 shows a statistical comparison between energy management and control for investigated references.

According to the statistical data, 80 out of 150 studies were conducted on the power management system. In fact, it reveals that the management of energy has gained more attention in the research community than energy control. Figure 4.2 clearly indicates that frequency and voltage were investigated in 54 out of 70 research papers. Moreover, the cost and emission functions were separately dealt with in 53 and 20 MG energy management studies, respectively [97].

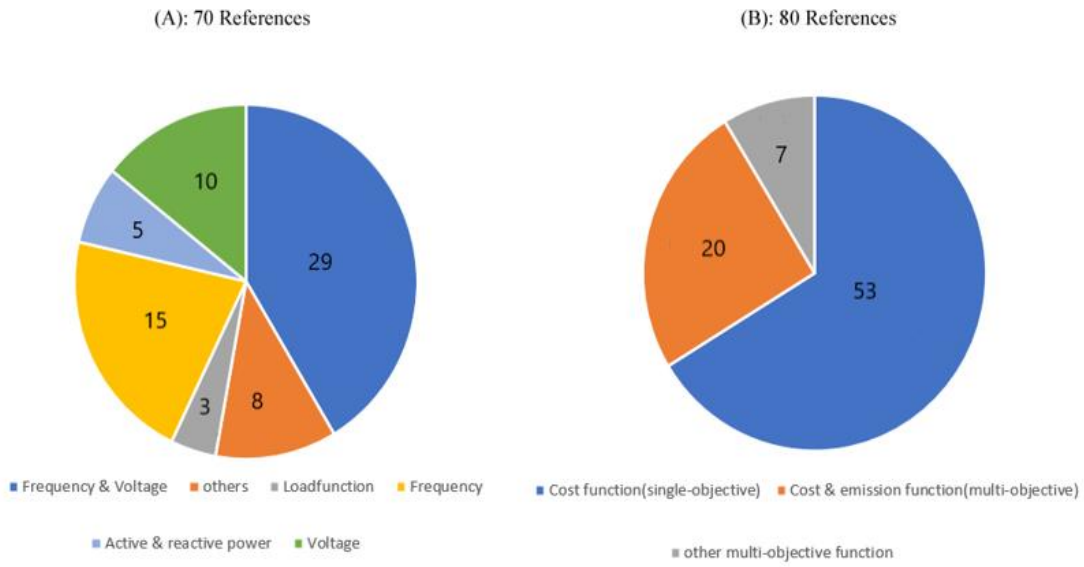


Figure 4.2. Statistical comparison between aspects of microgrid management in terms of control issues and energy management.

At any point in the MG, optimization may be applied to ensure the best operating conditions and address all necessary constraints. The process of MG setup, its maintenance, scheduling, operation, and activities involve different challenges and decision-making situations needing optimization in different application areas. Mathematically, an optimization problem requires finding the most optimal solution from the available options of feasible solutions. In simpler words, the optimization of hybrid MGs is roughly segregated into one of the three categories, including the control side, distribution side, and generation side [98].

Different kinds of optimization processes, both artificial intelligence-based and traditional ones, which have been reported in the literature, apply to MGs. Figure 4.3. presents practical methods for MG optimization.

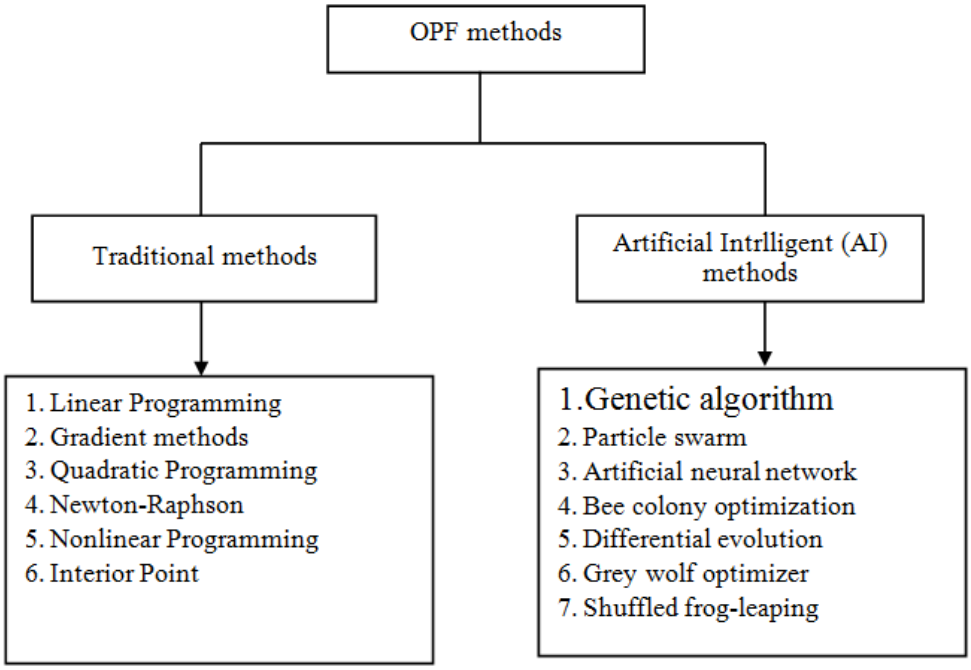


Figure 4.3. Classification of OPF methods.

Further in our work, the most frequently used optimization methods for MG are considered.

## 4.1. LINEAR PROGRAMMING

Linearization of the objective function and constraints is needed for linear programming formulation when non-negative variables are used.

In a study [99], an optimal power flow concept through a linear programming-based optimization method has presented. According to the results, the convergence of a five-bus 220 kV system was achieved within a single iteration and a considerable CPU time reduction. They recommended their process to run the Power System Control Division of the Florida Power and Light Company, which remained successful in a 15-bus system when real-time data was used.

Through their linear programming method, T.S. Chung et al. [100] attempted to minimize power losses and find the capacitor's optimal location within a distribution

system. A 14-bus system was used for calculations, and their process required matrix inversion, which thus saved the memory space and the computational time.

In a Spanish power generation system, another linear programming model by E. Lobato et al. [101] was proposed for OPF for reactive generator margins and power loss minimization. In the proposed methodology, capacitors and shunt reactors are discrete, and integer variables were used to model them. In each iteration, the constraints and the objective function were linearized.

DC power flow formulation is another concept that Rau, N. [102,103] has presented to simplify assumptions and the objective function linearization. It is given that the DC power flow constraint set is linear, which means that it requires no further constraint linearization. This concept differs from other linearization techniques because DC-OPF requires a single solving procedure to get the optimal solution, and it is non-iterative. Owing to the speed, simplicity, and robustness of DC-OPF, it is now a commonly applied industrial process.

### 4.2. GENETIC ALGORITHMS (GAs)

The nature of GAs is evolutionary, and they are search algorithms based on how natural genetics work [104,105]. For simultaneous search space exploration and performance enhancement of the generated solutions, GAs combine directed and stochastic search elements exploiting historical information from the guesses of the previous solutions [106]. Generally, at local optima, GAs avoid termination. It happens because the solutions are distributed throughout the search space, so random processes are used to find new solutions. As mentioned in a previous study, the solution eventually converges to a global optimum, specifically when the best solution exists within the solution pool, as mentioned in a previous study [107].

Genetic Algorithms (GAs) operate on the problem parameters' binary string (encoded), and they are not based on the actual system parameters. Every string can be considered a chromosome, which fully describes a single candidate solution to solve a problem. In simple form, Genetic Algorithms are iterative procedures. To generate new

populations (offsprings), three genetic operators (crossover, mutation, and selection) take place during each iteration (generation).

Using GAs, Bakritzs et al. [108] presented the economic dispatch problems. According to the researchers, their merits include effective GA coding to work on parallel machines, and there is no restriction of convexity on the generator's cost function. Compared to dynamic programming, GAs are superior, and it was observed through their performance observed in economic dispatch problems. The second GA solution's run time (the EGA method) increases proportionately with the system size.
In another study, Po-Hung Chen [109] used GA to present a major economic dispatch problem and a new encoding process through which a chromosome only has a normalized encoding incremental cost. He found no link/correlation between the total units and the total bits in a chromosome. The genetic approach has a unique characteristic, which is significant in intricate and large systems, so it accomplishes what other approaches fail to accomplish. Through the flexibility of the GA, the dispatch is more practical because of considering ramp rate limits, prohibited zone avoidance, and network losses. This process saves more time than the Lambda–iteration in large systems.

In their hybrid genetic algorithm, M. Younes and M. Rahl [110] combined GA with Mat power to deal with OPF, which included reactive as well as active power dispatches. To find a closer-to-global solution, they used GA and MATLAB to handle the OPF (also termed mat power) and found the global optimal. Before attempting to find the global solution, mat power helps adjust the control variables. According to the modified IEEE 57–bus system, they validated their method. Results show that a hybrid approach finds a better solution than the situation when either GA or Mat power is individually applied.

In a research paper, M.S. Kumari [111] formulated the OPF problem in the form of an optimization problem with multiple objectives and applied the optimal control settings to simultaneously minimize voltage stability issues, fuel cost, and power loss, for which she obtained a loss and voltage stability index that combines a new Decoupled Quadratic Load Flow (DQLF) solution with the Enhanced Genetic Algorithm (EGA)

for solving the OPF problem. She obtained a strong and dominated Pareto-optimal set using her approach called Strength Pareto Evolutionary Algorithm (SPEA).

### 4.3. PARTICLE SWARM OPTIMIZATION (PSO)

The PSO is an optimization process based on stochastic and population-based approaches, and it is a nature-based method observed in colonies of fish and birds. To find the required promising regions in a specific search space, the PSO uses a population. During the search, each particle/individual undergoes positional changes and moves to the decision space according to its own best experience.

To solve the traditional economic dispatch problem, El-Gallad et al. [112] presented the PSO-based approach. They formulated their objective function by combining non-differential regions and piece-wise quadratic cost functions rather than assigning a single convex function to each generating unit. The practical operating conditions, such as fuel types and valve-point effects, are the major reasons behind the innovation in the problem formulation. They also incorporated the balance of power, system demand, network losses, and generating capacity limits.

Using the valve-point effects, D.B. Attous [113] presented their economic dispatch problem. When the turbine's steam valves start opening, a valve point effect has rippling effects, which add to the generating units' curve. Their proposed process is based on PSO, which was examined and tested according to the standard IEEE 30-bus system. The PSO was declared as a competitive approach, which shows improved general convergence.

Using a new approach to calculate optimal power flow, S.Kumar [114] integrated PSO-fuzzy and GA-fuzzy optimization methods. The researcher tested four algorithms, including GA-fuzzy, FPSO, and PSO, to find a solution according to the modified IEEE 30 bus test system. Results show that integrating PSO and fuzzy with GA improved the average fitness performance obtained using optimal power flow. The comparison of results obtained through the integrated PSO-fuzzy and GA-Fuzzy

shows that the integrated method outperformed as compared to individual GA and PSO approaches. It was found that the synergetic approaches perform better.

To solve OPF by applying inequality constraints on the line flow, T. Saravanan [115] suggested a PSO technique and its application. He used a three-unit six-bus system, implemented the algorithm, and compared the results to the results of the linear programming method.

Using the power injection model of the FACTS device, the authors of [116] applied PSO to solve the optimization problem. They tested the proposed methodology using the 30-bus standard IEEE testing process before comparing the single-objective optimization results with/without the FACTS device.

### 4.4. MULTI-AGENT SYSTEMS (MAS)

The MAS system comprises certain agents, including intelligent agents, which perform together to achieve a global objective. Now it has emerged as one of the fastest-growing and most exciting research fields. MAS is the best choice in this context because when a microgrid undergoes MAS modeling, it helps make an intelligent system, for example, an intelligent microgrid or a smart grid. To implement computational, mathematical, and intelligent tools for decision-making modules, intelligent agents provide a platform. For all autonomous intelligent agents, a microgrid's MAS modeling provides a common communication interface that represents the network elements.

A fundamental MAS element is an intelligent agent [114], and the following typical characteristics define it: proactiveness, reactivity, and social-ability. Reactivity is the agents' ability to perceive the environment and timely response to gain their objectives. Proactiveness exhibits goal-directed behaviors. Social ability means their interaction with other agents to meet their design objectives. The mentioned factors show how is important MAS for developing a complex system.

Actually, MAS has several intelligent agents, which either compete or cooperate and negotiate or communicate with each other to achieve their individual and system goals. The agent environment diagram is presented in Figure 4.4.

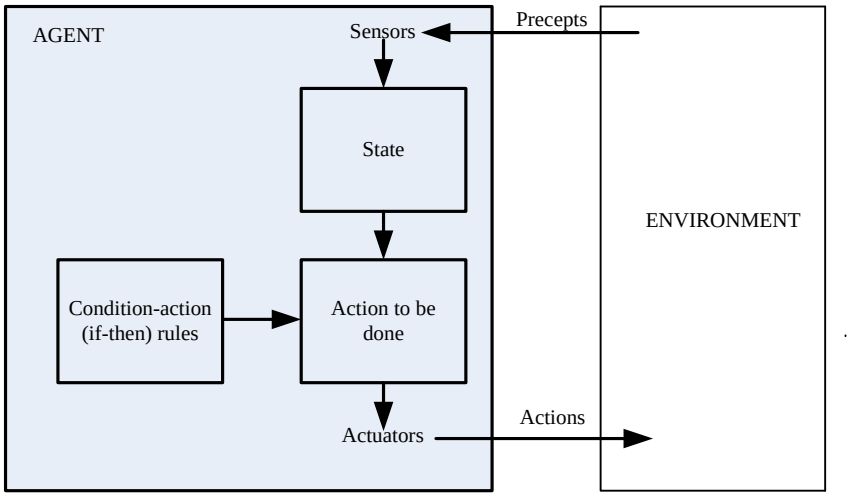


Figure 4.4. Agent environment diagram [112].

Research [115] shows the DERs' coordinating strategy in a microgrid. The author of the same study has discussed MAS's main characteristics and advantages for microgrids. MAS has gained remarkable significance as a power engineering topic, but identifying the key technical issues is still important [116,117], which will help adopt MAS effectively in the engineering framework. Some significant challenges include multi-agent platform selection and designing intelligent agents, which have characteristics such as proactiveness, social ability, and reactivity, according to standards of design ontologies, system security, and agent communication languages. Java Agent Development Framework (JADE), ZEUS, and VOYAGER platforms mostly apply for implementation of MAS. MACSimJX interface uses for interconnection simulation models, executed like in MATLAB/Simulation, with MAS platforms as close as possible to the real implementations. In Figure 4.5 is illustrated MACSimJX structure. This interface consists of client-server structure and agents.

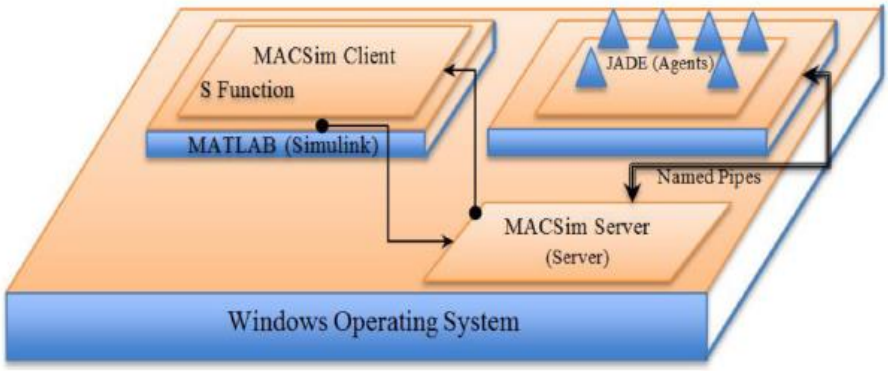


Figure 4.5. MACSimJX structure [117,121].

## 4.5. GREY WOLF OPTIMIZER (GWO)

Primarily, the GWO performs by mimicking grey wolves' leadership hierarchy and hunting mechanisms, which they exhibit in the natural environment. Four grey wolf types exist in each pack, including alpha, beta, delta, and omega. Moreover, their hunting process comprises three processes: searching encircling, and attacking prey, which are also performed during the optimization process.

As Mirjalili suggests, GWO is a novel and robust meta-heuristic method [33]. It is also an easy-to-understand and feasible-to-implement algorithm because it is nature and animal-inspired. The main GWO advantage is that it is adaptable, easy, and plain [34]. A few recent studies show that GWO may provide satisfying results when they were compared as compared to other popular and successful meta-heuristic concepts. For example, this happened when Mirjalili compared GWO with Gravitational Search Algorithm (GSA), differential evolution (DE), PSO, evolution strategy, and evolutionary programming through 29 test functions.

A study was conducted on exploration and exploitation processes in GWO and local optima avoidance [33]. Yahiaoui et al. [122] applied GWO to obtain an optimum hybrid energy system (HES) design equipped with a PV diesel generator battery. Using another approach, Yang et al. [123] applied GWO to determine WT proportional-integral controllers' optimal parameters at the maximum power point tracking (MPPT) using an enhanced fault ride-through capability. In a study by Ali et al. [124], GWO

was applied to obtain a polymer electrolyte membrane (PEM) fuel cell's model parameters. Another study [35] by Kamboj et al. shows that GWO can be used to handle the economic load dispatch problem in an electrical power system. Still, there is an insufficient and insignificant number of studies that compared different artificial intelligence methods and attempted to determine the optimum hybrid system components' configuration and sizes.

Another feature of mathematical modeling of a grey wolves' pack is their group hunting behavior, which has three phases: (a) prey track, chase, and approach; (b) prey encircling, harassing, and pursuing until it stops moving; and (c) attacking it.

The wolves' social hierarchy is mathematically modeled to solve any optimization problem that requires the best solution, which is called alpha (α). The second best and the third best are termed beta (β) and delta (δ), and other solutions are termed omega (ω).

### 4.5.1 Inspiration

In fact, grey wolves are Canidae species, so they are considered apex or topline predators, which means they are at the top place in the food chain. They mostly live in packs, and each pack has, on average, 5-12 members. An interesting aspect of their lifestyle is their strictly socially-dominant hierarchy, as Figure 4.4 indicates.

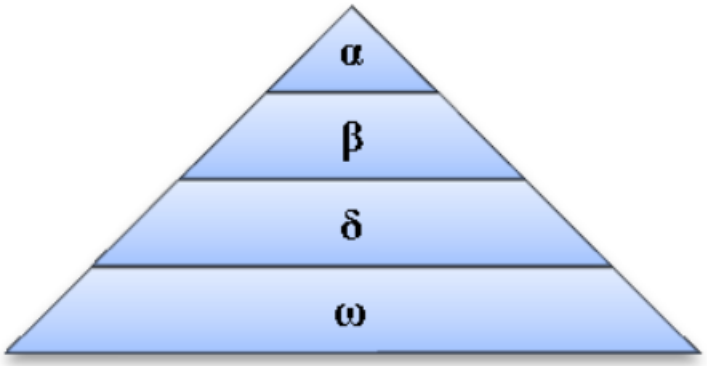


Figure 4.6. Grey wolf hierarchy (dominance decreases top-down).

A wolf-pack leader can be male/female and termed as alpha. An alpha wolf makes decisions regarding sleeping place, time to wake up, and hunting, to mention a few. The Alpha wolf dictates the whole pack's decisions, but some democratic behaviors become obvious when the alpha follows others. When all the pack members gather in one place, the members of the entire pack hold their tails down, and it is a sign of acknowledging alpha. The alpha wolf is dominant because others follow their orders [125,126]. Moreover, alphas only mate with their pack members, and they may not be the strongest but the best pack managers. It means that the pack management is more important for wolves than their leader's physical strength.

Grey wolves' second hierarchical level is beta, a subordinate wolf who assists alpha in decision-making and pack activities. Like alphas, they can be male or female, but they become alpha when an alpha wolf dies or gets too old. They respect an alpha, but it must command the wolves of lower levels. Moreover, a beta wolf reinforces the alpha's commands throughout a pack and provides essential feedback to the alpha.

Among grey wolves, the omega ranks the lowest because it acts as a scapegoat. They submit themselves to all the dominating wolves. It is obvious from the fact that they are allowed to eat after all the wolves are allowed to eat. On the surface, it seems as if the omegas are important to pack members, but observations show that when the pack loses the omega, it undergoes internal fights and issues. It is how wolves vent out frustration and violence. It helps keep the entire pack satisfied, sometimes takes care of the babies, and maintains the hierarchical structure.

Another category in wolf packs is the subordinate (also termed as delta), which submits to alpha and beta but dominates omegas. They include elders, scouts, caretakers, hunters, and sentinels. Normally, scouts watch the territorial boundaries and warn everyone in the pack when any type of danger emerges.

The sentinels assure the whole pack's safety while elders are either experienced alphas or betas. While hunting prey and food provision to the pack, the hunter wolves assist the leader in Hunting. The caretakers care for the wounded, sick, and weak wolves in a pack.

The grey wolves follow the following steps to carry out their hunting procedure [127]:

1- Track, search, chase, and approach the potential prey.
2- Harrass and encircle a prey until the prey no longer moves.
3- Attack the prey.

### 4.5.2. Mathematical Modeling and Algorithm

We have presented a few mathematical models which depict the grey wolves' tracking, attacking, social hierarchy, and encircling behaviors. After that, we have outlined the GWO algorithm.

#### 4.5.2.1. Social Hierarchy

To find the appropriate mathematical model for the wolves' social hierarchy, we use the term alpha (α) for the best GWO solution. In the same way, beta (β) and delta (δ) are the second-best and third-best solutions. The remaining candidate solutions are termed omega (ω): the top three (α, β, and δ) help the optimization process when the GWO algorithm is used. Obviously, ω wolves follow the three mentioned categories.

#### 4.5.2.2. Encircling prey

Wolves encircle their prey before they hunt it. Their encircling behavior can be mathematically described using the following model:

$$\vec{D} = \left|\vec{C}.\vec{X}_P(t) - \vec{X}(t)\right| \quad (4.1)$$

$$\vec{X}(t+1) = \vec{X}_P(t) - \vec{A}.\vec{D} \quad (4.2)$$

In this case, t shows the current iteration, $\vec{X}_P$ is the prey's position vector, $\vec{X}$, $\vec{A}$ and $\overrightarrow{C}$ represent coefficient vectors.

It is possible to calculate $\vec{A}$ and $\overrightarrow{C}$ as given below:

$$\vec{A} = 2\vec{a}.\overrightarrow{r_1} - \vec{a} \quad (4.3)$$

$$\vec{C} = 2.\overrightarrow{r_2} \tag{4.4}$$

Here, $r_1, r_2$ are the random vectors [0,1], and after iterations, $\vec{a}$ components have been linearly reduced from 2 to 0.

Fig. 3a shows the effects of equations 4.1 and 4.2, some possible neighbors, and a 2D positional vector. The mentioned figure also illustrates the wolf's position (X, Y) that changes/updates according to the prey's position (X*, Y*). The values of $\vec{A}$ and $\overrightarrow{C}$ vectors can be adjusted to attain places close to the best agent. Here, (X*-X, Y*) serves as an example that we can reach by adjusting $\vec{A} = (1,0)$ and $\overrightarrow{C} = (1,1)$. In Figure 4.5b, a grey wolf's possible updated positions are depicted in a 3D space. It is important to understand that wolves can reach any position that exists between the points because of the random vectors $\overrightarrow{r_1}$ and $\overrightarrow{r_2}$, as Fig. 4.5 illustrates. Thus, it is possible for a grey wolf to update its position in any random location in a space around the prey using Equations 4.1 and 4.2.

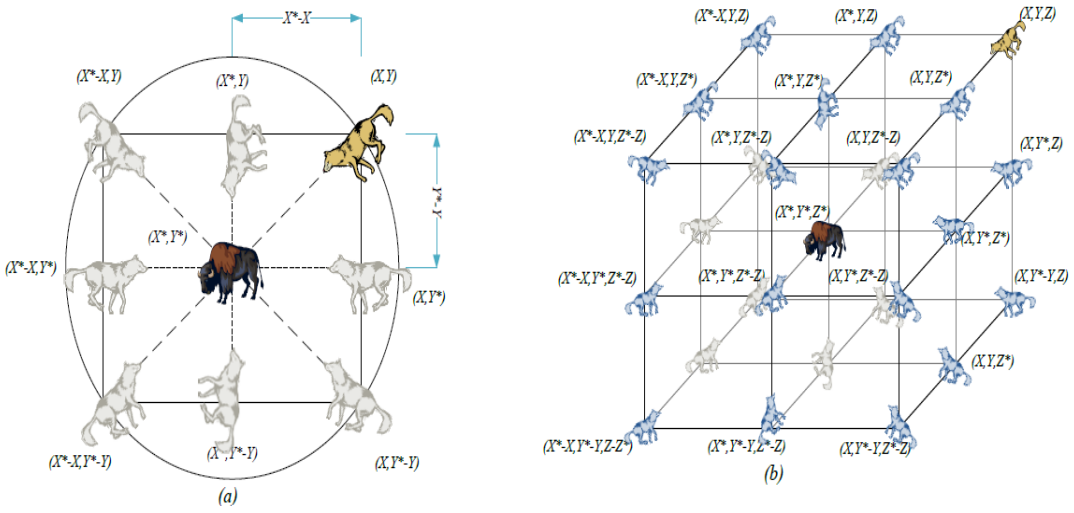


Figure 4.7. 2D and 3D position vectors and their next possible locations.

#### 4.5.2.3. Hunting

Normally, grey wolves recognize the prey's location before encircling it. Alpha wolf generally guides the hunt, whereas other wolves, such as beta and delta, may occasionally participate in hunting. But, in an abstract space, we have no idea about

the optimum location (prey). For mathematical simulation of their hunting behaviors, it is assumed that the alpha offers the best solution. At the same time, both beta and delta know the prey's location. Thus, they are the top three solutions, and now omegas must update their positions according to the best search agent's position. In this context, we proposed the following formulas.

$$\vec{D}_\alpha = \left|\vec{C}_1.\overrightarrow{CX}_\alpha - \overrightarrow{X}\right|, \overrightarrow{D_\beta} = \left|\vec{C}_2.\overrightarrow{X_\beta} - \vec{X}\right|, \overrightarrow{D_\delta} = \left|\overrightarrow{C_3}.\overrightarrow{X_\delta} - \overrightarrow{X}\right| \quad (4.5)$$

$$\overrightarrow{X_1} = \overrightarrow{X_\alpha} - \vec{A}_1.\left(\overrightarrow{D_\alpha}\right), \overrightarrow{X_2} = \overrightarrow{X_\beta} - \overrightarrow{A_2}.\left(\overrightarrow{D_\beta}\right), \overrightarrow{X_3} = \overrightarrow{X_\delta} - \overrightarrow{A_3}.\left(\overrightarrow{D_\delta}\right) \quad (4.6)$$

$$\vec{X}(t+1) = \frac{\overrightarrow{X_1}+\overrightarrow{X_2}+\overrightarrow{X_3}}{3} \quad (4.7)$$

Figure 4.5 exhibits the position updates of a search agent, keeping in view the positions of the top three types of wolves. It is obvious that within a circle, the final position would be randomly defined by alpha, beta, and delta, all of which estimate the prey's position, while the remaining wolves randomly change their positions around the prey.

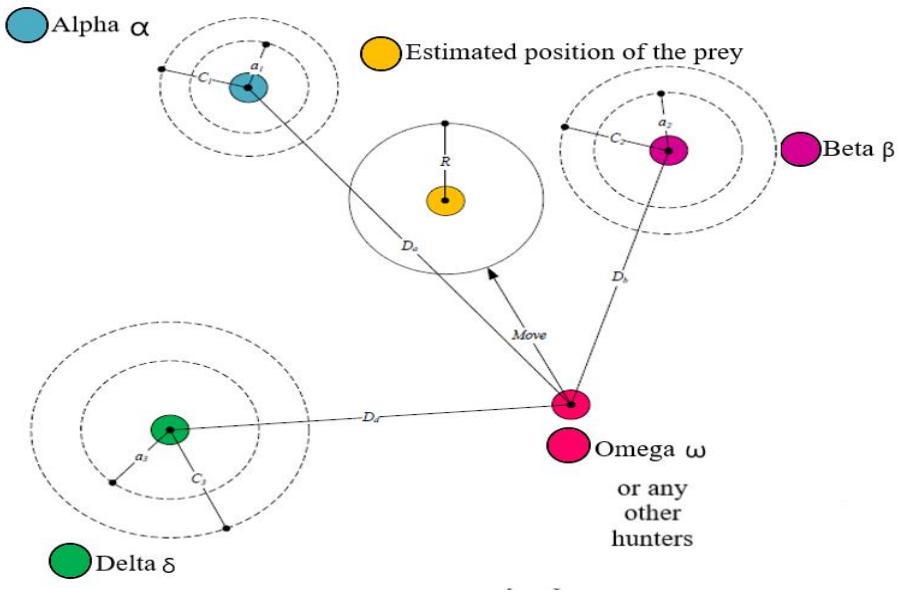


Figure 4.8. Position updating in GWO.

#### 4.5.2.4. Attacking Prey (exploitation)

It is mentioned earlier that wolves complete their hunting process when they attack their prey because it stops their movement. To create a mathematical model to express

the process grey wolves adapt to approach their prey, we reduced the vector $\vec{a}$ from 2 to 0 through iterations. In this context, $\vec{A}$ exists in the interval [-a, a] as a random value. The search agent's next position can be at any point between the prey's position and the current position. The random values of $\vec{A}$ are in [-1,1]. Figure 4.7a clearly indicates that |A|<1 urges wolves to attack in the prey's direction.

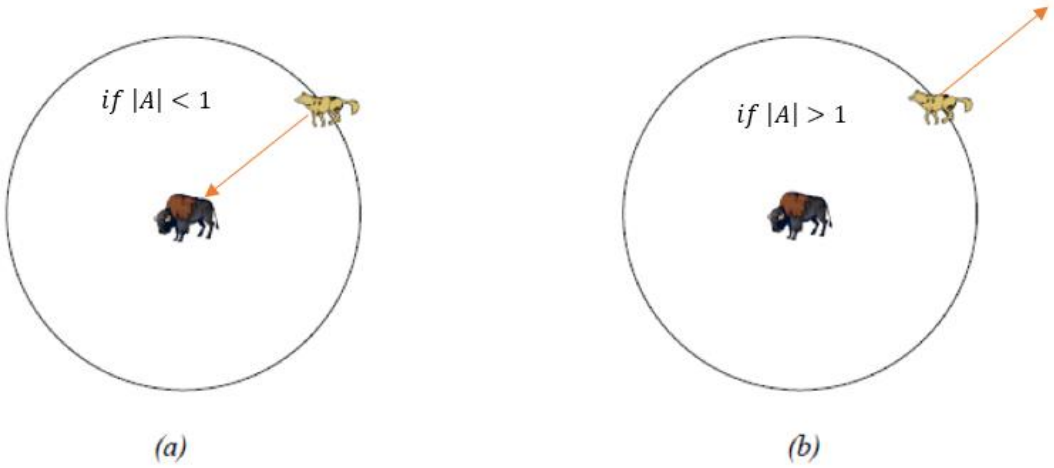


Figure 4.9. Attacking prey versus searching for prey.

It is clear from the proposed operators that the GWO algorithm directs and helps the search agents in updating their positions based on the locations that alpha, beta, and delta wolves have already acquired. It also helps to set the direction to attack the prey, but when attempting to find the local solutions, this algorithm can actually stagnate. It is correct that the proposed encircling process leads to some exploration, but in case a more comprehensive exploration is required, GWO requires more operators.

#### 4.5.2.5. Search for Prey (exploration)

It is already mentioned that grey wolves base their search on the positions of the leading wolves, but they diverge and then converge back again to launch an attack on the prey. To mathematically express divergence, we used $\vec{A}$ with random values (greater than 1 or less than -1). It means that a search agent will diverge from the prey, which emphasizes exploration and makes the GWO algorithm undergo a global search. In this case, |A|>1 urges grey wolves to diverge away from the prey to find better prey,

as illustrated in Figure 4.7b. In this context, $\vec{C}$ is a GWO component that helps exploration.

Equation 4.4 indicates that the $\vec{C}$ vector (random values in [0, 2]) provides random weights to a prey and either de-emphasizes (C<1) or emphasizes (C>1). Equation 4.1 shows the effect a prey has in defining the distance. It helps GWO exhibit more randomly during the optimization process, which leads to further exploration and avoids the local optima. In this case, contrary to *A*, *C* is not linearly decreased. We actually need *C* for providing random values to emphasize exploration both during the initial as well as final iterations. In the case of local optima stagnation, this component is quite helpful, specifically during the final iterations.

While approaching prey in nature, the *C* vector shows the impact obstacles have on the hunt. In nature, such obstacles exist in wolves' hunting paths that prevent them from making a quick and convenient approach to prey. It is the function of the vector *C*, and it can randomly assign a prey a specific weight that depends on the wolf's position, which makes it difficult and farther to reach, or this may be exactly the opposite (vice versa).

To conclude, the search for an optimized solution, or in other words, prey, initiates with creating a random grey wolves population (or candidate solutions) using the GWO algorithm. After a considerable number of iterations, three top wolves (alpha, beta, and delta) estimate the prey's position. Based on that, every candidate solution (wolf) changes (updates) its distance from the selected prey. To explore and exploit further, we reduced the parameter *a* from 2 to 0. When $|\vec{A}|$>1, the candidate solutions diverge from the prey, but when $|\vec{A}|$<1 is true, the candidate solutions converge towards the prey. At the end, when the end criterion is met, we terminate the GWO.

## PART 5

## ECONOMIC DISPATCH AND GREY WOLF OPTIMIZATION METHOD

At the present time, Distributed Generations (DGs) focused on renewable energy resources and their economic load dispatch problems are now getting more attention in microgrid system. Many research works on the cost-effective operation of microgrids have been established because they are environmentally sustainable, versatile and provide better quality of power [128,129]. Dynamic and static load dispatches are group of economic dispatch for power systems. However, the dynamic load dispatch is favored to the steady approach these days since this approach not only minimizes costs although it assists to communicate among all distribution power generators (DGs) [5,130]. However, owing to volatility, instability and unpredictability in renewable resources, the objective role of economic dispatch with a competitive approach is difficult to solve in the microgrid [7].

Solar PV technology helps to generate power with lowest cost and also enhance the environment factor to the environment. PV energy volatility, however will create numerous issues, such as economic losses from the hybrid power grid [131]. The economic dispatch of the Complex microgrid system considered the three related operating conditions such as grid connected mode and island modes, taking into account of renewable source abrupt changes due to change in environment conditions [9,132,133]. The dynamic programming approach responds extremely rapidly, helping to calculate the functionality of microgrid's in long-term and short-term operation of the microgrid system. The island mode with an energy storage device offers economic benefits and provides microgrid safety [10,11].

The scheduling of microgrid resources involves photovoltaic with battery energy storage, diesel engines with rotating reserve restrictions. Multi-objective optimization is carried out by addressing the environmental dilemma of microgrids [134,135]. To

solve the complex economic dispatch (CED) problem of the generating unit and to understand the consequences of the valve point, an updated differential evolution (UDE) has been added. The success of evolutionary programs on economic power dispatch (EPD) issues is analyzed and discussed in two sections. In grid-connected microgrid system with economic power dispatch, quadratic programming is often used. Comparisons are made that demonstrate that economic battery scheduling dependent on economic power dispatch in grid-connected mode and it reduces the total operating cost of the microgrid system [136,137]. The Monte Carlo simulation approach was used to test the suitability of an island mode of microgrid combined with the PV energy operating reserve. The particle swarm optimization technique was utilized to solve economic power dispatch problem in power systems with taking into account of nonlinear characteristics of the generator, these approaches help to more easily achieve higher performing solutions [138].

In this subchapter, mathematical simulation of the microgrid with complex economic power dispatch problem is developed in MATALB. The microgrid system consisting of following components, PV Power plant, Battery energy storage system and diesel gen-set system and this system operated in the following modes such as island mode and grid connected mode. The numerous restrictions are taken into consideration in order to enhance the microgrid system's performance and reliability. Analysis is conducted by considering the results of operating, maintenance and fuel cost for the scheduling of the systems in both modes. In operating costs, different variables such as cost of depreciation, cost of service control and cost effects of fuel usage are seen. To increase the output and reliability of the microgrid device, the restrictions of the rotating reserve are also included. The grid-connected mode is favored over the island mode, since it is very difficult to provide an efficient battery consumption solution. For the service, a battery with effective backup is needed in islanded mode. In the grid-connected mode, as per scheduling schemes, the overall cost of the microgrid device decreases by means of grey wolf optimization.

## 5.1. KARABUK UNIVERSITY MICROGRID MODELING

The Karabuk university microgrid device consists of different parts of the structure. Generating, storing and assembling. The segment that follows is discussion of the different models of DGs.

### 5.1.1. Solar PV Generation of Power and Calculation of Solar PV Costs

The photovoltaic (PV) panel output power is calculated using Equation (5.1) adopted from,

$$P_{PV} = 3.24 \times N_{PV}[1 - 0.0041 \times (T_{PV} - 8)] \times G_h \quad (5.1)$$

Where, solar output power (kW) is $P_{PV}$, $N_{PV}$ is generating capacity from all PV panels, $T_{PV}$ is temperature, and $G_{PV}$ is solar radiation at h time (kW/m$^2$). The clean energy subsidy includes state tax and federal solar panel incentive incentives. Therefore, the consideration of renewable energy conversion helps in the lowering of solar investment costs. The new decreased expenditure expense due to the renewable energy conversion consideration is estimated in the Eq. (5.2) in the following way:

$$C_P' = C_P - (C_P \times S_h) - [C_P \times (1 - S_h) \times F_h] \quad (5.2)$$

Where $C_P'$ reduces investment costs (\$/kW), $C_P$ is the true investment expense (\$/kW), $S_h$ is a national tax subsidy (percent) and $F_h$ is a state tax subsidy.

### 5.1.2. Battery Charging and Discharging Modeling

The formula for charging of Battery ($E_B(h) < 0$):

$$Q_C(h) = (1 - \alpha) \times Q_C(h - 1) - (E_B(h) \times \Delta h \times \eta_h) \quad (5.3)$$
$$-\eta_h \times E_B(h) \leq L_C \times Q_{Cmax}$$

The formula for discharging of Battery ($E_B(h) > 0$):

$$Q_C(h) = (1-\alpha) \times Q_C(h-1) - (E_B(h) \times \Delta h \times \eta_{h1}) \quad (5.4)$$

$$\frac{E_B(h)}{\eta_{h1}} \leq L_d \times Q_{Cmax} \quad (5.5)$$

The charging capacity, charging efficiency, discharge efficiency and self-discharge are expressed by $E_B(h)$, $\eta_h$, and $\eta_{h1}$ in percentage per hour, respectively. $L_C$ and $L_d$ are full rated power numbers. $Q_{Cmax}$, $Q_C(h)$, $Q_C(h-1)$ reflects the full power of the battery, the charge status of the battery in $h$ and $h-1$ cycles respectively.

### 5.1.3. Economic Load Dispatch in Microgrid

For the microgrid, the device operating cost $MG$ is listed below:

$$MG = MGC_{fuel} + MGC_{OM} + MGC_{DC} + GI\left(\sum Y_h^r R_h^r + C_{grid} + C_{diesel}\right) \quad (5.6)$$

$$MGC_{fuel} = L_{fc} \times E_i(h) \quad (5.7)$$

$$MGC_{OM} = L_{OM} \times E_i(h) \quad (5.8)$$

$$MGC_{DC} = \frac{DC}{E_{imax} \times 8760 \times FC} \times E_i(h) \quad (5.9)$$

$$DC = \frac{(I\_cost \times b \times (1+b)^m)}{((1+b)^m - 1)} \quad (5.10)$$

$$C_{grid} = a_2 + a_1 \times P_{G1} + a_0 \times {P_{G1}}^2 \quad (5.11)$$

$$C_{diesel} = a_2 + a_1 \times P_{G2} + a_0 \times {P_{G2}}^2 \quad (5.12)$$

Where $MGC_{fuel}$, $MGC_{OM}$, $MGC_{DC}$, $C_{grid}$ and $C_{diesel}$ illustrates the expense of fuel consumption, cost of service maintenance, cost of depreciation, cost of the grid and cost of diesel gen-set, respectively. $P_{G1}$ and $P_{G2}$ are power sharing of the grid and

diesel gen-set of the system. The spinning reserve price and the purchase power respectively reflect $Y_h^r \; and \; R_h^r$. $GI$ is equal to one and zero respectively in grid connected and island mode. $E_i(h)$ reflects the output power of the DGs, $L_{fc}$ and $L_{OM}$ reflects the fuel usage, operation control coefficients. $FC$, $DC$ and $I\_cost$ reflect the power factor, the cost of depreciation in kilowatt hours and the cost of installation, respectively. $b$ represents the rate of interest equal to 8% and $m$ represents the lifetime of DGs.

### 5.1.4. The Primary Objective Feature of The Microgrid System's Economic Load Dispatch

For the complex economic dispatch of the microgrid, the goal function is to minimize the aggregate cost with optimum detailed benefits.

$$minimize \; C_T = MG \tag{5.13}$$

The constraints used in the microgrid:

$$\sum_{i=1}^{N} E_i + P_{G1} + P_{G2} + E_B = P_{load} \tag{5.14}$$

$$E_{imin} \leq E_i \leq E_{imax} \tag{5.15}$$

$$P_{G1min} \leq P_{G1} \leq P_{G1max} \tag{5.16}$$

$$P_{G2min} \leq P_{G2} \leq P_{G2max} \tag{5.17}$$

$$E_{Bmin} \leq E_B \leq E_{Bmax} \tag{5.18}$$

$$Q_{Cmin} \leq Q_C \leq Q_{Cmax} \tag{5.19}$$

where: $E_{imin} \; and \; E_{imax}$ represents minimum and maximum limits of power generation of Solar PV.

$P_{G1min} and \; P_{G1max}$ represents minimum and maximum limits of power sharing of the grid.

$P_{G2min} and \; P_{G2max}$ represents minimum and maximum limits of power sharing of the diesel gen-set.

$E_{Bmin} \; and \; E_{Bmax}$ represents minimum and maximum limits of power sharing of the battery.

$Q_{Cmin} and\ Q_{Cmax}$ minimum and maximum limits of charge of the battery Set at 10% and 90% of the total power, respectively.

The microgrid consumes electricity from the grid if the $P_{G1}$ is positive, and the microgrid gives power to the grid if the $P_{G1}$ is negative. Similarly, the battery gets discharged if $E_B$ is positive, and the battery gets charged if $E_B$ is negative. The objective function mentioned in the equation (5.7) is optimized using grey wolf algorithm.

## 5.2. GREY WOLF OPTIMIZATION

A new population is based on the methodology of swarm intelligence, called the grey wolf optimizer, inspired by the nature and grey wolf attributes described in this section. Mirjalili et al. have applied this methodology (2014).

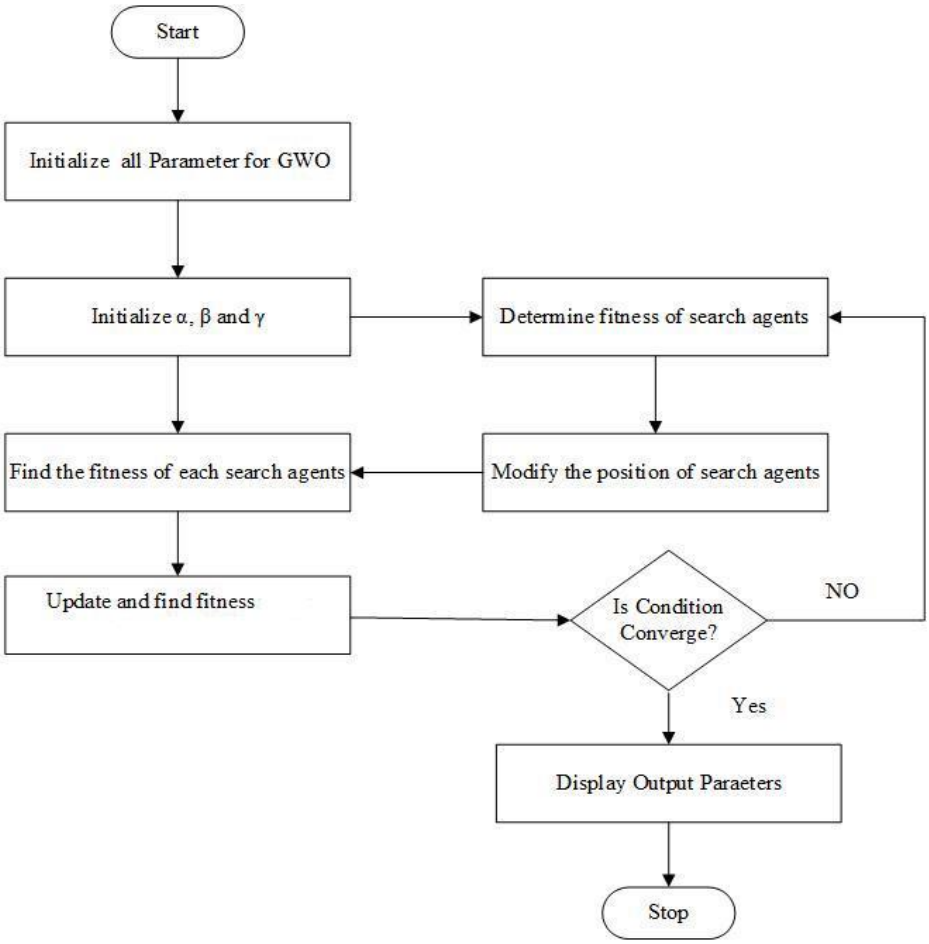


Figure 5.1. Flow chart for grey wolf optimization.

### 5.2.1. GWO Algorithm in Microgrid Economic Dispatch

The step-by-step GWO algorithm method for optimization of microgrid is given by:

1. Initialize all GWO algorithm input parameters, such as search agents-no (population size), number of control variables (problem dimension) by controller form, upper and lower search space limits, number of parameters of elitism, and total number of generations.
2. Search agents of grey wolves (i.e., power generation of grid, diesel gen-set) are randomly generated between upper and lower boundaries in the search space during the initialization process.
3. Calculate the fitness of every search agent in the search space and assign alpha, beta, delta wolves.
4. Updating the alpha, beta, and delta positions
5. Update the quest agent locations, like omega,
6. Finally, for each search agent, change the control variables (power generation of grid, diesel gen-set).
7. Check whether or not every search agent moves outside the search space and the randomly generated viable solution set is replaced by infeasible solutions.
8. For the next generation, sort the quest agent positions acquired in step 5 from the best value to the worst value and use them.
9. Switch to step 4 before fulfillment of the completion criteria.

The flow map of the optimal power generation of the microgrid using GWO algorithm is shown in Figure 5.1.

## 5.3. SIMULATION ANALYSIS OF ECONOMIC LOAD DISPATCH IN KBU MICROGRID

In this section, simulation of economic load dispatch of the Microgrid is explained in detailed. The specifications of the Microgrid are shown in the Table 5.1.

Table 5.1. Specification of KBU Microgrid.

| Component | Name | Size | Unit |
|---|---|---|---|
| Generator | Kohler 410kW Standby | 410 | kW |
| PV | Generic flat plate PV | 36.6 | kW |
| Battery Storage | Hitachi LL1500-W | 40 | kW |
| System Inverter | ABB Pro33 | 33.0 | kW |
| Utility | Safranbolu TEDAŞ | | |
| Critical Load | | 400 | kW |
| Non-critical Load | | 700 | kW |

Fuel usage coefficient, operation control coefficients, capacity factor, the cost of depreciation in kilowatt hours, the cost of installation, and the rate of interest and lifetime of DGs are presented in the Table 5.2.

Table 5.2. Parameter used in the operating cost of Microgrid.

| Description | Value | Unit |
|---|---|---|
| Fuel usage coefficient ($\boldsymbol{L_{fc}}$) | 0.8 | $/kW |
| operation control coefficient ($\boldsymbol{L_{OM}}$) | 0.4 | $/kW |
| capacity factor ($\boldsymbol{FC}$) | 0.9 | - |
| cost of installation ($\boldsymbol{I\_cost}$) | 1.02 | $/kW |
| Rate of interest *(b)* | 0.08 | % |
| lifetime of DGs *(m)* | 100 | Years |

The fuel cost coefficient of the grid and diesel gen-set is presented in the Table 5.3.

Table 5.3. Fuel cost coefficient of grid and diesel gen-set.

| Description | $\boldsymbol{a_0}$ | $\boldsymbol{a_1}$ | $\boldsymbol{a_2}$ |
|---|---|---|---|
| Grid | 0.004 | 5.3 | 500 |
| Diesel Gen-set | 0.042 | 7.8 | 101.5 |

Limit constraints for the different source of the Microgrid is shown in Table 5.4.

Table 5.4. Limit constraints for the different source of the Microgrid.

| Description | Minimum | Maximum | Unit |
|---|---|---|---|
| Grid Power | 0 | 800 | kW |
| Diesel Gen-set | 0 | 400 | kW |
| PV Panel | 0 | 36.6 | kW |
| Battery | 0 | 40 | kW |
| State of charge of battery | 20 | 100 | % |

The spinning reserve and purchasing power price for 24 hours are shown in the Figure 5.2.


Figure 5.2. Spinning reserve and purchasing of power price.

The PV power for each year has been collected for one year for solving economic load dispatch in micro grid. The PV panel output power for 24 hours in April 1$^{st}$ of 2019 is shown in the Figure 5.3. PV panel output for each month is shown in Figure 5.4.

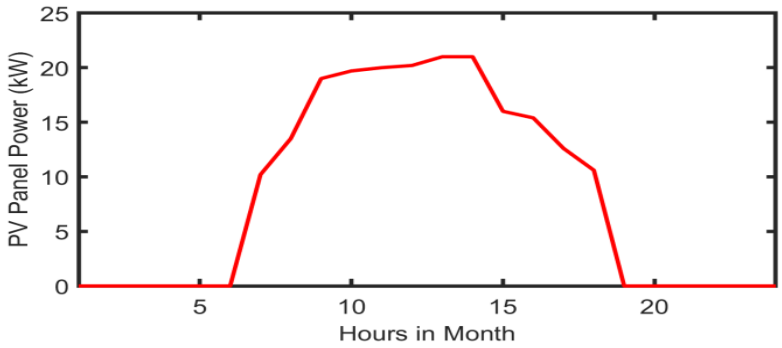


Figure 5.3. PV panel output power for 24 hours (1st April 2019).

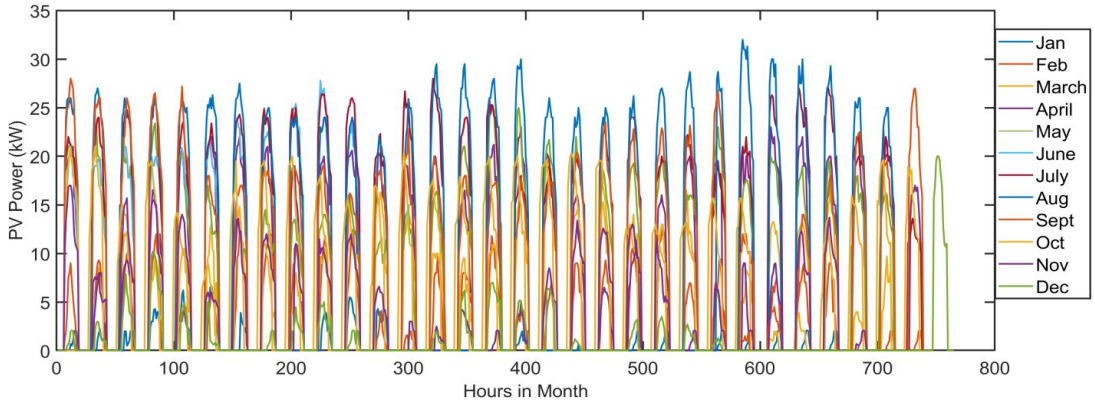


Figure 5.4. PV panel output power for 12 months (Year 2019).

The grey wolf algorithm for economic load dispatch for microgrid is developed in the MATLAB using m file script. The developed code was executed for all possible operating conditions. The optimization results for the 1st April 2019 is shown in Figure 5.5 and provided in the Table 5.5

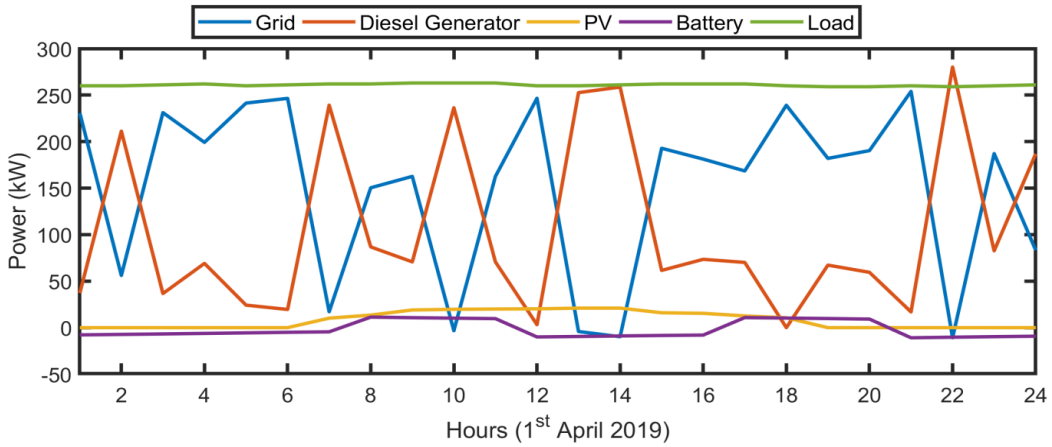


Figure 5.5. The grey wolf optimized result of micro grid (1st April 2019).

Table 5.5. KBU MG optimization results for 1st April 2019.

| Hour | Load (kW) | PV Power (kW) | Battery Power (kW) | Grid power (kW) | Diesel gen-set power (kW) | Total electricity cost ($/kW·h) | Mode of operation |
|---|---|---|---|---|---|---|---|
| **1** | 260 | 0.0 | -7.8 | 230.7 | 37.1 | 0.2392 | Battery charging mode + grid supply power + diesel gen-set supply power |
| **2** | 260 | 0.0 | -7.3 | 56.1 | 211.2 | 0.4449 | Battery charging mode + grid supply power + diesel gen-set supply power |
| **3** | 261 | 0.0 | -6.8 | 231.1 | 36.7 | 0.2391 | Battery charging mode + grid supply power + diesel gen-set supply power |
| **4** | 262 | 0.0 | -6.2 | 199.2 | 69.1 | 0.2589 | Battery charging mode + grid supply power + diesel gen-set supply power |
| **5** | 260 | 0.0 | -5.6 | 241.4 | 24.2 | 0.2331 | Battery charging mode + grid supply power + diesel gen-set supply power |
| **6** | 261 | 0.0 | -5.0 | 246.5 | 19.5 | 0.2348 | Battery charging mode + grid supply power + diesel gen-set supply power |
| **7** | 262 | 10.2 | -4.5 | 17.1 | 239.2 | 0.4997 | Battery charging mode + grid supply power + diesel gen-set supply power + PV supply the power |
| **8** | 262 | 13.5 | 11.3 | 150.4 | 86.8 | 0.2522 | Battery discharging mode + grid supply power + diesel gen-set supply power + PV supply the power |

Cont. Table 5.2

| | | | | | | | |
|---|---|---|---|---|---|---|---|
| **9** | 263 | 19.0 | 10.7 | 162.6 | 70.7 | 0.2371 | Battery discharging mode + grid supply power + diesel gen-set supply power + PV supply the power |
| **10** | 263 | 19.7 | 10.2 | -3.3 | 236.4 | 0.4826 | Battery discharging mode + grid receive power + diesel gen-set supply power + PV supply the power |
| **11** | 263 | 20.0 | 9.7 | 162.6 | 70.7 | 0.2378 | Battery discharging mode + grid supply power + diesel gen-set supply power + PV supply the power |
| **12** | 260 | 20.2 | -10.0 | 246.6 | 3.2 | 0.2218 | Battery charging mode + grid supply power + diesel gen-set supply power + PV supply the power |
| **13** | 260 | 21.0 | -9.5 | -4.2 | 252.7 | 0.5295 | Battery charging mode + grid receive power + diesel gen-set supply power + PV supply the power |
| **14** | 261 | 21.0 | -8.9 | -9.8 | 258.6 | 0.5463 | Battery charging mode + grid receive power + diesel gen-set supply power + PV supply the power |
| **15** | 262 | 16.0 | -8.4 | 192.9 | 61.5 | 0.2459 | Battery charging mode + grid supply power + diesel gen-set supply power + PV supply the power |

Cont. Table 5.2

| | | | | | | | |
|---|---|---|---|---|---|---|---|
| **16** | **262** | **15.4** | **-8.0** | **181.2** | **73.4** | **0.2547** | Battery charging mode + grid supply power + diesel gen-set supply power + PV supply the power |
| **17** | 262 | 12.6 | 10.8 | 168.5 | 70.1 | 0.2390 | Battery discharging mode + grid supply power + diesel gen-set supply power + PV supply the power |
| **18** | 260 | 10.6 | 10.3 | 239.1 | 0.0 | 0.2123 | Battery discharging mode + grid supply power + diesel gen-set supply power + PV supply the power |
| **19** | 259 | 0.0 | 9.8 | 182.0 | 67.2 | 0.2442 | Battery discharging mode + grid supply power + diesel gen-set supply power |
| **20** | 259 | 0.0 | 9.2 | 190.3 | 59.5 | 0.2388 | Battery discharging mode + grid supply power + diesel gen-set supply power |
| **21** | 260 | 0.0 | -10.9 | 254.0 | 16.9 | 0.2353 | Battery charging mode + grid supply power + diesel gen-set supply power |
| **22** | 259 | 0.0 | -10.3 | -10.8 | 280.1 | 0.6062 | Battery charging mode + grid supply power + diesel gen-set supply power |
| **23** | 260 | 0.0 | -9.7 | 187.1 | 82.6 | 0.2680 | Battery charging mode + grid supply power + diesel gen-set supply power |
| **24** | 261 | 0.0 | -9.2 | 83.3 | 186.8 | 0.4034 | Battery charging mode + grid supply power + diesel gen-set supply power |

From the Table 5.5, the operation of Microgrid classified into six and each mode is highlighted in different color for better understanding of the optimized data. The Battery charging mode + grid supply power + diesel gen-set supply power is highlighted in orange color. Battery charging mode + grid supply power + diesel gen-set supply power + PV supply the power is highlighted in green color. Battery discharging mode + grid supply power + diesel gen-set supply power + PV supply the power is highlighted in yellow color. Battery discharging mode + grid receives power + diesel gen-set supply power + PV supply the power is highlighted in blue color. Battery charging mode + grid receives power + diesel gen-set supply power + PV supply the power is highlighted in grey color. Battery discharging mode + grid supply power + diesel gen-set supply power is highlighted in red color. From these results, grey wolf optimization is effectively optimizing the economic load dispatch of the considered microgrid system. The optimization results of each month are shown in Appendix A.

In this chapter, we used the different agent values and implemented in the proposed method. Also, we calculated the efficiency of these parameter in the cost of the energy. This scenario is shown in Table 5.6.

Table 5.6. The energy cost related to GWO agent values.

| **Number of search agents** | **Grid** | **Diesel Generator** | **Load** | **PV** | **Battery** | **Total energy (kW)** | **Total Cost ($/kW·h)** |
|---|---|---|---|---|---|---|---|
| 5 | 99.777 | 175.789 | 281.317 | 7.287 | 1.549 | 284.402 | 0.4675 |
| 10 | 112.051 | 163.526 | 281.317 | 7.287 | 1.549 | 284.415 | 0.4381 |
| 15 | 118.963 | 156.612 | 281.317 | 7.287 | 1.549 | 284.412 | 0.4096 |
| 20 | 129.095 | 146.482 | 281.317 | 7.287 | 1.549 | 284.414 | 0.3924 |
| 25 | 145.775 | 129.8046 | 281.317 | 7.2872 | 1.5493 | 284.416 | 0.3874 |
| 30 | 144.9619 | 130.6142 | 281.317 | 7.2872 | 1.5493 | 284.4126 | 0.3562 |

As seen in Table 5.6 the PV, Battery and Load are not changed in all scenarios, and PV, Battery and Load are fixed to 7.2872 kW, 1.5493 kW and 281.3176 kW, respectively. However, Grid and Diesel generator values are changed. The lowest total electricity cost value is 0.3562 $/kW·h that is obtained if number of agents as 30. The

highest energy value for the Grid is obtained as 145.775 kW and 175.7890 kW for diesel generator, respectively when we select the number of agents as 25 and 5. That mean refers to that the 5 agents and 25 agents value are best values for the GWO algorithm where total electricity cost value are 0.4675 $/kW·h and 0.3874 $/kW·h, respectively.

# PART 6

# COMPARISON OF MULTI-AGENT BASED AND GREY WOLF OPTIMIZATION METHODS RESULTS

In this chapter, a multi-agent system (MAS) of KBU MG has been designed and conducted on the JADE platform and merged with the KBU MG simulation model on the MATLAB/Simulink. Also, the accompanying simulation outcomes are discussed and compared with GWO results.

## 6.1. MULTI-AGENT SYSTEM STRUCTURE OF KBU MG

Multi-agent based MG structure of KBU Engineering faculty has been designed. Multi-agent based KBU MG consists of the following agents:

- ***Control Agent (CA)***: This agent is responsible to control of the system frequency and voltage and acts to change MG mode to island mode at a common coupling point (PCC). It also delivery signals to DERs.
- ***DER Agent***: DER agent collects the information related to distributed generation sources. Additionally, it observes and controls power levels of DER.
- ***Load Agent (LA)***: This agent consists of data of loads profiles like critical load and non-critical load profiles.

Figure 6.1 shows the block diagram for proposed MAS of KBU MG.

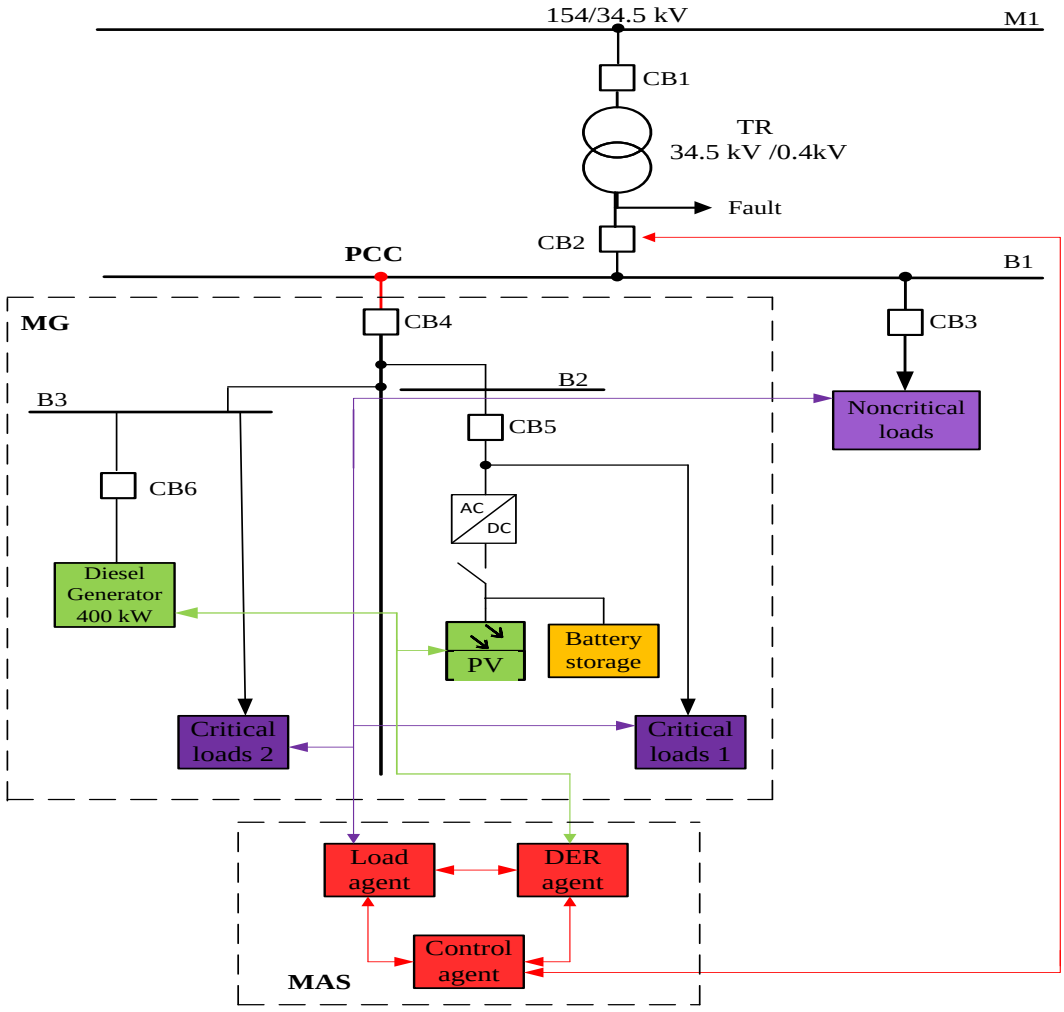


Figure 6.1. Multi-agent based KBU MG control.

The same technical characteristics of KBU MG components (see Table 5.1) have been utilized for designing and implementation of MAS [139].

Flow-chart of MAS based control is shown in Figure 6.4.

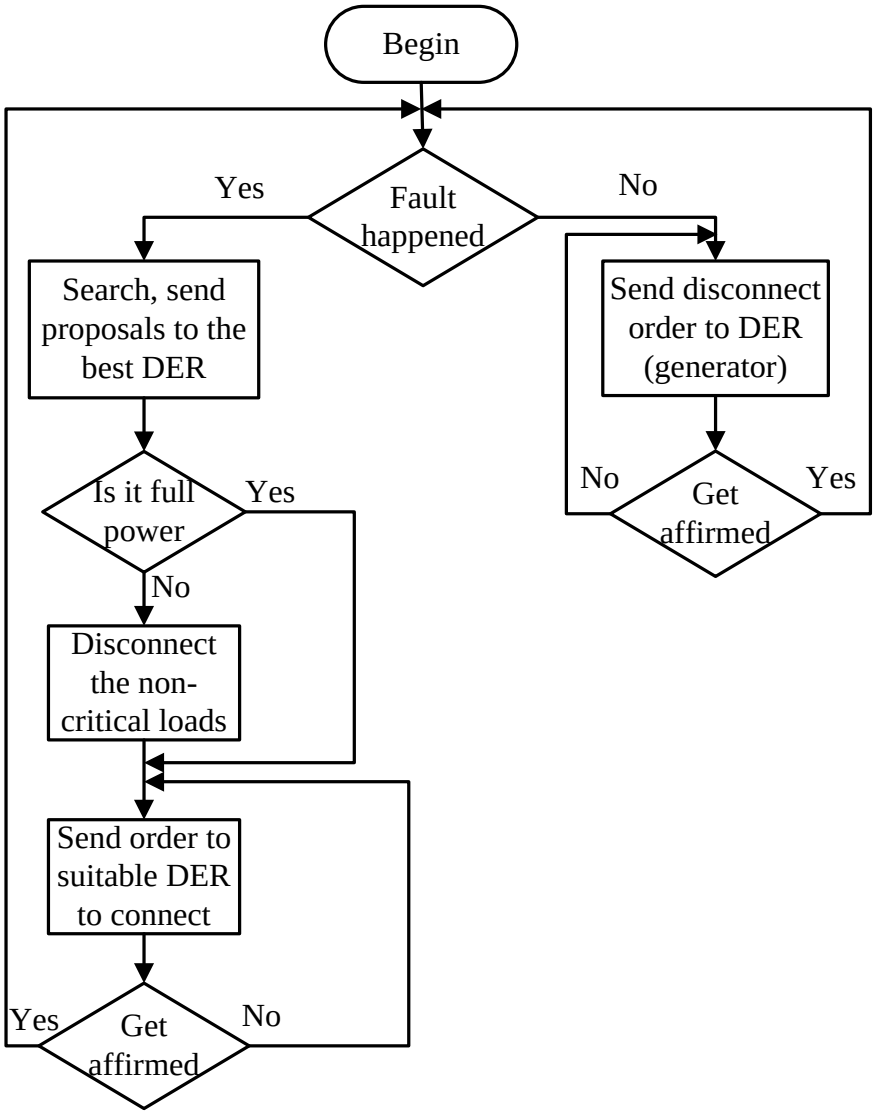


Figure 6.2. Flow-chart of multi-agent based control.

## 6.2. MICROGRID SIMULATION CIRCUIT DESCRIPTION

According to the Figure 6.1 the Microgrid simulation circuit and MAS control implementation can be explained. The simulation testbed in MATLAB/Simulink contains of two DERs (PV panels and diesel generator), grid interface for connecting the PV panels to the network, three loads (critical load 1, critical load 2 and non-critical load).

Firstly, KBU MG is simulated using MATLAB/Simulink to obtain main results (voltages and currents of critical load 1, critical load 2, and non-critical load). Then

these results have transmitted to JADE platform to examine the operation of MAS and estimate the functioning of MAS. Microgrid disconnection during fault status or power outage for securing loads (critical loads) with the available energy of DERs is the main goal of the MAS. In islanded operation mode, if the loads are greater than the capacity of DERs, then non-critical loads should be disconnected.

## 6.3. OPTIMIZATION OF MICROGRID

The goal of MAS-based microgrid optimization is to present the effectively controlled view of MG in a active distribution network by increasing economic advantages. MAS has been proposed to control and make a power balance between load demand and generated power by grid and DERs to provide efficiency and reduce fuel cost of MG.

### 6.3.1. Proposed Approach

The main concept behind the suggested approach is designing a representative agent for each microgrid component. This methodology largely depends on the agents' and their elements' abilities to exchange information. This information exchange is bi-directional. In the first direction, measurements, such as power, voltage, and current, are regained. The second direction relates to physical aspects of a microgrid, and it performs various significant functions, such as ON/OFF, circuit breaking, and mode conversion (grid-connected to island or vice versa). It means that a multi-agent system submits to the microgrid's intelligent interface while every agent is already installed on the system.

MAS architecture of KBU MG is shown in Figure 6.3 which comprises of two distributed energy resources (PV panels and generator) and three loads. The following MG components and function are represented by the local agents:

- DERs are represented as power generation agent.
- Loads as load agent for loads.
- To control connection/disconnection MG to main grid at PCC is represented by control agent.

- Delivery data and connection – monitoring agent.

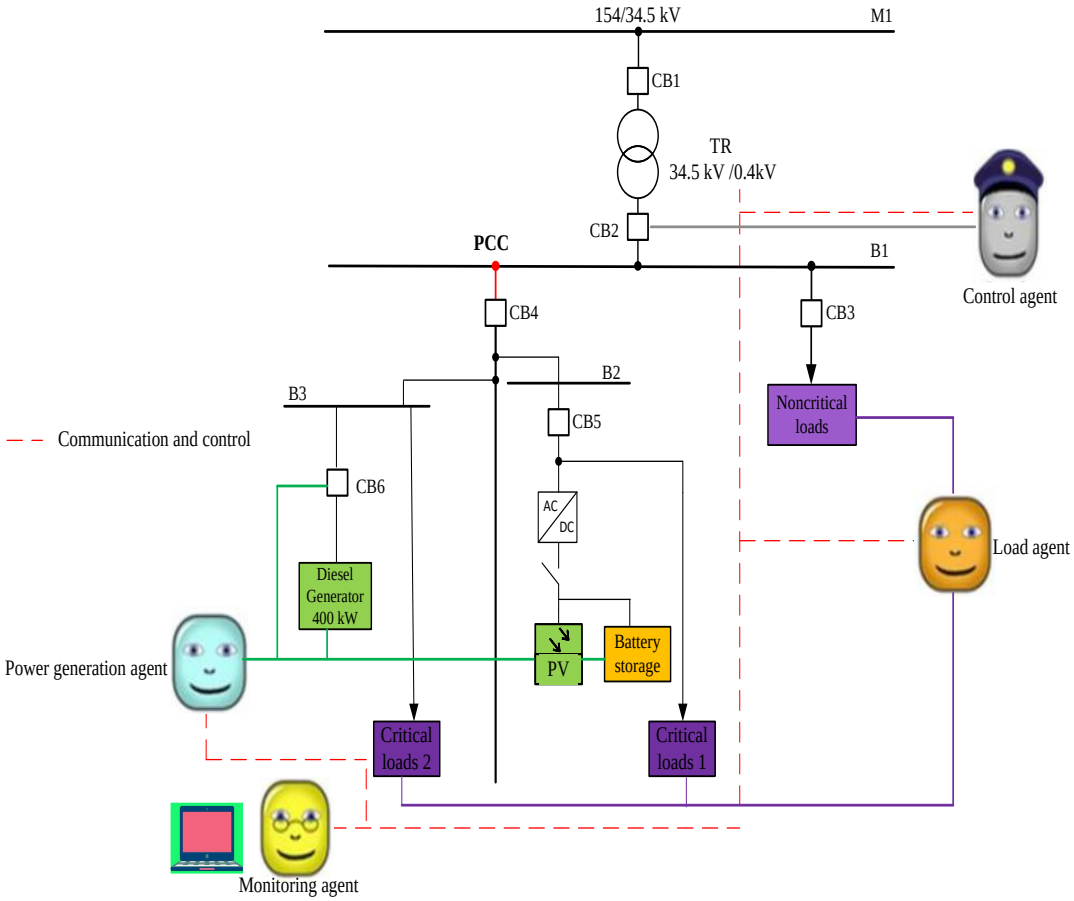


Figure 6.3. MAS architecture of KBU MG.

The precept of the proposed management approach depends on information exchanged by messages between agents to make appropriate decisions. The proposed algorithm for the management of operation is represented in Figure 6.4. It is imperative to take note of that the drawn graph shows both the program of management and the cooperation among agents. Where: Pd is demand for power, Ppv is the produced power from PV panels and Pgen is the produced power from the generator. The multi-agent system should be capable to manage events, for example, the demand for power. For this event, and as we know the operation modes of the MG are grid/island modes. In this study, two cases are possible for island mode:

- If the amount of produced power from the PV panels is greater than or equal to the demand for power Pd, loads are fed according to messages exchanged among the power generation agent and load agent.
- If the produced power from PV panels not sufficient to feed loads the power generation agent transmits power request to the generator to be compensated for power shortages.

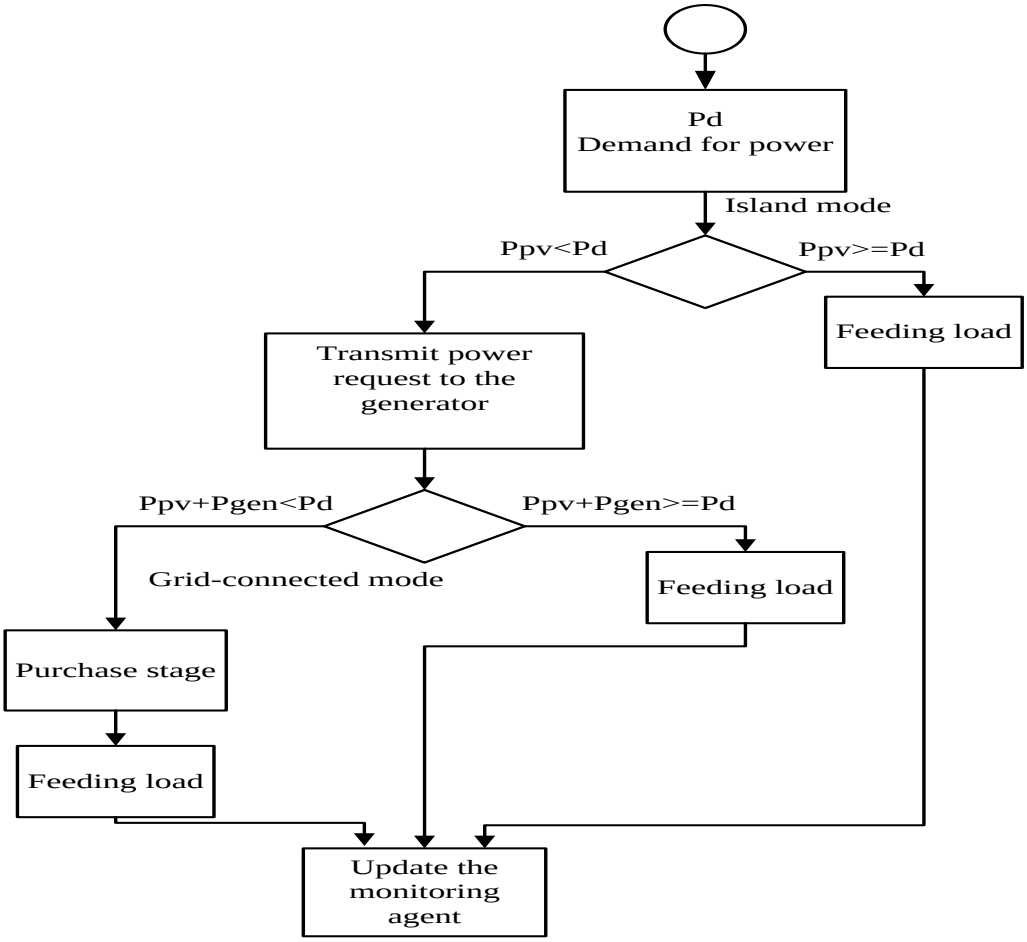


Figure 6.4. Operation of MG depending on the proposed management algorithm.

If the amount of power from PV panels and generator is not enough to feed all loads, the management of this case relies upon the operation mode of the MG. The control agent connects the main grid to the MG and starts a power purchase stage. The multi-agent system takes decisions dependent on an optimization algorithm which determines the minimal cost of power.

### 6.3.2. Implementation of Agents

In this subsection, the functions and responsibilities of the following agents have been conducted on JADE platform:

- Load agent: It is responsible for specifying the amount of load demand or power which is received from the microgrid and main grid, also it informs power generation agent and control agent by details.
- Power generation agent: It is used to control the power generation from the PV panels, generator and main grid based on settings of the load demand or load power from the load agent.
- Control agent: It controls the operation modes of the MG (grid-connected mode and island mode) depended on the details which are received from power generation and load agents.
- Monitoring agent: The monitoring agent is used to display the actual load power, power generation, system efficiency and operation modes of the system according to information from the load agent, power generation agent and control agent.

## 6.4. SIMULATION RESULTS AND ANALYSIS

MAS is implemented on the JADE platform and interconnected with MATLAB/Simulink via MACSimJX.
Two load profile settings (is how much amount of maximum load connected to the system) with fourteen cases have been used for the purpose of testing the proposed approach.

Based on load profile settings the amount of power that generation units will supply to the loads is the main task of the MAS.

Once as the simulation begins, the agents initiate to perform their tasks. The agents initiate communications and share information between each other and JADE

exchanges information with MATLAB/Simulink through MACSimJX. Figure 6.5 demonstrates a graphical user interface (GUI) of the sniffer agent.

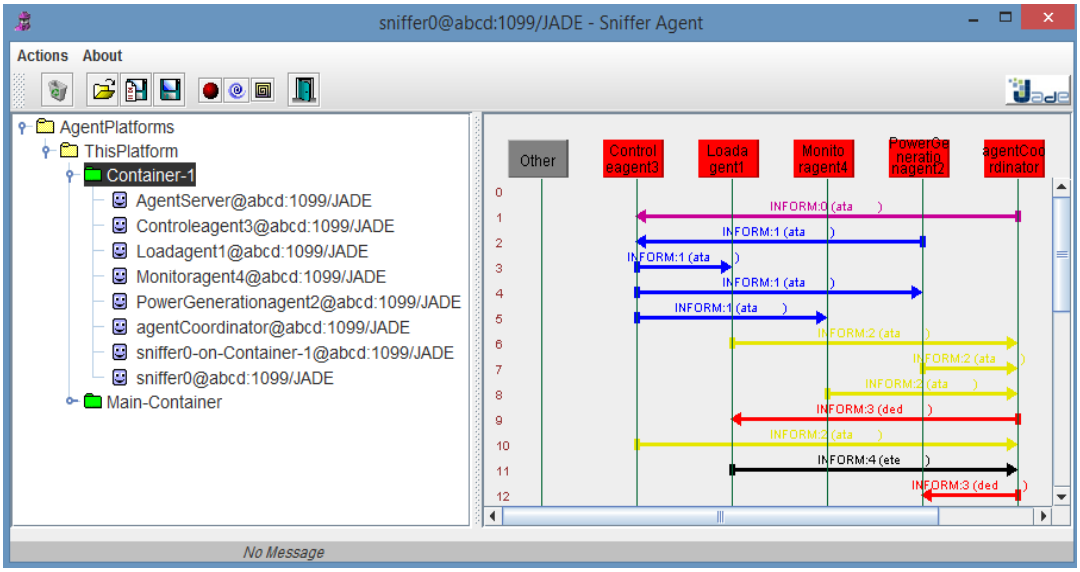


Figure 6.5. Communication and interaction among agents.

The outcomes of performance of the proposed agents for each load profile setting have been displayed. In Table 6.1 are given loads profile settings for different conditions. The total loads profile setting (Laod1, Load 2, Load 3) without MAS is given on Table 6.1 and its graphical view is shown in Figure 6.6.

Table 6.1. Loads profile setting.

| TIME (sec) | LOAD 1 (kW) | LOAD 2 (kW) | LOAD 3 (kW) | TOTAL (kW) |
|---|---|---|---|---|
| 0-0.1 | 17 | 195 | 0 | 17 |
| 0.1-0.2 | 0 | 195 | 0 | 195 |
| 0.2-0.3 | 17 | 195 | 0 | 212 |
| 0.3-0.4 | 0 | 0 | 550 | 550 |
| 0.4-0.5 | 17 | 0 | 550 | 567 |
| 0.5-0.6 | 0 | 195 | 550 | 745 |
| 0.6-0.7 | 17 | 195 | 550 | 762 |

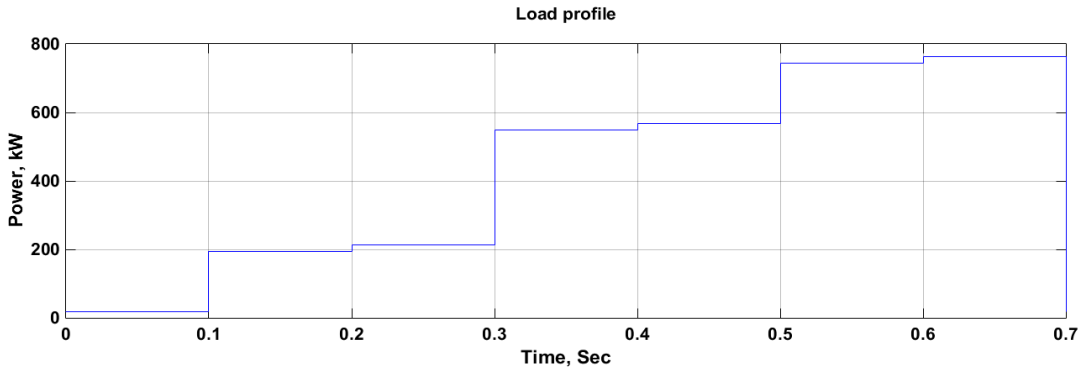


Figure 6.6. Total load profile setting.

Table 6.2 shows operation modes of microgrid during different loads.

Table 6.2. Operation modes of the microgrid during different loads.

| **TIME (sec.)** | 0-0.1 | 0.1-0.2 | 0.2-0.3 | 0.3-0.4 | 0.4-0.5 | 0.5-0.6 | 0.6-0.7 |
|---|---|---|---|---|---|---|---|
| **LOAD (kW)** | 17 | 195 | 212 | 550 | 567 | 745 | 762 |
| **OPERATION MODES** | Island mode | Island mode | Island mode | Grid mode | Grid mode | Grid mode | Grid mode |

The load profile setting performance under suggested MAS is shown in Figure 6.7**.**

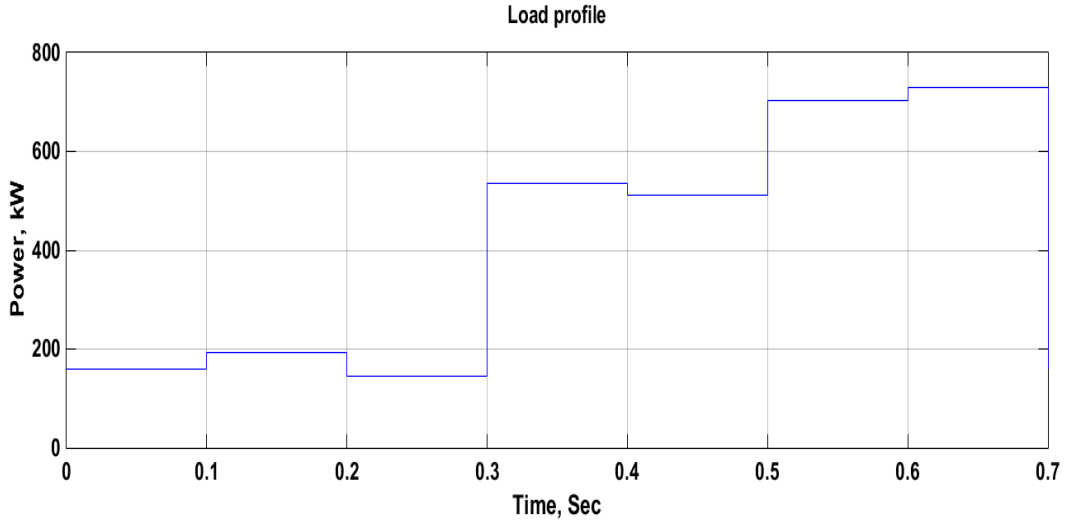


Figure 6.7. Load profile setting performance using MAS.

In Figure 6.8 we can see the power balance of "PV – diesel generator – main grid" system.

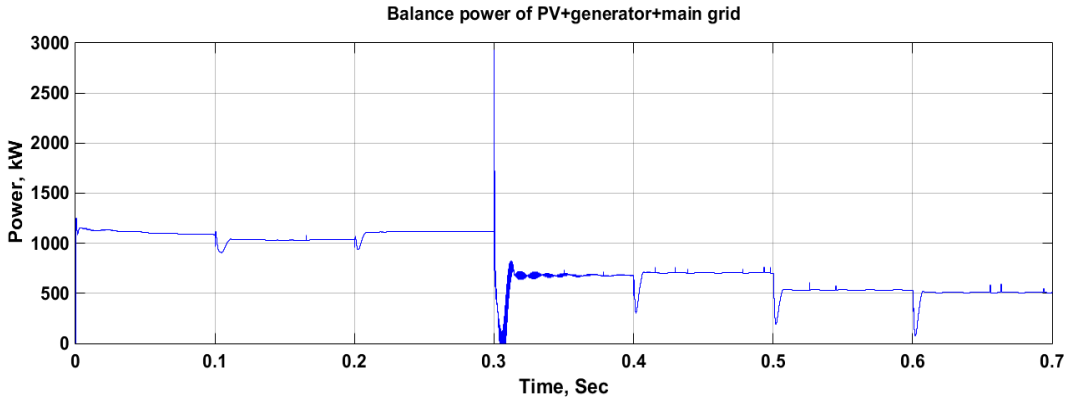


Figure 6.8. Power balance "PV – generator – main grid" system.

## 6.5. COMPARISON GREY WOLF OPTIMIZATION AND MAS RESULTS

In this subchapter, GWO and MAS optimization results of KBU MG are compared. Using limit constraints for the different source of the KBU MG (see Table 5.4) we determined daily the spinning reserve and purchasing power price based on MAS. The spinning reserve and purchasing electricity price for 24 hours which are obtained using MAS are shown in the Figure 6.9.

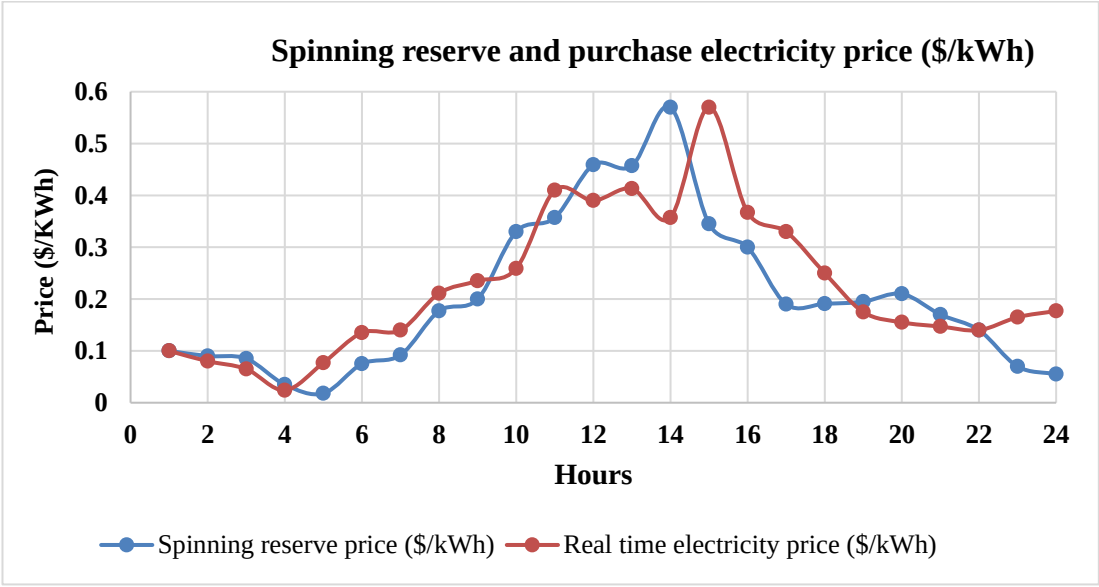


Figure 6.9. Spinning reserve and purchasing electricity price.

The comparison of the spinning reserve and purchasing electricity price optimization results between GWO and MAS techniques are presented in Figure 6.10. It should be

noted, the electricity prices accepted by GWO are more lesser than the electricity prices in MAS.

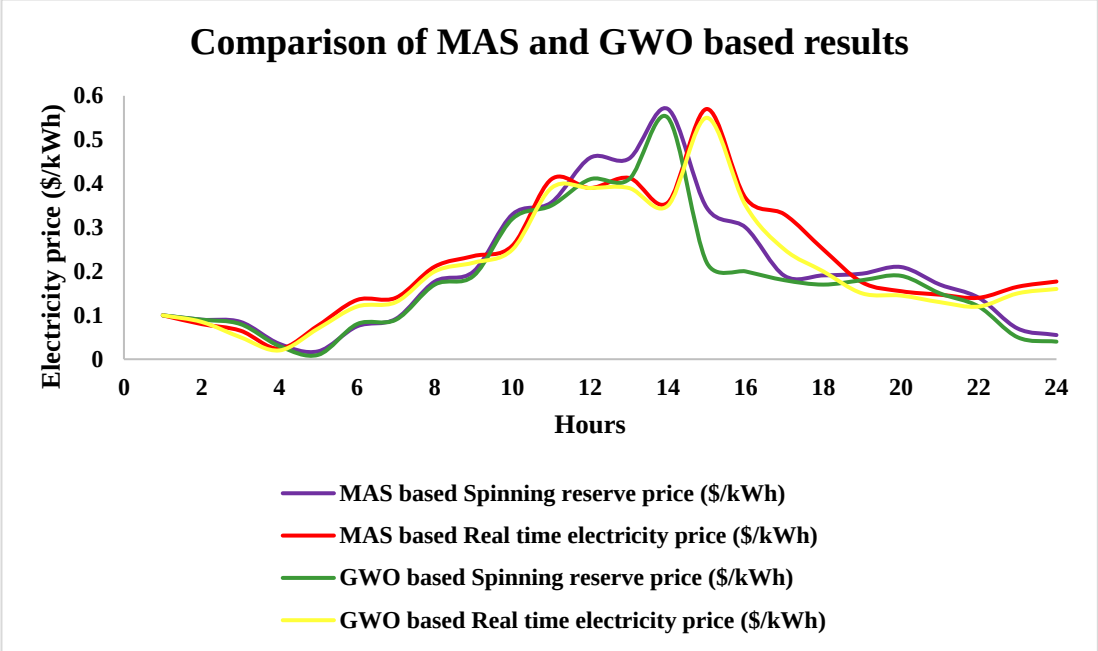


Figure 6.10. The comparison optimization results of GWO and MAS techniques.

The PV panel output power based on MAS for 24 hours (April 1st of 2019), and the comparison of PV panel output power between two methods are shown in the Figure 6.11 and Figure 6.12, respectively. The comparison two method results show that PV power generated by GWO method is lesser more than PV power generated using MAS.

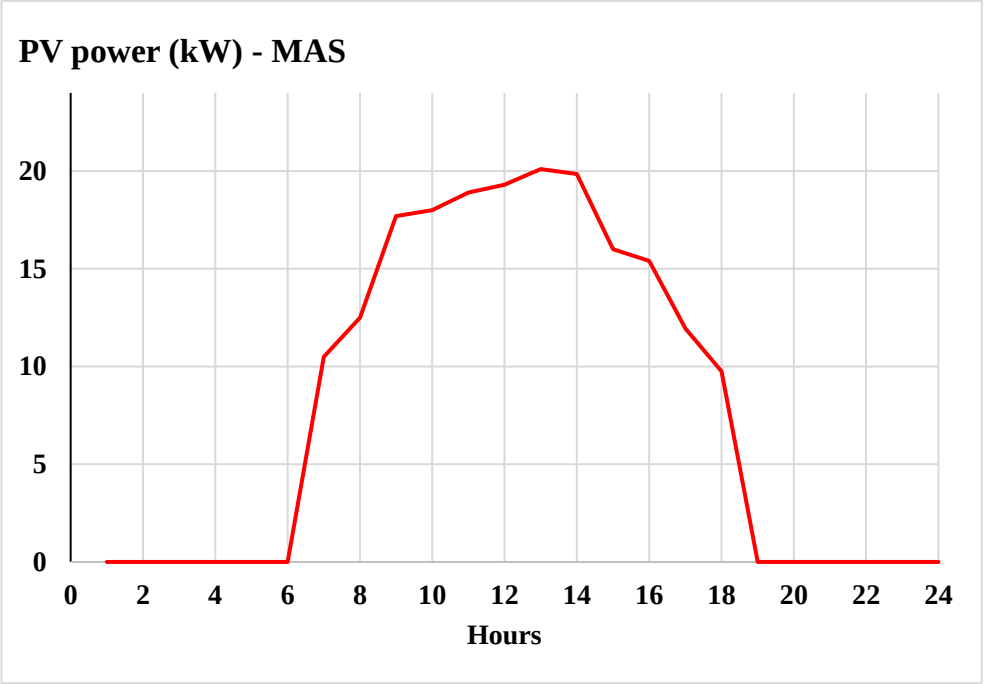


Figure 6.11. PV power of 24 hours based on MAS (1st April 2019).

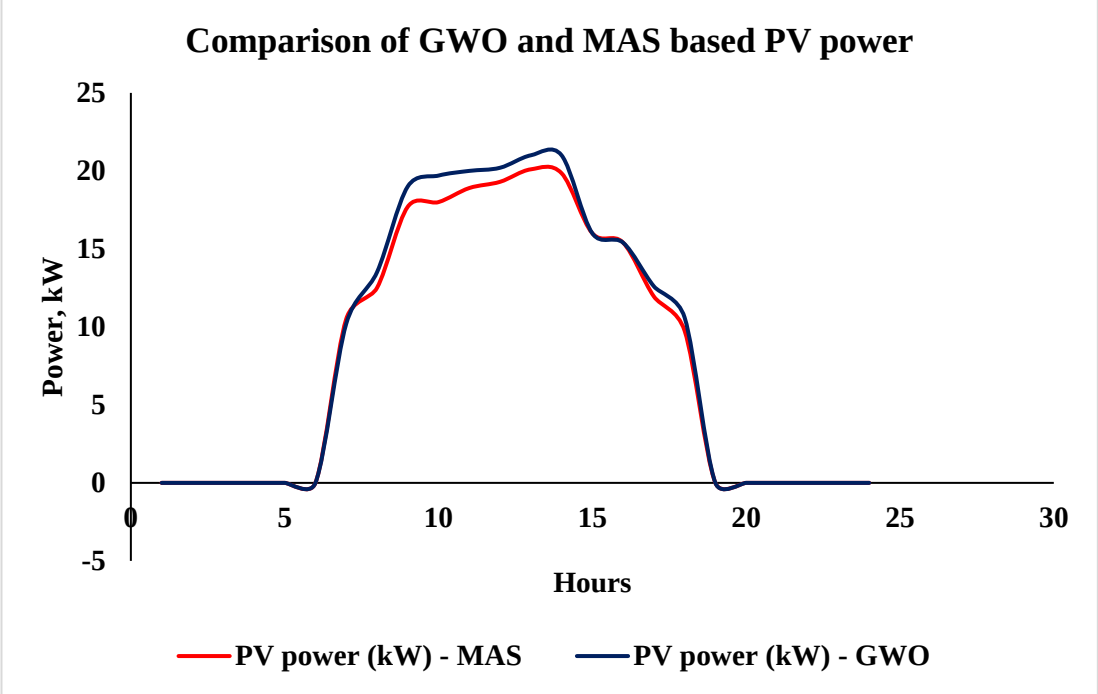


Figure 6.12. Comparison of PV panel power based on MAS and GWO methods.

## PART 7

## CONCLUSION

The traditional distribution network is usually connected to the main network, which feeds the loads alone. The distance between the load and the mains is relatively long, which causes high losses and voltage drops in the network. The use of renewable energy sources has brought many advantages. The first advantage of using renewable sources is that the reliability of the system is improved because it is often powered by multiple energy sources. The second point is to reduce the distance between the power generator and the power consumer; Of course, the disadvantages of renewable energy sources are changes and uncertainty of renewable energy sources, which can be eliminated by using energy storage devices.

In this research, quantitative and qualitative evaluation of renewable energy sources and energy storage resources are presented. At each level of problem evaluation, optimization takes place over a 24-hour period, one hour to one hour. Power distribution is two-way; This means that energy consumption and energy sales to the grid are possible, and the cost of energy consumption is also considered.

To minimize the fuel cost, maintenance cost, operating cost of the MG system grey wolf optimization technique has applied in this work. The MG system which is considered in this research work contains of: PV generation unit; battery energy storage device and diesel generator. The numerous restrictions are taken into consideration in order to enhance the MG system's performance and reliability. Analysis is conducted by considering the results of operating, maintenance and fuel cost for the scheduling of the systems in both modes – island and grid-connected modes. The grid-connected mode is favored over the island mode, since it is very difficult to provide an efficient battery consumption solution. For the service, a battery with effective backup is needed in islanded mode. In the grid-connected mode, as per

scheduling schemes, the overall cost of the microgrid device decreases by means of grey wolf optimization. The detailed investigation is carried out on power dispatch optimization and cost minimization in island mode and grid-connected mode of the microgrid system for all scheduling scheme with taking into account the impact of running costs.

It also discusses of MAS applications in MG and how to apply the suggested approaches for different modes operation of MG system.

Finally, GWO and MAS optimization results of KBU MG have been compared.

## 7.1. THESIS CONTRIBUTIONS

The following contributions have been made in this research work:

- The mathematical modelling of the PV panel, diesel engine, and battery in microgrid system along with economic power dispatch (EPD) problem is developed and analyzed.
- The dynamic EPD optimization is carried out using grey wolf optimization for both operating modes of the MG, i.e. island and grid-connected modes.
- MAS has developed for a KBU MG containing control agent, DER agent, and load agent.
- The results based on Grey wolf optimization technique and MAS of the spinning reserve and purchasing electricity price optimization KBU MG have compared.

## 7.2. RECOMMENDATION FOR FUTURE WORKS

Summarizing the thesis contributions, the following recommendations can be proposed for future works:

- The analyzing the protection of grid-connected microgrid and utilizing GWO technique for grid-connected hybrid microgrid.

- Microgrid considering with a different distributed generation, including wind energy, PV-systems, fuel cell for various types of distribution network.
- The comparison of GWO technique with swarm intelligence optimization methods such as genetic algorithm, particle swarm optimization, and ant colony.

## REFERENCES


1. Driesen, J. and Katiraei, F., "Design for distributed energy resources", ***IEEE Power and Energy Magazine***, 6 (3): 30-40 (2008).

2. Sun, Q., Li, Z. and Zhang, H., "Impact of distributed generation on voltage profile in distribution system", ***IEEE Book Impact of distributed generation on voltage profile in distribution system***, 249-252 (2009).

3. Tan, K., So, P., Chu, Y. and Chen, M., "Coordinated control and energy management of distributed generation inverters in a microgrid", ***IEEE transactions on power delivery***, (28) 2: 704-713 (2013).

4. Hirsch, A., Parag, Y., and Guerrero, J., "Microgrids: A review of technologies, key drivers, and outstanding issues," ***Renew. Sustain. Energy Rev.***, 90: 402–411 (2018).

5. Wang, X., Ji, Y., Wang, J., Wang, Y. and Qi, L., "Optimal energy management of microgrid based on multi-parameter dynamic programming," ***Int. J. Distrib. Sens. Networks,*** 16 (6): 1-12 (2020).

6. Calderaro, V., Conio, G., Galdi, V., Massa, G. and Piccolo, A., "Active management of renewable energy sources for maximizing power production," ***Int. J. Electr. Power Energy Syst.***, 57: 64–72 (2014).

7. Pattanaik, J. K., Basu, M. and Dash, D. P., "Dynamic economic dispatch: a comparative study for differential evolution, particle swarm optimization, evolutionary programming, genetic algorithm, and simulated annealing," ***J. Electr. Syst. Inf. Technol.***, 6 (1): 1-7 (2019).

8. Ioannou, A., Angus, A. and Brennan, F., "Risk-based methods for sustainable energy system planning: A review, **"*Renew. Sustain. Energy Rev.***, 74: 602–615 (2017).

9. Li, Y., Yang, Z., Li, G., Zhao, D. and Tian, W., "Optimal scheduling of an isolated microgrid with battery storage considering load and renewable generation uncertainties," ***IEEE Trans. Ind. Electron.***, 66 (2): 1565–1575 (2018).

10. Cagnano, A., Bugliari, A. C. and De Tuglie, E., "A cooperative control for the reserve management of isolated microgrids," ***Appl. Energy***, 218: 256–265 (2018).

11. Hajiaghasi, S., Salemnia, A. Hamzeh, M., "Hybrid energy storage system for microgrids applications: A review, **"*J. Energy Storage***, 21: 543–570 (2019).

12. Ahmad, J., Imran, M., Khalid, A., Iqbal, W., Ashraf, S.R., Adnan, M., Ali, S.F. and Khokhar, K.S., "Techno economic analysis of a wind-photovoltaic-biomass hybrid renewable energy system for rural electrification: A case study of Kallar Kahar", ***Energy***, 148: 208-234 (2018).

13. Das, B. K., Al-Abdeli, Y. M. and Kothapalli, G., "Effect of load following strategies, hardware, and thermal load distribution on stand-alone hybrid CCHP systems", ***Appl. Energy***, 220: 735-753 (2018).

14. Delgado, C., and Dominguez-Navarro, J. A., "Optimal design of a hybrid renewable energy system", ***In Proceedings of the 2014 Ninth International Conference on Ecological Vehicles and Renewable Energies*** (EVER), Monte-Carlo, Monaco, 25–27 March (2014).

15. Dufo-López, R., Bernal-Agustín, J. L. and Contreras, J., "Optimization of control strategies for stand-alone renewable energy systems with hydrogen storage", ***Renew Energy***, 32 (7): 1102-1126 (2007).

16. Luna, A. C., Meng, L., Diaz, N. L., Graells, M., Vasquez, J. C., and Guerrero, J. M., "Online Energy Management Systems for Microgrids: Experimental Validation and Assessment Framework", ***IEEE Trans. Power Electron***, 33 (3): 2201-2215 (2018).

17. Chaouachi, A., Kamel, R. M., Andoulsi, R. and Nagasaka, K., "Multiobjective intelligent energy management for a microgrid", ***IEEE Trans. Ind. Electron***, 60: 1688–1699 (2013).

18. Li, H., Eseye, A.T., Zhang, J., and Zheng, D., "Optimal energy management for industrial microgrids with high-penetration renewables", ***Prot. Control Mod. Power Syst***, 2 (1): 1-14 (2017).

19. Marzband, M., Azarinejadian, F., Savaghebi, M., and Guerrero, J. M., "An optimal energy management system for islanded microgrids based on multiperiod artificial bee colony combined with markov chain", ***IEEE Syst. J***, 1: (3) 1712-1722 (2017).

20. Ei-Bidairi, K. S., Nguyen, H. D., Jayasinghe, S. D. G. and Mahmoud, T. S., "Multiobjective Intelligent Energy Management Optimization for Grid-Connected Microgrids", ***IEEE International Conference on Environment and Electrical Engineering and 2018 IEEE Industrial and Commercial Power Systems Europe*** (EEEIC/I&CPS Europe), 1-6 (2018).

21. Ogunjuyigbe, A. S. O., Ayodele, T. R. and Akinola, O. A. "Optimal allocation and sizing of PV/Wind/Split-diesel/Battery hybrid energy system for minimizing

life cycle cost, carbon emission and dump energy of remote residential building", ***Appl. Energy***, 171 (C): 153-171 (2016).

22. Wu, N., Wang, H., "Deep learning adaptive dynamic programming for real time energy management and control strategy of micro-grid", ***J. Clean Prod***, 204 (3): 1169-1177 (2018).

23. Zhuo, W., "Microgrid energy management strategy with battery energy storage system and approximate dynamic programming", ***In Proc. of the 2018 37th Chinese Control Conference (CCC)***, Wuhan, China, 25–27 July, 7581-7587 (2018).

24. Raju, L., Morais, A.A., Rathnakumar, R., Ponnivalavan, S., and Thavam, L.D., "Micro-grid grid outage management using multi-agent systems", ***In Proc. of the 2017 Second International Conference on Recent Trends and Challenges in Computational Models (ICRTCCM)***, Tindivanam, India, 3–4 February, 363-368 (2017).

25. Karavas, C.S., Kyriakarakos, G., Arvanitis, K.G., and Papadakis, G., "A multi-agent decentralized energy management system based on distributed intelligence for the design and control of autonomous polygeneration microgrids", ***Energy Convers. Manag***, 103: 166-179 (2015).

26. Lu, T., Ai, Q., and Wang, Z., "Interactive game vector: A stochastic operation-based pricing mechanism for smart energy systems with coupled-microgrids", ***Appl. Energy***, 212: 1462-1475 (2018).

27. Hu, W., Wang, P., and Gooi, H.B., "Towards optimal energy management of microgrids with a realistic model", **In Proc. of the 2016 Power Systems Computation Conference (PSCC)**, 1-7 (2016).

28. Zachar, M., and Daoutidis, P., "Energy management and load shaping for commercial microgrids coupled with flexible building environment control", ***J. Energy Storage***, 16: 61-75 (2018).

29. Wu, Z., Tazvinga, H., and Xia, X., "Demand side management of photovoltaic-battery hybrid system", ***Appl. Energy***, 148: 294-304 (2015).

30. Astaneh, M., Roshandel, R., Dufo-López, R., and Bernal-Agustín, J. L., "A novel framework for optimization of size and control strategy of lithium-ion battery based off-grid renewable energy systems", ***Energy Convers. Manag***, 175 (1): 99-111 (2018).

31. Yadav, N., and Kumar, D., "Microgrid economic load dispatch including storage and reserve", ***IEEE 8th Power India International Conference*** (PIICON), 1-6 (2018).

32. Han, X. S., Gooi, H. B. and Kirschen, D. S., "Dynamic economic dispatch: feasible and optimal solutions", ***IEEE Trans. power Syst***, 16 (1): 22–28 (2001).

33. Faris, H., Aljarah, I., Al-Betar, M. A., and Mirjalili, S., "Grey wolf optimizer: A review of recent variants and application", ***Neural Computing and Applications***, 30: 413-423 (2018).

34. Mirjalili, S., Mirjalili, S. M., and Lewis,A., "Grey wolf optimizer", ***Advances In Engineering Software***, 69: 46–61 (2014).

35. Kamboj, V. K., Bath, S. K., and Dhillon, J., "Solution of non-convex economic load dispatch problem using grey wolf optimizer" ***Neural Computing and Applications***, 27 (5): 1301–16 (2016).

36. Gupta, P., Kumar, V., Rana, K. P. S., and Mishra, P., "Comparative study of some optimization techniques applied to Jacketed CSTR control", ***4th International Conference on Reliability, Infocom Technologies and Optimization (ICRITO)***, Noida, 1–6 (2015).

37. B. Lasseter, "Microgrids. Distributed power generation", ***in Proc. Of IEEE Power Eng. Soc. Winter Meet***, Jan, 146–149 (2001).

38. Myles, W., Miller, J., Knudsen, S., and Grabowski, T., "Electric power system asset optimization", ***Energy Sector Planning and Analysis (ESPA)***, 20 (2011).

39. Campbell, R. J., and Lowry, S., "Weather-related power outages and electric system resiliency", ***CRS***, Washington D.C. (2012).

40. Hatziargyriou, N., "Microgrids: architectures and controls", ***Wiley-IEEE Press***, Chichester, United Kingdom, 341 (2014).

41. Hatziargyriou, N., Jenkins, N., Strbac, G., Lopes, J.A.P., Ruela, J., Engler, A., Oyarzabal, J., Kariniotakis, G., and Amorim, A., "Microgrids-large scale integration of microgeneration to low voltage grids", ***ConseilInt. des Grands Reseaux Electriques***, Paris, France, Tech. Report (2006).

42. Lede, A. M. R., Molina, M. G., Martinez, M. and Mercado, P. E. "Microgrid Architectures for Distributed Generation: A brief review", ***2017 IEEE PES Innovative Smart Grid Technologies Conference - Latin America (ISGT Latin America)***, 1-6 (2017).

43. Katiraei, F., Iravani, R., Hatziargyriou, N., and Dimeas, A., "Microgrids management", ***IEEE Power and Energy Magazine***, 6: 54-65 (2008).

44. Mahmoud, M. S., Hussain, S. A. and Abido, M.A., "Modeling and control of microgrid", ***Journal of the Franklin Institute***, 351 (5): 2822-2859 (2014).

45. Kanellos, F. D., Tsouchnikas, A. I. and Hatziargyriou, N. D., "Micro-grid simulation during grid-connected and islanded modes of operation", ***International Conference on Power Systems Transients (IPST'05)***, (2005).

46. Katiraei, F. M., Iravani, R., and Lehn, P.W., "Micro-grid autonomous operation during and subsequent to islanding process", ***IEEE Trans.PowerDeliv***, 20 (1): 248–257 (2005).

47. Kakigano H., Miura Y., and Ise T., "Low-voltage bipolar-type DC Micro Grid for super high-quality distribution", ***IEEE Trans Power Electron***, 25 (12): 3066 – 3075 (2010).

48. Justo, J. J., Mwasilu, F., Lee, J., and Jung, J. W., "AC-microgrids versus DC-microgrids with distributed energy resources. A review", ***Renewable and Sustainable Energy Reviews***, 24: 387-405 (2013).

49. Dobakhshari, A. S., Azizi, S., and Ranjbar, A.M., "Control of microgrids: aspects and prospects", ***International Conference on Networking, Sensing and Control*** (ICNSC), 38–43 (2011).

50. Patrao, I., Figueres, E., Garcerá, G., and R. González-Medina, "Microgrid architectures for low voltage distributed generation" ***Renewable and Sustainable Energy Reviews***, vol. 43, pp. 415-424 (2015).

51. Unamuno, E., and Barrena, J. A., "Hybrid ac/dc microgrids—Part I: Review and classification of topologies", ***Renewable and Sustainable Energy Reviews***, 52: 1251-1259 (2015).

52. Parhizi, S., Lotfi, H., Khodaei, A., and Bahramirad, S., "State of the Art in Research on Microgrids", ***IEEE Access,*** 3: 380-925 (2015).

53. Olivares, D. E., Mehrizi-Sani, A., Etemadi, A.H., "Trends in Microgrid Control", ***IEEE Trans. Smart Grid***, 5: 1-15 (2014).

54. Mushtaq, A., Hojabri, M., Humada, A.M., Daniyal, H.B., and Frayyeh, H.F., "An Overview on Microgrid Control Strategies", ***Int. J. Eng. Adv. Technol***, 4 (5): 93-98 (2015).

55. Meng, L., Shafiee, Q., Ferrari-Trecate, G., Karimi, H., Fulwani, D., Lu, X., and Guerrero, J. M. “Review on Control of DC Microgrids and Multiple Microgrid Clusters”, ***IEEE Journal of Emerging and Selected Topics in Power Electronics***, 5 (3): 928 – 948 (2017).

56. Feng, W., Jin, M., Liu, X., Bao, Y., Marnay, C., Yao, C., and Yu, J., “A review of microgrid development in the United States – A decade of progress on policies, demonstrations, controls, and software tools”, ***Appl. Energy***, 228: 1656-1668 (2018).

57. Tucci, M., and Ferrari-Trecate, G., “A scalable, line-independent control design algorithm for voltage and frequency stabilization in AC islanded microgrids”, ***Automatica*** 111: 1-7 (2020).

58. Cintuglu, M.H., Youssef, T., and Mohammed, O.A. "Development and application of a real-time testbed for multiagent system interoperability: A case study on hierarchical microgrid control", ***IEEE Transactions on Smart Grid***, 9 (3): 1759-1768, (2016).

59. Gao, F., Kang, R., Cao, J., Yang, T., and Mod. J., “Primary and secondary control in DC microgrids: a review”, ***Modern Power Syst. And Clean Energy***, 7: 227-242 (2019).

60. Yamashita, D.Y., Vechiu, I., and Gaubert, J.P., “A review of hierarchical control for building microgrids”, ***Renew. Sustain. Energy***, ***Rev***. 118 (2020).

61. Meng, L., Sanseverino, E.R., Luna, A., Dragicevic, T., Vasquez, J.C., Guerrero, J.M., “Renewable and Sustainable Energy Reviews”, ***Renew. Sustain. Energy***, ***Rev***. 60 (2016).

62. Cook, M. D., Trinklein, E. H., Parker, G. G., Robinett, R. D., Weaver, W. W., “Optimal and Decentralized Control Strategies for Inverter-Based AC Microgrids” ***Energies***, 12 (18) (2019).

63. Li, L., Han, Y., Yang, P., Huang, Q., Zhang, Z., and Xu, Y., “A new distributed control strategy for DC microgrids with droop coefficient correction and DC bus voltage restoration” ***IEEE Innovative Smart Grid Technologies – Asia (ISGT Asia)***, Chengdu, China, (2019).

64. Guerrero, J. M., Member, S., Vasquez, J. C., Matas, J., Vicuña, L. G., and Castilla, M., “Hierarchical control of droop-controlled AC and DC Microgrids – A general approach toward standardization,” ***IEEE Trans. on Industrial Electronics,*** 58 (1): 158–172 (2011).

65. Alwal, L., Kihato, P., and Kamau, S., "A review of control strategies for microgrid with PV-wind hybrid generation systems", ***Proceedings of the Sustainable Research and Innovation Conference***, Kenya, (2018).

66. Delgoshaei, P., and Freihaut, J.D., "Development of a Control Platform for a Building-Scale Hybrid Solar PV-Natural Gas Microgrid", ***Energies, MDPI***, 12 (21): 1-30 (2019).

67. Yu, H., Niu, S., Zhang, Y., and Jian, L., "An integrated and reconfigurable hybrid AC/DC microgrid architecture with autonomous power flow control for nearly/net zero energy buildings", ***Appl. Energy***, 263 (1) (2020).

68. Bintoudi, A.D., et al., "Novel hybrid design for microgrid control", ***IEEE PES Asia-Pacific Power and Energy Engineering Conference*** (APPEEC), 1-6 (2017).

69. Gu, Y., Yang, H., Sun, W., Chi, Y., Li, W., He, X., and CSEE J., "Hierarchical Control of DC Microgrids Combining Robustness and Smartness", ***Power and Energy Syst***, 6 (2): 384-393 (2020).

70. Vechiu, I., Llaria, A., Curea, O., Camblong, H., Comput Int., "Control of power converters for microgrids", ***Math. Electr. Electron. Eng***, 30 (1): 300–309 (2011).

71. Siddique, A. B., Munsi, S., Sarker, S.K., Das, S. K., and Islam, R., "Voltage and current control augmentation of islanded microgrid using multifunction model reference modified adaptive PID controller" ***Int. J. Electr. Power Energy Syst***, 113 (2019).

72. Pham, X. H. T., "Power sharing strategy in islanded microgrids using improved droop control", ***Electr. Power Syst, Res***. 180: 106164 (2020).

73. Vandoorn, T. L., De Kooning J. D. M., Meersman, B., and Vandevelde, L. "Review of primary control strategies for islanded microgrids with power-electronic interfaces", ***Renew Sustain Energy Rev***, 19: 613–28 (2013).

74. Malik, S. M., Sun, Y., Huang, W., Ai, X., Shuai, Z., "A Generalized Droop Strategy for Interlinking Converter in a Standalone Hybrid Microgrid", ***Appl. Energy***, 226 (2018).

75. Liu, Y., Han, Y., Lin, C., Yang, P., and Wang, C., "Design and implementation of droop control strategy for DC microgrid based on multiple DC/DC converters", ***IEEE Innovative Smart Grid Technologies –*** Asia, (ISGT Asia), Chengdu, China, 3896-3901 (2019).

76. Peyghami-Akhuleh, S., Mokhtari, H., Davari, P., Loh, P.C., and Blaabjerg, F., "Smart power management of DC microgrids in future milligrids", ***in Proc. IEEE EPE ECCE*** Europe, (2016).

77. Babazadeh-Dizaji, R., Hamzeh, M., and Hekmati, A., "A frequency-based economical-sharing strategy for low-voltage DC microgrids", ***Int. J. Electr. Power Energy Syst***, 118 (2020).

78. Li, F., Lin, Z., Qian, Z., and Wu, J., "Active DC bus signaling control method for coordinating multiple energy storage devices in DC microgrid", ***IEEE Second International Conference on DC Microgrids (ICDCM***), Nuremburg (2017).

79. Peyghami, S., Mokhtari, H., Davari, P., Loh, P.C., and Blaabjerg, F., "On Secondary Control Approaches for Voltage Regulation in DC Microgrids ", ***IEEE Trans. Ind. Appl***, 53 (5) (2017).

80. Heydari, R., Dragicevic, T., and Blaabjerg, F., "High-bandwidth Secondary Voltage and Frequency Control of VSC-based AC Microgrid", ***IEEE Trans. Power Electron***, 34 (11): 11320-11331 (2019).

81. Humada, A. M., et al, "Modeling of PV system and parameter extraction based on experimental data: Review and investigation", ***Solar Energy***, 199: 742–760 (2020).

82. Mellit, A., Benghanem, M., and Kalogirou, S.A., "Modeling and simulation of a stand-alone photovoltaic system using an adaptive artificial neural network: Proposition for a new sizing procedure", ***Renewable Energy***, 32: 285–313 (2007).

83. Chouder, A., Silvester, S., Taghezouit, B., and Karatepe, E., "Monitoring, modelling and simulation of PV systems using LabVIEW", ***Solar Energy***, 91: 337-349 (2013).

84. Koutroulis, E., and Kalaitzakis, K., "Development of an integrated data-acquisition system for renewable energy sources systems monitoring", ***Renewable Energy***, 28: 139–152 (2003).

85. Almagrahi, N., "Modeling, control and techno-economic analysis of Karabuk university Microgrid", PhD thesis, ***Institute of graduate programs***, Karabuk, 60-65 (2020).

86. Mellit, A., Kalogirou, S. A., Hontoria, L., and Shaari, S., "Artificial intelligence techniques for sizing photovoltaic systems: A review", ***Renewable and Sustainable Energy Reviews***, 13: 406–419 (2009).

87. Zitouni, N., Andoulsi, R., Sellami, A., Mami, A., and Hassen, A., "A new Bond Graph Model of a Water Disinfection System Based on UV Lamp Feed by Photovoltaic Source: Simulation and Experimental Results", ***J. Automation & Systems Engineering***, 5 (2): 79-95 (2011).

88. Gawthrop, P. J., & Bevan, G. P., "Bond-graph modeling: a tutorial introduction for control engineer", ***IEEE Control Systems***, 27 (2): 24-45 (2007).

89. Umesh R. B., and Umanand, L., "Bond graph toolbox for handling complex variable", ***IET Control Theory Appl***, 3 (5): 551-560 (2009).

90. Park, R. H., "Two-reaction theory of synchronous machines", ***American Institute of Electrical Engineers, Transactions of the***, 48: 716–727 (1929).

91. Anderson, P. M., and Fouad, A. A., "Power System Control and Stability", Second Edition, ***John Wiley and Sons, Inc***, New York, 553 (2003).

92. Xiao, W., Dunford, W.G., and Capel, A., "A Novel Modeling Method for Photovoltaic Cells", ***IEEE Power Electrics Specialists Conference***, 1950–1956 (2004).

93. Ding, F., Li, P., Huang, B., Gao, F., Ding, C. and Wang, C., "Modeling and simulation of grid-connected hybrid photovoltaic/battery distributed generation system", in ***Proceedings of the China International Conference on Electricity Distribution (CICED '10)***, 1–10 (2010).

94. Zhong, Q. C. and Zeng, Y., "Universal Droop Control of Inverters with Different Types of Output Impedance", ***IEEE Access***, 4: 702–712 (2016).

95. Ren, H., Xiang, A., Teng, W., and Cen, R., "Economic optimization with environmental cost for a microgrid" , ***IEEE Power Energy Soc. Gen. Meet***, 071003: 1–6 (2012).

96. Meng, L., Shafiee, Q., Trecate, G. F., Karimi, H., Fulwani, D., Xiaonan Lu, and Guerrero, Josep. M., "Review on Control of DC Microgrids", ***IEEE J. Emerg. Sel. Top. Power Electron***, 5 (3): 928–948, (2017).

97. Jirdehib, M., Tabara, V. S., Ghassemzadeha, S., and Tohidia, S., "Different aspects of microgrid management: A comprehensive review", ***Journal of Energy Storage***, 30: 101457 (2020).

98. Fathima, A. Hina., and Palanisamy, K., "Renewable and Sustainable Energy Reviews", ***Renewable & Sustainable Energy Reviews***, 45: 431–446 (2015).

99. Mukherjee, S. K. “Optimal power flow by linear programming based optimization”, ***Proceedings IEEE Southeastcon '92***, 2: 527-529 (1992).

100. Chung T. S., and Shaoyun, Ge., “A recursive LP-based approach for optimal capacitor allocation with cost-benefit consideration”, ***Electric Power Syst. Research***, 39: 129-136 (1997).

101. Lobato, E., Rouco, L., Navarrete, M. I., Casanova, R., and Lopez, G., “An LP-based optimal power flow for transmission losses and generator reactive margins minimization”, ***IEEE Porto Power Tech Proceedings in Proc, Portugal***, 3: 5 (2001).

102. Rau, N., “Issues in the path toward an RTO and standard markets”, ***IEEE Trans. Power Syst***, 18 (2): 435–443 (2003).

103. Rau, N., “Optimization Principles: Practical Applications to the Operation and Markets of the Electric Power Industry”, ***Wiley/IEEE Press,*** Hoboken (2003).

104. Haupt, R., “Practical Genetic Algorithms”, ***Wiley/IEEE Press,*** New York (2004).

105. Tang, K., and Kwong, S., “Genetic Algorithms: Concepts and Designs”, ***Springer***, Berlin (1999).

106. Kamal, M., Rahman, T., and Musirin, I., “Application of improved genetic algorithms for loss minimisation in power system”, Proceedings ***National Power and Energy Conference,*** 258–262 (2004).

107. Rudolph, G., “Convergence analysis of canonical genetic algorithms”, ***IEEE Trans. Neural Netw***, 5: 96–101 (1994).

108. Bakritzs, A., Perirtridis V., and Kazarlis, S., “Genetic Algorithm Solution to the Economic Dispatch Problem”, ***IEE Proc. – Generation Transmission Distribution***, 141 (4): 377-382 (1994).

109. Po-Hung Chen and Hong-Chan Chang, “Large-Scale Economic Dispatch by Genetic Algorithm Discover”, ***IEEE Transactions on Power Systems***, 10 (4): 1919 – 1926 (1995).

110. Younes, M., Rahli, M., and Abdelhakeem-Koridak, L., “Optimal Power based on Hybrid Genetic Algorithm”, ***Journal of Information Science and Engineering***, 23: 1801-1816 (2007).

111. Kumari, S. M. and Maheswarapu, S. “Enhanced Genetic Algorithm based computation technique for multi-objective Optimal Power Flow solution”, ***Electrical Power and Energy Systems***, 32: 736–742 (2010).

112. El-Gallad, A. I., El-Hawary, M., Sallam, A. A., and Kalas, A., “Swarm intelligence for hybrid cost dispatch problem”, ***in Proc. Canadian Conf. Elect. Comput. Eng***, 2: 753–757 (2001).

113. Ben Attous, D., “Particle swarm optimization based optimal power flow for units with non-smooth fuel cost functions”, ***International Conference on Electrical and Electronics Engineering – ELECO,*** 377-381 (2009).

114. Kumar, S., and Chaturvedi, D. K., “Optimal power flow solution using fuzzy evolutionary and swarm optimization”, ***Electrical Power and Energy Systems***, 47: 416–423 (2013).

115. Saravanan, T., Saritha, G., and Srinivasan, V.,”Optimal Power Flow Using Particle Swarm Optimization”, ***Middle-East Journal of Scientific Research***, 20 (11): 1554-1560 (2014).

116. Praveen, J., and Srinivasa B., “Single objective optimization using PSO with Interline Power Flow Controller”, ***International Electrical Engineering Journal***, 5 (12): 1659-1664 (2014).

117. Wooldridge, M., and Weiss, G., “Intelligent Agents”, (Ed.), Multi-agent Systems, ***The MIT Press***, Cambridge, 3–51 (1999).

118. Logenthiran, T., Srinivasan, D., and Khambadkone, A. M., “Multi-agent system for energy resource scheduling of integrated microgrids in a distributed system”, ***Electric Power Systems Research***, 138-148 (2011).

119. McArthur, S. D., Davidson, E. M., Catterson, V. M., Dimeas, A. L., Hatziargyriou, N.D., Ponci, F., and Funabashi, T., “Multi-agent systems for power engineering applications – Part I: Concepts, approaches, and technical challenges”, ***IEEE Transactions on Power systems***, 22 (4): 1743-1752 (2007).

120. McArthur, S. D., Davidson, E. M., Catterson, V. M., Dimeas, A. L., Hatziargyriou, N. D., Ponci, F., and Funabashi, T., “Multi-Agent Systems for Power Engineering Applications – Part II: Technologies, Standards, and Tools for Building Multi-agent Systems”, ***IEEE Transactions on Power system***, pp.1753-1759 (2007).

121. Robinson, C.R., Mendham, P., and Clarke, T., “MACSimJX: A tool for enabling agent modelling with Simulink using JADE’, ***Journal of Physical Agents***, (2010).

122. Yahiaoui, A., Fodhil, F., Benmansour, K., Tadjine, M., and Cheggaga. N., "Grey wolf optimizer for optimal design of hybrid renewable energy system PV-diesel generator-battery: Application to the case of Djanet city of Algeria", ***Solar Energy***, 158: 941–51 (2017).

123. Yang, B., Zhang, X., Yu, T., Shu, H., and Fang, Z., "Grouped grey wolf optimizer for maximum power point tracking of doubly-fed induction generator-based wind turbine" ***Energy Conversion and Management***, 133: 427–43 (2017).

124. Ali, M., El-Hameed, M. A., and Farahat. M. A., "Effective parameters' identification for polymer electrolyte membrane fuel cell models using grey wolf optimizer" ***Renewable Energy***, 111: 455–62 (2017).

125. Precup, R. E., David, R., Szedlak-Stinean, A. L., Petriu, E. M., and Dragan. F., "An easily understandable grey wolf optimizer and its application to fuzzy controller tuning", ***Algorithms***, 10 (2): 68 (2017).

126. Mech, L. D., "Alpha status, dominance, and division of labor in wolf packs", ***Canadian Journal of Zoology***, 77: 1196-1203 (1999).

127. Muro, C., Escobedo, R., Spector, L., and Coppinger, R., "Wolfpack (Canis lupus) hunting strategies emerge from simple rules in computational simulations," ***Behav. Process***., 88 (3): 192–197 (2011).

128. Vankadara K., and Raglend, I. J., "A review to economic dispatch of hybrid microgrids" **, *Serbian J. Electr. Eng***, 16 (2): 233–246 (2019).

129. Badal, F. R., Das, P., Sarker, S. K., and Das, S. K., "A survey on control issues in renewable energy integration and microgrid", ***Prot. Control Mod. Power Syst***, 4: 8 (2019).

130. Maharsi, A. L., Wijaya, F. D., and Mustika, I. W., "Cost-based power distribution optimization scheduling in microgrid", **in *Proc. 3rd International Conference on Science and Technology-Computer***, *(ICST)*, 87–92 (2017).

131. Antony, A., Wang, Y. D., and Roskilly, A. P., "A detailed optimisation of solar photovoltaic/thermal systems and its application.", ***Energy Procedia***, 158: 1141–1148 (2019).

132. Paliwal, N. K., Singh, A. K., and Singh, N. K., "Economic energy scheduling of grid connected microgrid with diesel engine and reserve constraint", ***IEEE Region 10 Humanitarian Technology Conference (R10-HTC)***, 1–6 (*2016).*

133. Han, X. S., Gooi, H. B., and Kirschen, D. S., "Dynamic economic dispatch:

feasible and optimal solutions" , ***IEEE Trans. power Syst***, 16 (1): 22–28 (2001).

134. Phommixay, S., Doumbia, M. L., and St-Pierre, D. L., "Review on the cost optimization of microgrids via particle swarm optimization", ***Int. J. Energy Environ. Eng***, 11 (1): 73–89 (2020).

135. Zheng, W., Wu, W., Zhang, B., Sun, H., Guo, Q., and Lin, C., "Dynamic economic dispatch for microgrids: A fully distributed approach", in ***IEEE/PES Transmission and Distribution Conference and Exposition (T&D)***, 1–3 (2016).

136. Fan, S., He, G., Guo, B., and Wang, Z., "A user energy management system (UEMS)-based microgrid economic dispatch model", ***IEEE PES Asia-Pacific Power and Energy Engineering Conference (APPEEC)***, 1–6 (2017).

137. Paul, T. G., Hossain, S. J., Ghosh, S., Mandal, P., and Kamalasadan, S., "A quadratic programming based optimal power and battery dispatch for grid-connected microgrid", ***IEEE Trans. Ind. App***, 54 (2): 1793–1805 (2018).

138. Wang, Y., Wang, L., Xu, L., and Sun, J., "Monte Carlo based operating reserve adequacy evaluation of a stand-alone microgrid considering high penetrations of correlated wind energy", ***3rd International Conference on Information Science and Control Engineering (ICISCE)***, 1356–1360 (2016).

139. Issa, A., "Multi-agent system based Microgrid control", PhD thesis, ***Institute of graduate programs,*** Karabuk, 62-75 (2020).

# APPENDIX A.

## KBU MG OPTIMIZATION RESULTS FOR EACH MONTH

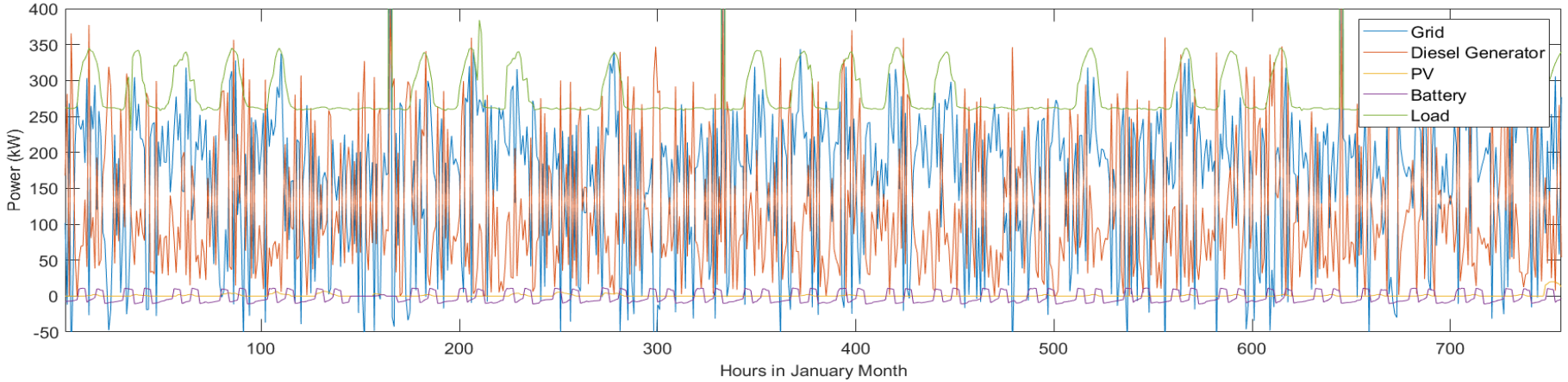
Power (kW)
Hours in January Month
Grid
Diesel Generator
PV
Battery
Load

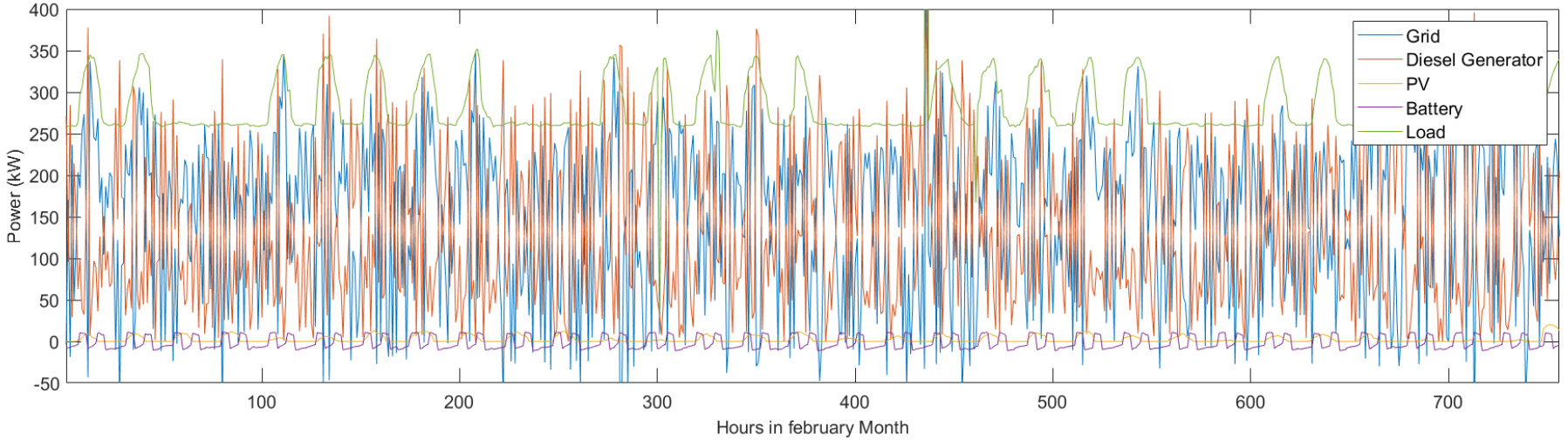
Power (kW)
Hours in february Month
Grid
Diesel Generator
PV
Battery
Load

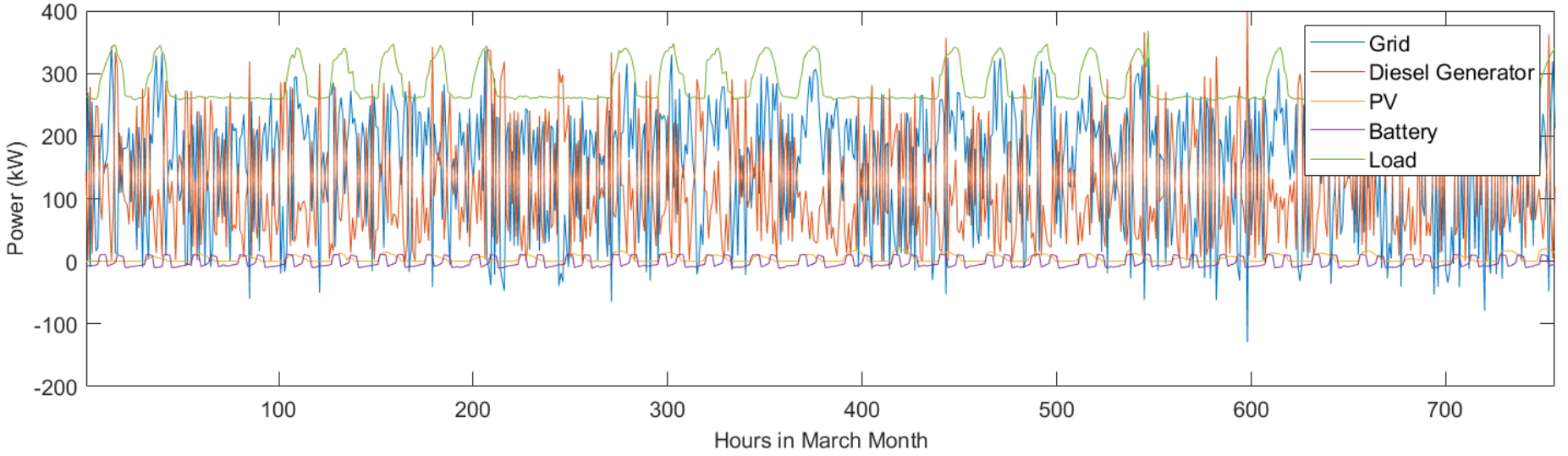
Power (kW)
400
300
200
100
0
-100
-200
100
200
300
400
500
600
700
Hours in March Month
Grid
Diesel Generator
PV
Battery
Load

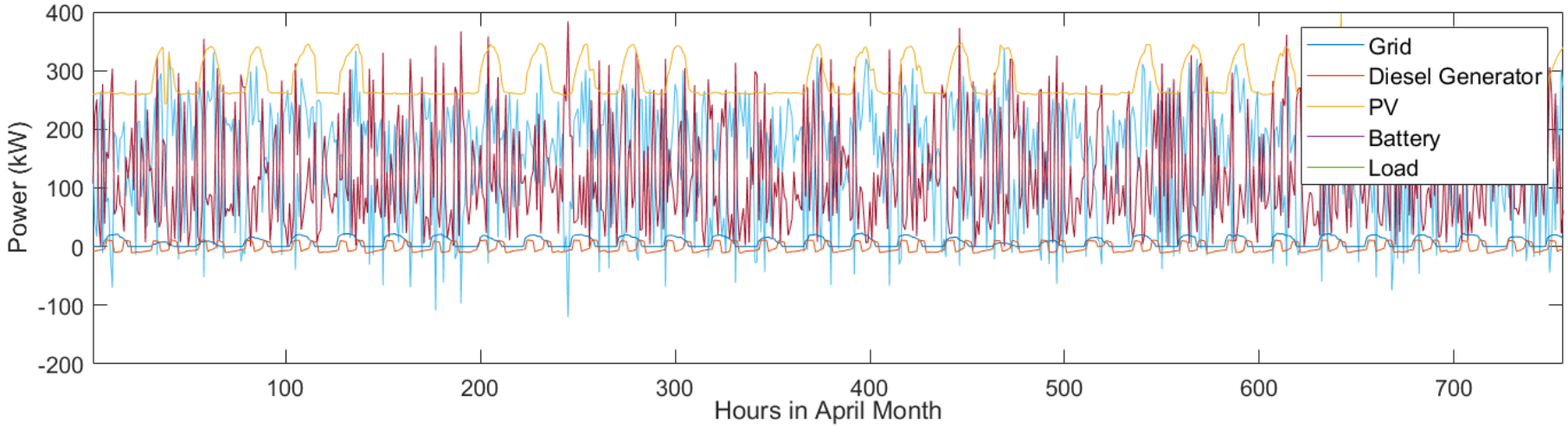
Power (kW)
400
300
200
100
0
-100
-200
100
200
300
400
500
600
700
Hours in April Month
Grid
Diesel Generator
PV
Battery
Load

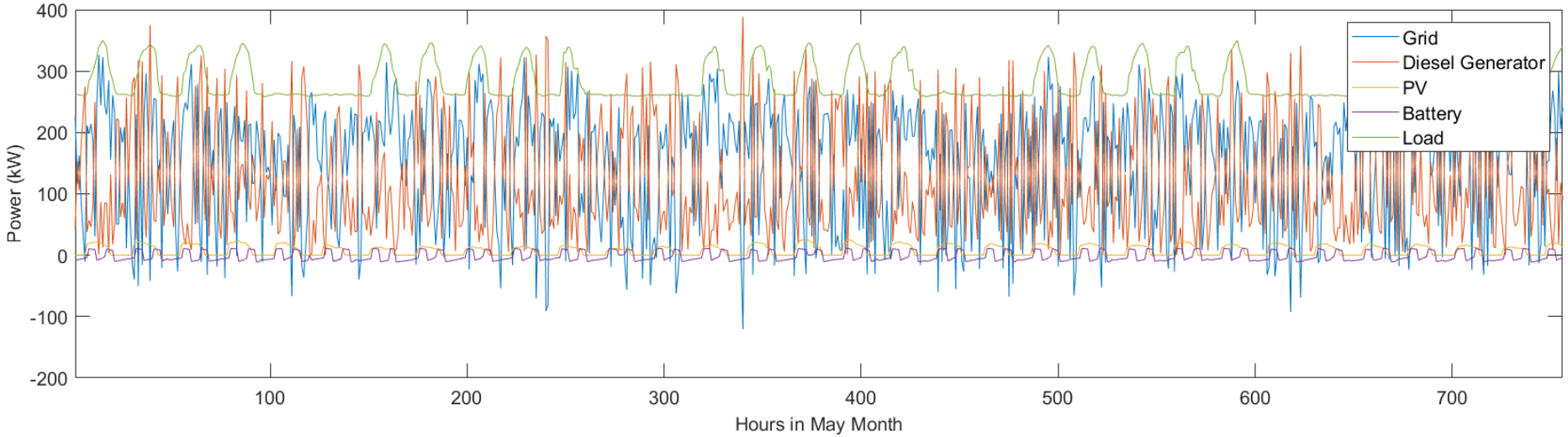
Power (kW)
Hours in May Month
Grid
Diesel Generator
PV
Battery
Load

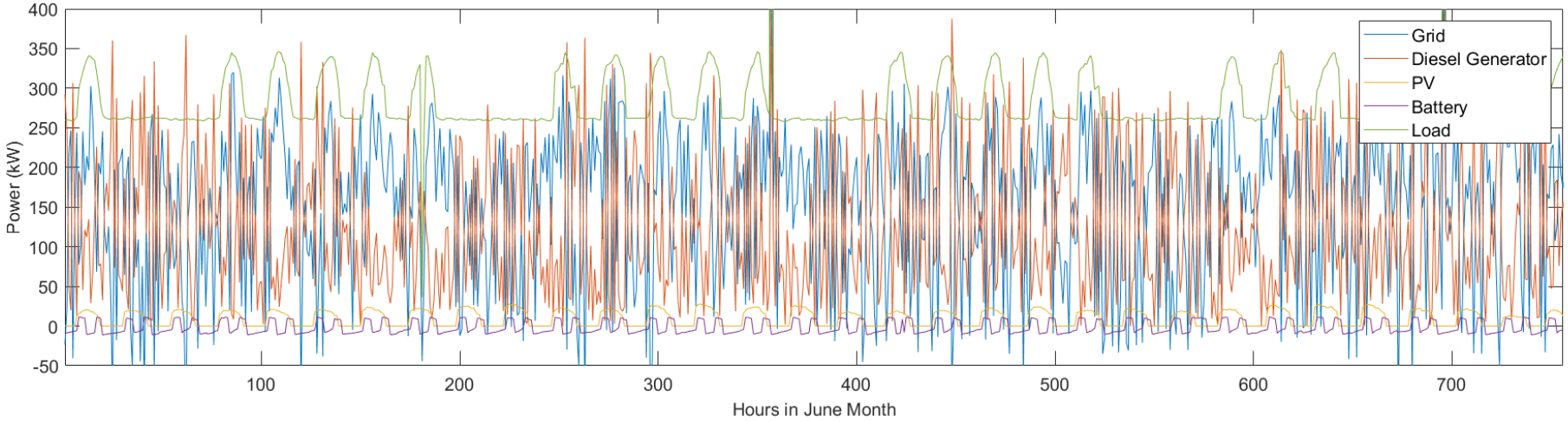
Power (kW)
Hours in June Month
Grid
Diesel Generator
PV
Battery
Load

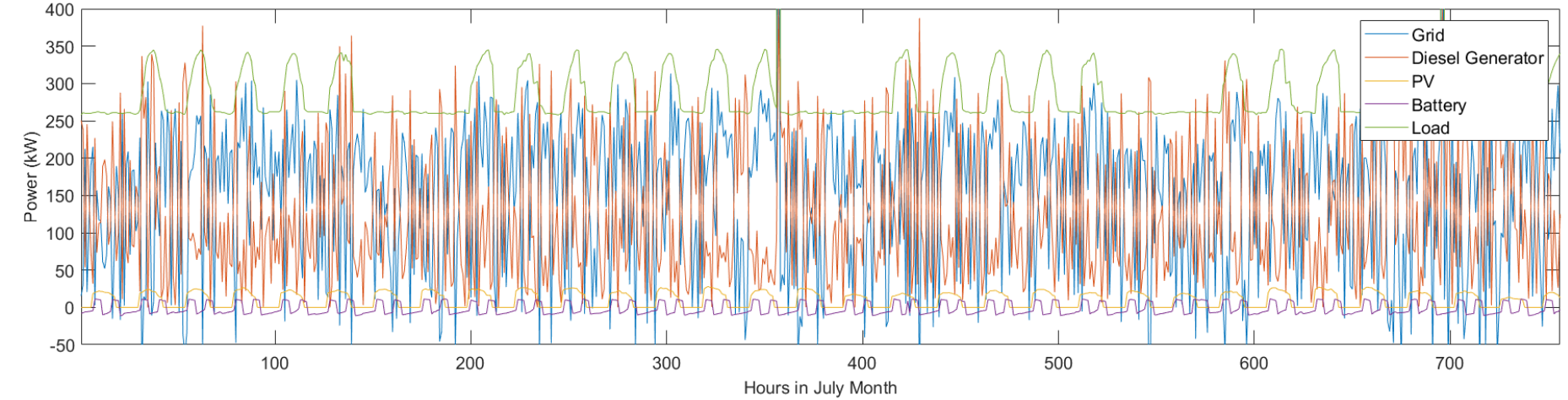
Power (kW)
Hours in July Month
Grid
Diesel Generator
PV
Battery
Load

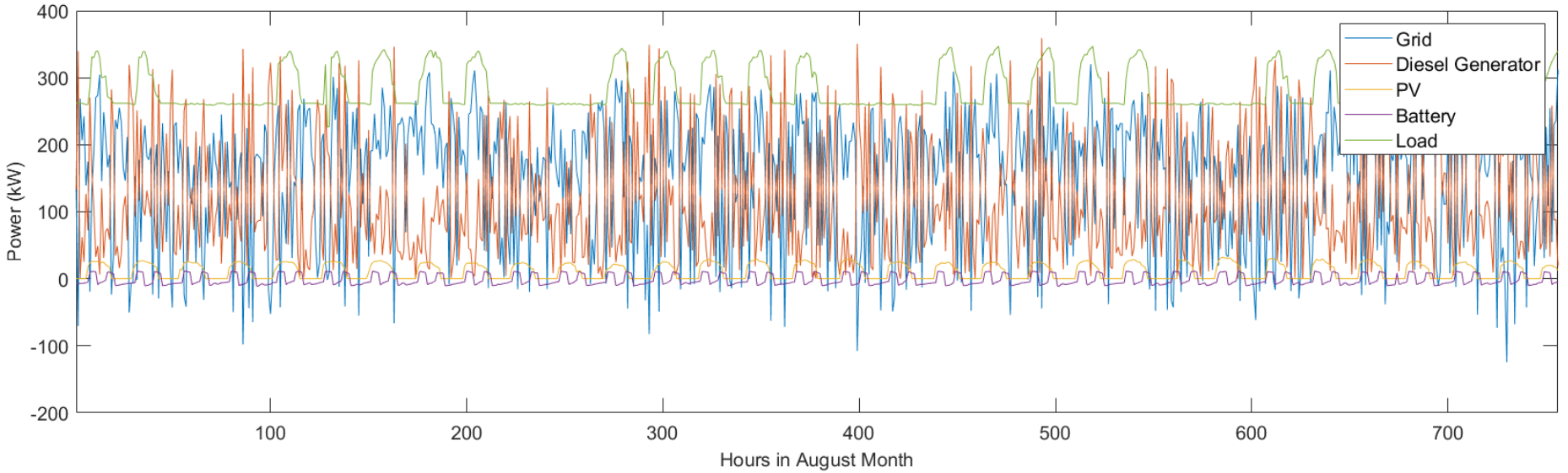
Power (kW)
Hours in August Month
Grid
Diesel Generator
PV
Battery
Load

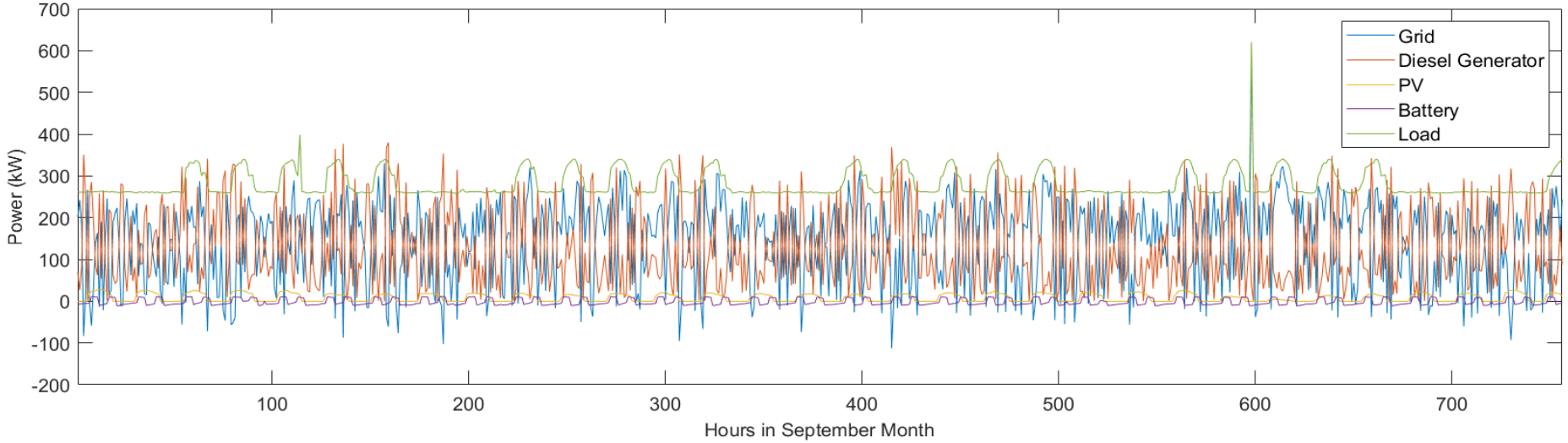
Grid
Diesel Generator
PV
Battery
Load
Power (kW)
Hours in September Month

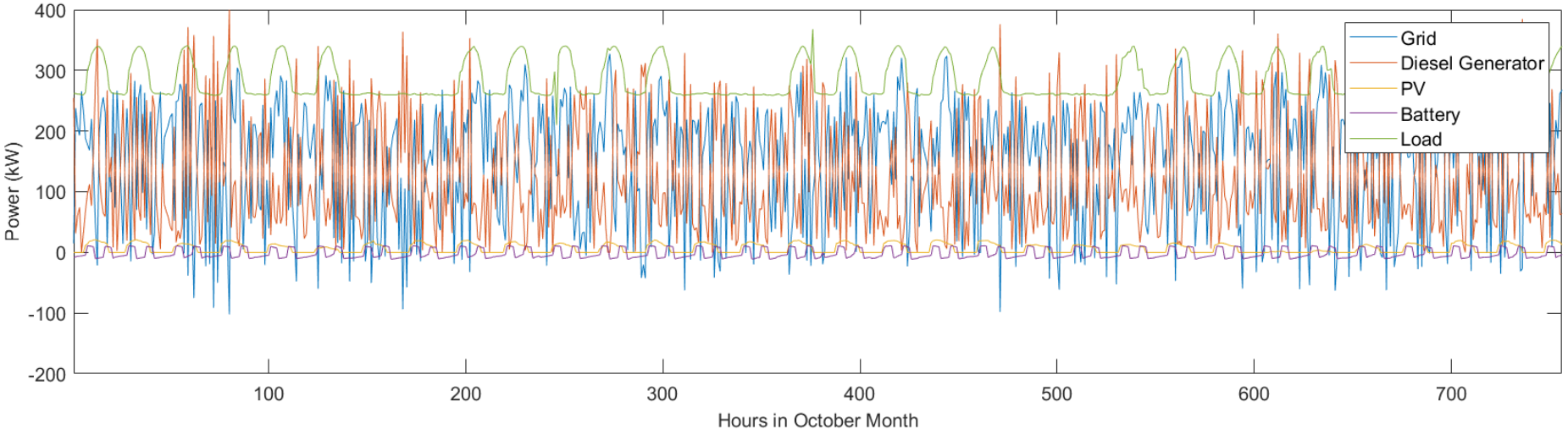
Grid
Diesel Generator
PV
Battery
Load
Power (kW)
Hours in October Month

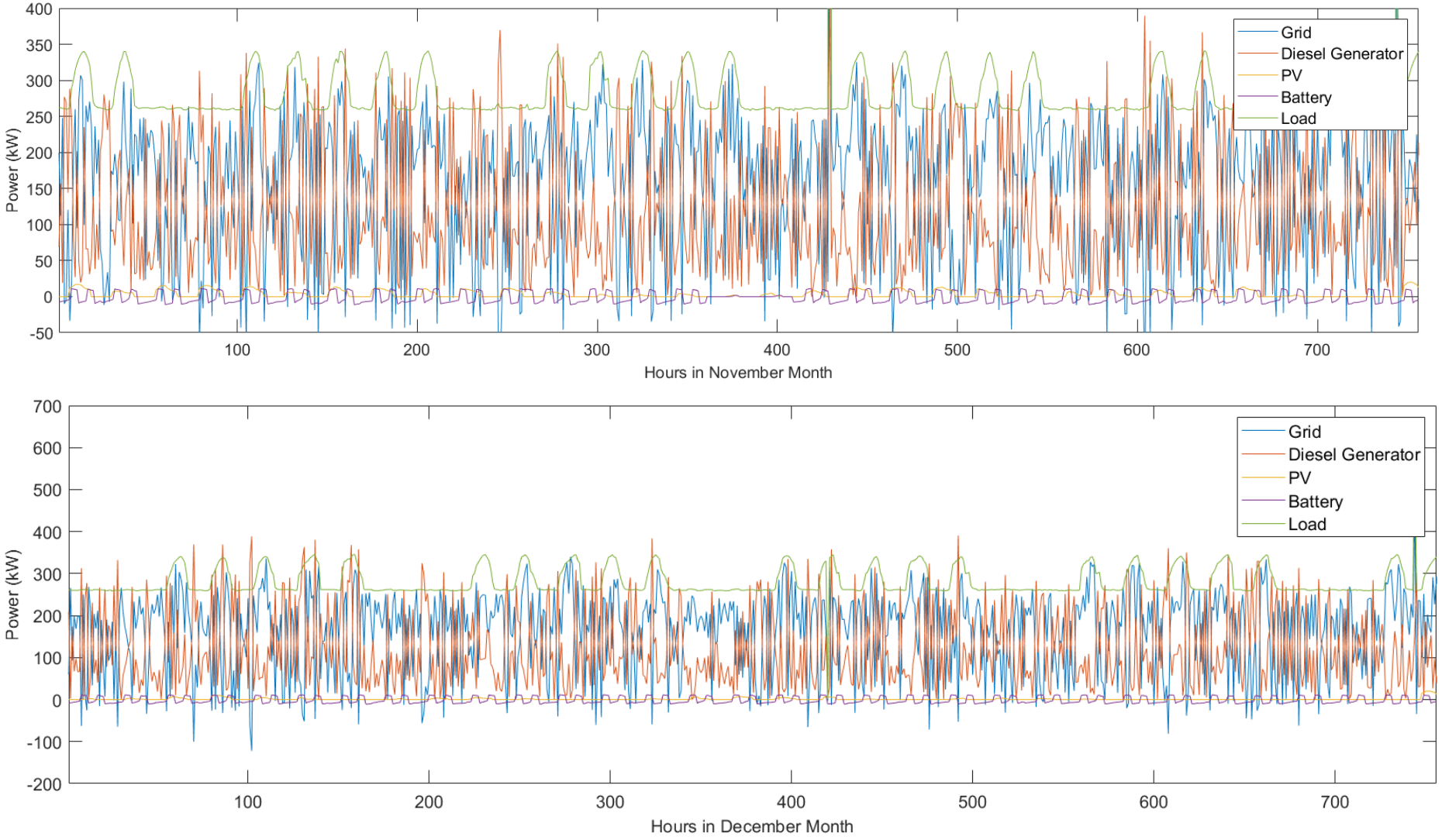
Power (kW)
Hours in November Month
Grid
Diesel Generator
PV
Battery
Load
Power (kW)
Hours in December Month
Grid
Diesel Generator
PV
Battery
Load

# APPENDIX B.

# PUBLISHED PAPERS

**ESCI-indexed Journal**

1. Aljribi, S., Yusupov, Z. “Grey wolf optimized economic load dispatch including battery storage in microgrid”, ***Journal of Polutechnic***, (2022)

## RESUME

Salem Faraj Alarabi ALJRIBI graduated primary and preparatory education in Beni Walid (Libya) city. He completed high school education in Electrical Engineering. He graduated Master program in Cracow University of Technology, Department of Electric and Computer Engineering in Cracow (Poland), 2005. In 2006, he started working at the higher institute of heavy machinery as a lecturer. He started his Ph.D. education program at Karabük University in Department of Electrical-Electronics Engineering in 2015.

## CONTACT INFORMATION

Address: Karabük University
Institute of Graduate Programs
Demir-Çelik Campus/KARABUK
E-mail: aljribi@gmail.com